The Pennsylvania State University
APPLIED RESEARCH LABORATORY
P.O. Box 30
State College, PA 16804

SOUND PROPAGATION IN THE ATMOSPHERE: ANALYSIS OF SIGNAL AMPLITUDE AND PHASE TEMPORAL AND SPATIAL VARIATIONS

by

S. R. Solomon
D. W. Thomson

Technical Report No. TR 91-007
June 1991

Supported by:
Office of Naval Research

L.R. Hettche, Director
Applied Research Laboratory

Distribution unlimited

REPORT DOCUMENTATION PAGE

Form Approved
OMB No. 0704-0188

1. AGENCY USE ONLY (Leave blank)	2. REPORT DATE	3. REPORT TYPE AND DATES COVERED
	June 1991	

4. TITLE AND SUBTITLE

SOUND PROPAGATION IN THE ATMOSPHERE: ANALYSIS OF SIGNAL AMPLITUDE AND PHASE TEMPORAL AND SPATIAL VARIATIONS

5. FUNDING NUMBERS

N00014-86-K-0688

6. AUTHOR(S)

S. R. Solomon, D. W. Thomson

7. PERFORMING ORGANIZATION NAME(S) AND ADDRESS(ES)

Applied Research Laboratory
Penn State University
P. O. Box 30
State College, PA 16804

8. PERFORMING ORGANIZATION REPORT NUMBER

TR-91-007

9. SPONSORING/MONITORING AGENCY NAME(S) AND ADDRESS(ES)

Office of Naval Research
800 North Quincy Street
Arlington, VA 22217-5000

10. SPONSORING/MONITORING AGENCY REPORT NUMBER

11. SUPPLEMENTARY NOTES

12a. DISTRIBUTION/AVAILABILITY STATEMENT

Unlimited

12b. DISTRIBUTION CODE

13. ABSTRACT *(Maximum 200 words)*

Temporal and spatial variations of the signal amplitude and phase were studied by use of a well developed atmospheric sound propagation prediction model. Modifications were made to this ray tracing model to incorporate the calculation of phase. Full documentation on the original and its modifications were provided. Two case studies were performed using actual meteorological data as input. The first study was representative of long distance (25 km) sound propagation in a mountainous region. The second was representative of sound propagation over much shorter distances (600 m) in a forest environment. The results of both signal amplitude and phase were displayed in a statistical format. This format was an aid to analyzing and explaining the temporal and spatial variabilities.

14. SUBJECT TERMS

atmosphere, sound propagation, model, ray tracing, temporal variations, spatial variations

15. NUMBER OF PAGES

193

16. PRICE CODE

17. SECURITY CLASSIFICATION OF REPORT	18. SECURITY CLASSIFICATION OF THIS PAGE	19. SECURITY CLASSIFICATION OF ABSTRACT	20. LIMITATION OF ABSTRACT
Unclassified	Unclassified	Unclassified	Unlimited

ABSTRACT

Temporal and spatial variations of the signal amplitude and phase were studied by use of a well developed atmospheric sound propagation prediction model. Modifications were made to this ray tracing model to incorporate the calculation of phase. Full documentation on the original and its modifications were provided. Two case studies were performed using actual meteorological data as input. The first study was representative of long distance (25 km) sound propagation in a mountainous region. The second was representative of sound propagation over much shorter distances (600 m) in a forest environment. The results of both signal amplitude and phase were displayed in a statistical format. This format was an aid to analyzing and explaining the temporal and spatial variabilities.

TABLE OF CONTENTS

TABLE OF CONTENTS (Continued)

TABLE OF CONTENTS (Continued)

LIST OF FIGURES

LIST OF FIGURES (Continued)

LIST OF FIGURES (Continued)

LIST OF FIGURES (Continued)

LIST OF FIGURES (Continued)

LIST OF FIGURES (Continued)

LIST OF FIGURES (Continued)

LIST OF FIGURES (Continued)

LIST OF TABLES

Chapter 1

INTRODUCTION

Properly used, ray tracing can be a powerful method for predicting and analyzing the characteristics of sound propagated through the atmosphere. This thesis discusses the use of a sophisticated ray tracing program, RAYPS, for examining the properties of sound propagated over ranges of a few hundred meters to several 10's of kilometers. The computer program was originally developed for analysis of noise impact in areas surrounding natural or artificial sources. By distributing an array of fictitious targets along the specific topography the sound pressure level (SPL) can be predicted as it might be measured using an array of correspondingly placed microphones. This propagation model accounts for atmospheric absorption and reflection loss at the ground as well as ray refraction in the atmosphere.

Under the direction of Dr. Dennis W. Thomson the initial version of RAYPS was coded by Dr. William H. Mach (dec.) with occasional assistance by one of his Ph. D. students, Michael Moss. Due to rapidly deteriorating health, Dr. Mach was neither able to complete parts of the program nor documentation of it. Those tasks thus became a part of this thesis study. Calculations to evaluate the phase of the rays at each of the targets and to perform the coherent summation of the multipath signals were also functions added to the model.

With the model completed and tested, it was then used for several case studies of environmental sound propagation. One case study was performed using actual terrain and meteorological data from a region of complex, mountainous terrain. Several data sets representing the evolution of the meteorological conditions throughout two different days were run. In particular the temporal (diurnal) fluctuations of both the sound pressure level (amplitude) and signal phase were examined. Statistical parameters such as mean values and standard deviations were used to summarize the nature of the predicted fluctuations. The dependence of the variability on spatial range was also investigated. Statistical output such as cumulative relative frequency distributions as well as histograms were also used to parameterize the predicted noise levels. Such methods ought to be more widely used in environmental noise impact assessment programs.

Understanding outdoor sound propagation requires knowledge of how waves propagate in a medium which every day typically alternates between being highly stable and unstable. Meteorologists define that part of the atmosphere which exhibits such behavior to be the boundary layer. It is characterized by mixing "...generated by frictional drag as the Atmosphere moves across the rough and rigid surface of the Earth, and by the 'bubbling-up' of air parcels from the heated surface (Oke, 1978, p. 4)." One property of turbulence is that as it mixes the air, it creates fluxes of physical quantities -- momentum, sensible heat, latent heat, particles, pollutants, etc.. Acousticians are primarily concerned with the flux-dependent vertical profiles of wind, temperature, and humidity for it is they which determine the

shape of the sound speed profile.

Acoustic and electromagnetic waves traveling in such a medium are refracted, absorbed, and scattered. In this thesis we are principally concerned with line-of-sight propagation. The term line-of-sight will mean propagation along paths in which refraction and reflection (at the ground) are the primary propagation mechanisms. The propagation need not be literally line-of-sight, i.e. within visual range, for rays can be refracted into regions behind blocking terrain. Forward scattering by turbulence will not be considered. Experiments now in progress at Penn State indicate that it is not the dominant factor controlling signal behavior over paths of the type considered in this thesis. But at time scales larger than those normally associated with turbulence atmospheric refractive indices are still always changing both spatially and temporally. As a result the amplitude and phase of propagating waves through the atmosphere are also constantly changing.

Many experimenters have studied the amplitude and phase fluctuations of waves propagated over line-of-sight atmospheric paths. The papers listed below are representative of the types of studies and analyses which have been performed. For example, during the period when substantial interest existed in the performance of microwave relay links Janes et al. (1965, 1970) compared the phase and amplitude variations of different radiowave frequencies. Fried's (1969) paper is an example of an optical study in which amplitude scintillations of starlight were investigated. The amplitude and phase spectra reported by Tatarski for optical waves were shown by Clifford and Brown (1970)

to be a good approximation for acoustical waves. Little (1969) discussed specifically the comparison between electromagnetic and acoustical waves.

Few studies on amplitude and phase fluctuations exist in the field of acoustics. Some include Wessels and Velds (1983), Herzog et al (1988), Mandics (1971), and Nesterova et al. (1987). In their study of sound bending over barriers, Wessels and Velds used frequency of occurrence and percentage of time to describe the fluctuations of the acoustical signals. Herzog et al. conducted a computer simulation in which they examined the sound pressure levels for long-range propagation. Mandics included both amplitude and phase variations. Nesterova et al. concentrated on phase variations.

Although the main purpose of Mandics' study was to compare statistical quantities evaluated from an experiment to those derived from theory, his original results provide examples we can use for comparison with the results from RAYPS. Mandics' experiment involved a single source emitting two frequencies within the range from 1 kHz to 4 kHz. At one end of an inclined 67 meter line-of-sight propagation path he set up a receiving array of eight transducers distributed transversely to the path. The amplitude from each array element and the phase difference between each two adjacent array elements were recorded sixty times a second. A single record lasted up to 23 minutes; a new record was taken every hour. Some of the raw data, taken during an "...active time of the day (around noon)..." (Mandics, 1971, p.38), showed fluctuations within a 4 dB range for amplitude and 60° for phase difference. During a less

active time, just before sunset, the fluctuations were slower and diminished in range.

Nesterova, et al. provided another example of acoustic phase fluctuations. Their experiment employed a single source emitting sound at frequencies of 10 and 30 Hz. The phase difference was measured between two in-line sensors -- one placed 20 meters from the source and the other at 420 meters. Measurements were recorded once every minute. The paper illustrated results from the times 2140 to 2251. They claimed that over this period (at a time of an inversion), "...the phase difference changed by approximately 100°...(Nesterova, 1987, p. 158)." Nesterova, et al.'s major claim was that although the wind in the direction of sound propagation might change only slightly, the phase difference could change considerably.

RAYPS can simulate a line-of-sight experiment at any of the eight octave multiple frequencies in the range from 63 to 8000 Hz. The signal phase and amplitude are recorded at targets every 100 meters along the direction of propagation for distances up to 25 kilometers away from the source. Signal fluctuations can be computed along arbitrary source-receiver bearings. Half hour intervals were used as they were sufficient to evaluate diurnal variations, the latter being a problem of particular interest in environmental noise impact studies.

Chapter 2

THEORETICAL CONCEPTS EMPLOYED IN THE REFRACTION MODEL

In the introduction, a brief description of the model was presented. Originally the model was designed simply to create ray traces and, thereby, also to predict sound pressure levels at various locations. As a part of this thesis study the necessary modifications were made to also allow prediction of the signal phase at the same locations. In RAYPS, the path an acoustic ray will follow is determined by the sound speed profile. This profile is strongly dependent upon the meteorological variables of temperature and wind with lesser contributions from moisture. Although horizontal homogeneity has been assumed for the speed of sound profile, the meteorological variables contributing to this profile are allowed to and do vary temporally. It is the temporal variability of the combined atmospheric parameters that controls the temporal changes in the ray traces. An "instantaneous" ray trace can be used to determine an "instantaneous" sound pressure level. Calculation of the sound pressure level involves not only the divergence/convergence of a ray pair, but also the reflection coefficient of the ground, and the path-integrated, frequency dependent, absorption by the atmosphere. In the expanded version of the model the travel time and reflection coefficient are used to evaluate the signal phase. Each aspect of the model's calculations will be explained completely in the following sections.

2.1. SOUND SPEED CALCULATIONS

Outdoor sound propagation in the earth's surface and boundary layers can be treated as an acoustic wave traveling in a fluid medium with a non-zero ambient flow. The speed of sound in a quiescent medium is primarily dependent upon the thermodynamic parameters: density, or temperature and static pressure. For atmospheric propagation vapor pressure must sometimes be considered as well. Wind creates the non-zero ambient flow. Thus, its speed with respect to the direction of propagation must also be included in determining the speed of sound. For typical atmospheric conditions the relative importance of the above parameters has been discussed by Thomson (1987). Using derivatives he shows for a typical, neutral (as defined meteorologically) atmosphere, how changes in the vapor pressure, pressure, temperature and wind with height effect the speed of sound (Thomson, 1987, p. 26). Wind and temperature are shown to be the dominant variables.

The sound speed is proportional to the square root of temperature (in degrees Kelvin).

$$C_T = (20.05)T^{1/2}.$$

The component of the wind in the direction which the sound is traveling (source - receiver line) adds to the speed of sound.

$$C = C_T + u_{comp}$$

$$u_{comp} = |U| \cos (\theta_u - \theta_r)$$

where $|U|$ is the magnitude of the wind speed,

θ_u is the wind direction, and

θ_r is the compass bearing which represents the line drawn from the source to the receiver. Hence, the effective speed of sound is azimuthally dependent.

Both the wind speed and direction, and the temperature normally vary with height, and in turn, so does the sound speed. As sound rays travel through levels of varying sound speed they are continuously refracted upward or downward. In terms of Snell's law, the rays going through horizontally stratified layers of varying indices of refraction will always locally be bent toward the medium with a lower speed. Mathematically Snell's law is represented by the equation

$$\frac{\cos\theta_1}{c_1} = \frac{\cos\theta_2}{c_2} = \ldots \frac{\cos\theta_n}{c_n}.$$

It assumes that the angles are measured from the boundary separating the two media. See Figure 2.1. When not at a turning point, the model calculates the angle of the ray in the new medium by use of the equation: $\theta_2 = \arccos\ (c_2 * \frac{\cos\theta_1}{c_1})$.

In an isothermal atmosphere, wind gradients will completely determine the variation of sound speed with height. Generally wind speeds increase with height. Thus as sound rays propagate downwind they are usually refracted down toward the ground. Upwind the converse occurs. As another limiting case consider the situation in which the atmosphere is calm, i.e there is no wind. Only temperature gradients are then present. During the day in the presence of a large positive thermal lapse rate, temperature decreasing with height, the rays will bend upward. On the other hand, at night, when an inversion is often present, and temperature increases with height (a negative

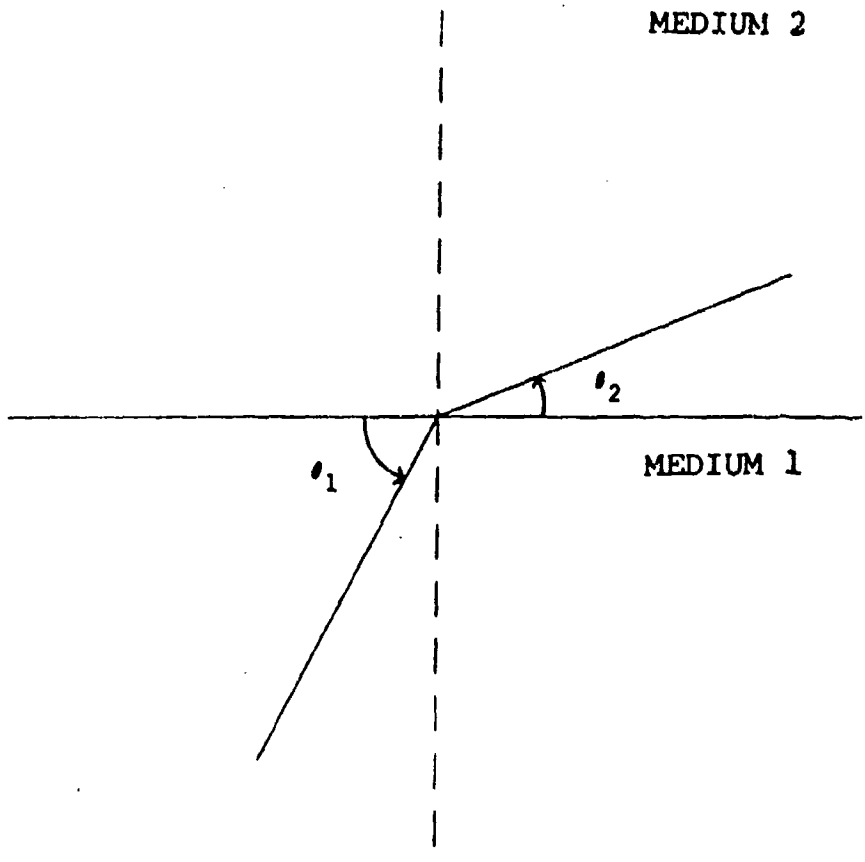

Figure 2.1. The Angles Used in Snell's Law

lapse), the rays will bend downward. Note the meteorological convention that when speaking of temperature the lapse rate is the negative of the temperature gradient. Hence, a positive lapse rate is one in which the temperature decreases with height and negative when the temperature increases.

Normally, both the wind and temperature effects must be considered simultaneously. Thomson (1987, p. 27) shows that for most noise propagation situations the wind speed profile dominates except when winds are light. But at near ranges when gradients in the first one to two meters above the ground are of greatest importance, contributions from both the wind and temperature are often comparable.

All of the meteorological variables important to the sound propagation also fluctuate in time. Thus RAYPS was designed to use multiple sequential sets of meteorological data.

2.2. SOUND PRESSURE LEVEL CALCULATIONS

In RAYPS, transmission, reflection, and absorption are all included in the calculation of the sound pressure level at each target location. Clay and Medwin define transmission loss as "the difference between the source level and the SPL ... (1977, p. 82)." Note that losses due to reflection and absorption are not included in the above definition. It is assumed that changes in SPL are due solely to ray focusing and defocusing. According to Clay and Medwin this focus-related transmission loss can be estimated by using the change in separation of closely spaced rays as they converge or diverge

(1977, p. 91). Assuming that no power can flow across the rays, the power between two rays ($\Delta\Pi$) calculated near the source is the same as that calculated between the same two rays at a horizontal distance r. The power close to the source is calculated by assuming that within a few wavelengths the curvature of the rays is small enough to be negligible. The relevant geometry is shown in Figure 2.2. Thus,

$$\Delta\Pi = \frac{P_o^2}{\rho_o c_o}(2\pi R_o \sin\theta_o) R_o \Delta\theta,$$

where $\rho_o c_o$ is the impedance and P_o is the pressure at the reference radius R_o. At a distance r from the source

$$\Delta\Pi = \frac{2\pi r L P^2}{\rho c},$$

where ρc is the impedance and P is the pressure at r. Clay and Medwin set both power differences equal to one another and solve for P^2.

$$P^2 = \frac{P_o^2 R_o^2 \rho c \sin\theta \Delta\theta_o}{\rho_o c_o r L}.$$

They also suggest that the vertical separation between the two rays h is easier to determine rather than the perpendicular separation L. Therefore, by making the substitution $L = |h*\sin\theta|$

$$P^2 = \frac{P_o^2 R_o^2 \Delta\theta}{rh} \frac{\rho c}{\rho_o c_o} \frac{|\sin\theta_o|}{|\sin\theta|}.$$

Defining the transmission loss in dB to be $TL = -20*\log(P/P_o)$

$$TL = 10*\log\left(\frac{r}{R_o}\right) + 10*\log\left(\frac{h}{R_o \Delta\theta}\right) - 10*\log\left(\frac{\rho c}{\rho_o c_o}\right) - 10*\log\left(\frac{\sin\theta_o}{\sin\theta}\right).$$

The model takes the reference radius to be one meter. Each term in the sum is found individually and then totaled.

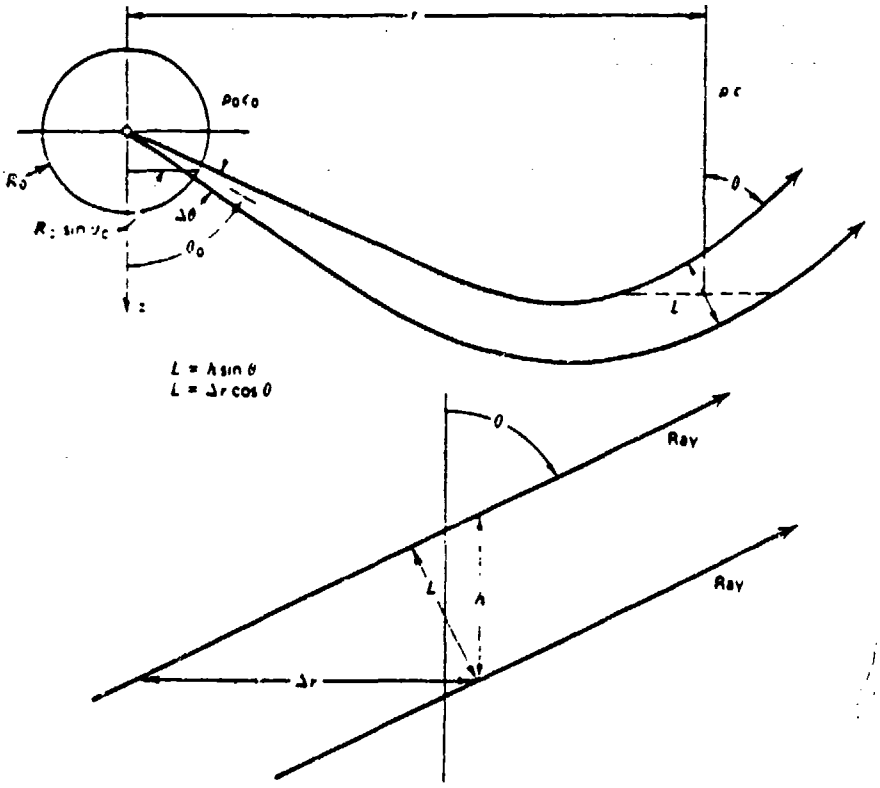

Figure 2.2. The Geometry Used in the Calculation of Power between Two Rays (Reproduced from Clay and Medwin, 1977, p. 92)

Reflection of the sound at the ground also causes a loss in the final SPL. Chessel (1977) expresses the pressure reflection coefficient for a plane sound wave as:

$$R_p = \frac{Z_2 \sin\theta_1 - Z_1 \sin\theta_2}{Z_2 \sin\theta_1 + Z_1 \sin\theta_2}$$

where Z_1 is the characteristic impedance of the air and Z_2 is the characteristic impedance of the ground. θ_1 and θ_2 are the angles of incidence and refraction, respectively. By rearranging this equation and using Snell's law, $\cos\theta_2 = (k_1/k_2)*\cos\theta_1$,

$$R_p = \frac{\sin\theta_1 - Z_1/Z_2(1 - (k_1^2/k_2^2)*\cos^2\theta_1)^{1/2}}{\sin\theta_1 + Z_1/Z_2(1 - (k_1^2/k_2^2)*\cos^2\theta_1)^{1/2}}.$$

k_1 and k_2 are the propagation constants for the two media. Chessel discusses the frequency dependence upon both the ground impedance and propagation constant. Use in the model of Chessel's general equation consists of several substitutions. The characteristic impedance of the air becomes $\rho_o c_o$ measured just above the surface of the ground. Complex values for the impedance of the ground Z_2, and the propagation constant of the ground, k_2, are supplied (Chessel, 1977). Finally, k_1 of the air becomes ω/c_o, where c_o is also defined just above the surface. Both the frequency and speed of sound in air are known prior to the reflection coefficient calculations. These alterations cause the coefficient to be defined as:

$$R_p = \frac{Z_2 \sin\theta_1 - \rho \cdot c \cdot \left(1 - \frac{\cos^2\theta_1}{\frac{c^2k^2}{\omega^2}}\right)^{1/2}}{Z_2 \sin\theta_1 + \rho \cdot c \cdot \left(1 - \frac{\cos^2\theta_1}{\frac{c^2k^2}{\omega^2}}\right)^{1/2}}.$$

The model takes the magnitude of this complex pressure reflection coefficient and converts it into a dB loss (RL).

$$RL = 20*\log(|R_p|).$$

Atmospheric attenuation is the remaining term contributing to the final SPL. ANSI Standard S1.26-1978 explains in detail the mechanism behind the atmospheric absorption. It includes tables that give the absorption coefficient as a function of frequency, temperature, and relative humidity. The tabulated coefficients give the number of decibels attenuated for each one hundred meters of travel. The sound pressure level at a given location depends, of course, upon the losses along the total ray path to that location. The final calculated SPL is, thus, determined by subtracting all three losses -- transmission, reflection and absorption -- from the source level.

2.3. PHASE CALCULATIONS

In a paper by Lahti and Tuominen (1981), multipath summation and multiple boundary reflections are discussed with respect to sound

propagation in the atmosphere. They express the phase of an individual ray as:

$$\phi_i = \omega T_i + \sum_{j=1}^{n} \psi_{ij};\ i = 1,2,3 \ldots m.$$

In this equation m is the number of rays, n is the number of reflections, T_i is the travel time of an individual ray, ω is the frequency of concern and ψ_{ij} is the phase from the complex reflection coefficient for the j^{th} reflection. This model uses the equation to determine the phase of an individual ray. For the model

$$\psi_{ij} = \arctan\ (Im(R_p)/Re(R_p))$$

where R_p is calculated in the same manner as for the sound pressure levels and individually for each bounce for each ray. ωT_i can be verified through the use of units.

$$\frac{Rads}{s} * s = rads,$$

a unit describing phase. Thus, in the above manners, this sound propagation simulation model outputs ray traces, sound pressure levels, and phase.

Chapter 3

DOCUMENTATION OF RAYPS

The various input files for the program, the running of it, and its output files are explained in this section. One feature of the program is the ease with which meteorological data, topography, and the number of projected rays and their angles can be changed. Additional information is requested once the program begins running. This information defines certain parameters for that run such as, times, frequencies, bearings, etc. The program itself consists of many routines working together to predict the characteristics of the propagated sound. The output files facilitate permanent storage and plotting of the results.

3.1. INPUT FILES

3.1.1. METEOROLOGICAL DATA

The meteorological data file containing the temperature, wind and humidity profiles is crucial to all of the following calculations. Each meteorological data file is named after the day it represents. The first two characters designate the month and the next two the date. Usually this file has the extension '.dat.'

Each day contains the above dated profiles at half hour intervals. The temperature is followed by the u and v components of

the wind and, finally, the humidity mixing ratio. Normally each profile is a set of thirty points corresponding to data recorded at one hundred meter height intervals. Temperature is specified in degrees Kelvin, and wind in meters per second. For each half hour, there are also three additional lines of data at the beginning of the set. The first line contains the date. The current half hour is posted in the second line. And finally, the temperature, u and v wind components, and mixing ratio at the height of ten meters is listed on the third. One disadvantage of the half hour interval format is that data only on the hour or half hour can be used. If measurements of different time intervals need to be processed, then a separate mapping to half hour intervals is required. For example, to do so data from 0600, 0605, 0610, and 0615 can be assigned the times (labels) 0600, 0630, 0700, and 0730, respectively, in the meteorological data file.

3.1.2. ABSORPTION COEFFICIENTS

In determining the sound pressure level it is essential, especially at frequencies in excess of about 1 KHz to include the atmospheric absorption coefficient, i.e. the dB loss per one hundred meters traveled. This absorption coefficient is frequency, temperature and relative humidity dependent. A separate program, COEF.FOR, written by William Syrett reads in the temperature and mixing ratio from the meteorological file and produces a table of absorption coefficients. The table is arranged to provide coefficients for each of the eight octave frequencies at each time.

The name of the output from COEF.FOR is assigned to be the first four characters (the date) from the meteorological file plus 'ac.dat.' This output is used as input for the ray tracing model.

3.1.3. TOPOGRAPHY

A topography file containing the height of the ground relative to the height at the source, along each bearing of interest must also be provided. In the present version of the program the height may range from -400.0 m to 3000.0 m. The first column indicates the distance (km) out from the source at which each topographic value is reported. The horizontal resolution is usually set to 500.0 m, the maximum distance being 25 kilometers. The following columns then list the height at the different bearings. The first number in each column is the bearing in degrees, north being zero and east being ninety. Presently there can be up to nine bearings with an azimuthal resolution of twenty degrees. To create a "flat" topography a line in subroutine PROD can set all the elements in the topography array to zero. The topography file may be given any name. This name, however, must correspond to the file opened in the main program as unit 27.

3.1.4. LAUNCH ANGLE DATA

In the first two lines of the input file ANGDAT.DAT some parameters are initialized. The first line contains the source height, and the maximum and minimum heights to trace each ray. The

second line sets the total number of rays to be used by the program. The rest of the input file primarily lists the angles of the rays that leave the source. The user can specify up to 155 pairs of rays to be emitted from the source. A horizontal ray is annotated as zero degrees. The rays that initially are aimed upwards have positive angles and those aimed downwards negative. The rays are listed in pairs differing by a small angle, $\partial\theta$. A suggested value is $\partial\theta$ = .001°. The divergence or convergence of the rays in each pair is used to determine the transmission loss at a horizontal distance (Clay, 1977, p.91).

All these input files allow the program to run for different locations and/or conditions. The topography may be changed or the meteorological data may be altered, either because a different meteorological environment needs to be studied or a different day needs to be run. Depending upon the conditions, different numbers of rays may be needed. For example, on certain days rays launched above ten degrees may always refract upwards and never return to the ground. On other days, fifteen degrees may be the critical angle. The flexibility of the input files caters to the model's use for individual noise impact studies.

3.2. ROUTINES

3.2.1. INTRODUCTION

After all of the necessary input data files have been created, the program may be executed. Any user of RAYPS ought to understand both the attributes and the limitations of the model. The following subsections describe the main program and its subroutines. They document the purpose of and algorithms in each routine. The description basically consists of a written explanation of each routine's flow chart. All of the supplementary flow charts are included in the appendix. For some routines the description also includes the mathematical steps which have been coded.

The primary application of this model is for predicting sound propagation through a temporally varying atmosphere. In the original model both ray traces and sound pressure level (SPL) graphs were created to represent this variability. First the model traces refrangible sound rays at particular times along the specified bearings. Secondly it calculates the sound pressure levels of chosen frequencies at each "target," i.e. normally every 100 meters, for each bearing for each time. Further explanations of these output files are included in section 3.3.

The model performs its calculations through use of the following algorithm. It loops through the desired times and bearings (RAYPS), tracing the rays one pair at a time (CALRAY). Once a pair is traced, the SPLs at each target are calculated for each frequency (SOUNDP).

New values from each pair are then added to running totals kept for each target. The tracing and calculations are repeated for each pair until all are completed.

3.2.2. RAYPS

The main program, RAYPS, performs all the management tasks for the model. It begins by prompting the user with questions that qualify the run. The information requested includes the meteorological file, the times and bearings of interest, the cutoff horizontal distance, the frequencies of interest, and whether or not the ray trace is to be saved to an output file. The meteorological file refers to the file mentioned in section 3.1.1. The user has the choice of individual times, i.e. times he selects himself, or all the times available for that day. If the user decides to select the times, then the model immediately prompts for how many and what times. The times are entered in ascending order in 24 hour clock time. As indicated earlier the model only processes hour or half hour times. However, if all times are chosen then a flag is set to read in all the half hour data sets and the output is also produced as a time series. Later in the series of questions the user is asked for which radial (bearing) and gate (target) the time series is to be kept. The default bearing and target distance are 60° and 2000.0 m, respectively. After the times data, the bearings are set up. It is only necessary to enter the first and last bearings. The model loops through the bearings at twenty degree intervals starting with the

first and ending with the last. It is important that the difference between the first and last bearing be evenly divisible by twenty. Next a horizontal cut off distance (DMAX), in meters, is called for. This is the distance to which the rays will be traced. DMAX can be no larger than 25 km. How many and what frequencies are entered in next. The choice of eight frequencies corresponds to the centers of the major octave bands -- 63, 125, 250, 500, 1000, 2000, 4000, and 8000 Hz. Finally, the user can opt to save or not to save the ray traces to file. All these questions and answers serve to guide the model's calculations.

Once all the initial set up is completed, the model begins to loop through each of the selected half hours. For each of the half hours the subroutine PROD is called with the NMAX flag set to two, allowing the subroutine to read in the meteorological data, i.e. the variables TEMP, U, V, and QM, and to set them up as profiles. Further explanation of this subroutine will be found in section 3.2.3. After the profiles are set up, absorption coefficients are then read in from the "*AC.DAT" file. For each selected frequency for the current half hour an output file to store the sound pressure levels is created.

The program now begins a loop through each bearing. If the ray traces are to be saved, then an output file for the current bearing and half hour is created. Further explanation of both these output files exists in section 3.3. Next, the main program calls a series of subroutines -- PROD, DATIN, SPDATA, and CALRAY. PROD, now with NMAX set to one, serves mainly to read in the topographical data. DATIN calculates the speed of sound profile from the wind and temperature

data. SPDATA calls a subroutine that cubically splines the data. Cubic splines are performed on the speed of sound as it depends upon temperature (C) only, the temperature (TEMP), the wind along the current bearing direction (U), and the speed of sound due to both temperature and wind (CPU). The last subroutine CALRAY performs the ray tracing for all the rays. It also calls the subroutine that calculates the SPL's. Creating the ray trace file and calling the series of subroutines is repeated for each bearing. After all the bearings are completed the whole process begins again for the next half hour. Once all the specified half hours are completed the main program, and hence a particular run, is finished.

3.2.3. PROD

As mentioned above, the subroutine PROD performs two functions depending upon how the flag NMAX is set. The first function establishes the wind, temperature and mixing ratio profiles. The second task establishes the topography for the current bearing. It also defines the vertical structure of the profiles. Details of the vertical structure will be described later.

The PROD subroutine directs itself towards the first task if NMAX is greater than one, i.e. two. It begins by calling the subroutine READDAT, a subroutine that reads in all the data from a half hour set from the meteorological data file. Next it calculates the gradient from 100.0 meters to ten meters of the temperature profile (TGRAD). TGRAD is used in the following subroutine call to

SURF. SURF calculates the wind components and the temperatures at 0.0 m and -400.0 m. The PROD subprogram combines both these special values and the 100 m interval values read in by READDAT into the profile arrays. The final task of this first function is to change the u and v components at each level in the profile into the wind speed and direction by calling the subroutine WSWD.

If NMAX = 1 then PROD directs itself towards the second objective, mainly preparing the topographic array and defining the vertical structure. This section of the subprogram begins by reading in the topography for all bearings into an array called DAVIS. The number of bearings is limited to nine. The DAVIS array is two dimensional, the first dimension representing a horizontal location and the second representing a bearing. If the second index equals one, however, it represents the horizontal structure instead of the first bearing. The horizontal structure is built out of 0.5 kilometer intervals. PROD copies this structure into its own array X and converts the data from kilometers to meters. Next, the subroutine copies the part of DAVIS that represents the current bearing's topography into the array TOP. Afterwards the vertical structure is set up. This structure, the array Z, lists the elevations of interest. The first three are special. They are heights at -400.0, 0.0, and 10.0 meters. The rest of the array includes vertical heights at every hundred meters, starting at 100.0 and ending at 3000.0 meters. The main purpose of PROD is to establish the profiles whether it be the vertical profile of meteorological data or the horizontal profile of topographical data. It manages the data so that it can be

easily accessed by other subroutines.

3.2.4. READDAT

READDAT is a simple program that reads in data from the meteorological file. First it reads in the hour and the minutes of the current data set. Next it reads in the temperature, the u and v wind components, and the mixing ratio values at ten meters. It then reads in the temperature at one hundred meter intervals, followed likewise by the u and v components. Finally the mixing ratio at every one hundred meters is read. Only one half hour data set is read in each time READDAT is called. Whether or not this half hour is to be used is determined in RAYPS.

3.2.5. SURF

The purpose of subroutine SURF is to calculate the wind components and the temperature at the "surface," corresponding to zero meters elevation, and at the "bottom," -400.0 m elevation. Since the topography is normalized so that the elevation at the source is zero meters, the use of negative topographical elevations is possible. The model currently limits the absolute bottom to -400.0 meters. Given the data at 10.0 and 100.0 m the values at 0.0 and -400.0 m are linearly extrapolated. The wind components, however, at the "bottom" are special in that they are forced to have a zero value in order to conform to the assumption of no slip at the ground (Panofsky, 1984 p.

120). SURF begins the extension of the temperature and wind profiles to heights below ten meters.

3.2.6. WSWD

As mentioned above, the function of WSWD is to convert the u and v components at each height into a wind speed (WS) and a wind direction (WD) at each height. Since U and V are vector components the direction and magnitude of the wind can be found trigonometrically,

$$WS = \sqrt{u^2+v^2}$$

and WD depends upon the arctan ($\frac{u}{v}$). The result from the IBM's Fortran function datan (double precision arctan) is changed into degrees and then mapped onto a coordinate system which has been rotated by ninety degrees. WSWD performs this mapping task through a lengthy if-else statement. Having the wind described as a direction and magnitude makes it easier to calculate its contribution to the speed of sound along the source-receiver compass bearing.

3.2.7. DATIN

DATIN is the subroutine that calculates the speed of sound from the meteorological profiles. The calculations in this subroutine follow the relations discussed in section 2.1. First it determines the sound velocity profile (C) from the temperature profile. Next the component of the wind along the direction of the current bearing (U)

is computed at the different heights. Finally the two numbers C and U are added together for the total sound velocity (CPU). An option of keeping the total sound velocity constant as a function of height is also incorporated into the program. Commenting out the line cpu (j) = c (j) + u (j) and adding in the line cpu (j) = 339.0d0 will accomplish this task. Upon completion of the subroutine DATIN a sound velocity profile is created.

3.2.8. SPDATA

The next subroutine, SPDATA, completes the extension of all the profiles into the negative elevations. The function of this subroutine is to spline the data so that values between -400.0 meters and 0.0 meters can be inferred. The actual splining is conducted by the subroutine SPLINE. SPDATA sets up parameters so that SPLINE can be called.

The first task involved in SPDATA is to define the number of points to be splined in the vertical direction. Next, the lower and upper limits for the splining processes are defined -- -400.0 and 3000.0 meters. The size of the interval can then be calculated directly; the difference between the limits is divided by the number of points to be splined. Finally SPLINE is called separately for C, TEMP, U, and CPU. Upon completion of this subroutine the profiles are ready to be used.

3.2.9. SPLINE

The SPLINE subroutine performs a cubic spline interpolation on a set of data. Basically data from a specified number of points are transformed into data for a different specified number of points. For the profiles this results in the addition of points at -300.0, -200.0, and -100.0 meters. This subroutine is the last used to generate the required sound speed profiles.

3.2.10. CALRAY

The critical calculations in the model, RAYPS, are performed in subroutine CALRAY. CALRAY traces all of the rays and calls SOUNDP, the subroutine that computes the SPLs. It uses Snell's law to predict the trajectories of the rays through the atmosphere. The sound velocity profile for the current time and the topography for the current bearing are singled out for use in this subroutine. The tracing is a matter of continually finding the new vertical and horizontal position of each ray, checking the boundary conditions each time. These boundary conditions include the top of the atmospheric boundary layer, the ground's complex topography, and the maximum horizontal distance. CALRAY also keeps track of which rays hit which targets. This information is necessary for SOUNDP.

CALRAY begins with reading in the angles (in degrees) of all the rays, i.e. both rays of all the pairs. This information is found in the file ANGDAT.DAT. The difference between the two rays of each pair

is calculated and converted into radians. This difference is the same for each pair. It is used later in determining the sound pressure level of each propagated ray pair. Next, each ray angle is converted into radians. The necessity for using radians is dictated by the intrinsic trigonometric Fortran functions.

The next section initializes the variable RCPUNOT also to be used in SOUNDP. RCPUNOT, $\rho_o c_o$, is the density of air at the height of the source times the speed of sound at the same height. A subroutine, ZINT, is used to get the temperature and sound velocity at the current height, in this case the source height. With the temperature ρ_o can be found.

$$\text{RHNOT} = \rho_o = 0.34838 * (\frac{825.0}{\text{TZHT}})$$

and consequently,

$$\text{RCPUNOT} = \rho_o c_o = \text{RHNOT} * \text{CPUSHT}.$$

Upon completing the above calculations CALRAY is ready to begin ray tracing. If the ray trace is to be saved, the routine first transfers the topography to the ray tracing file. The routine starts to loop through the pairs of rays. For each ray pair an initializing process is performed. This means the beginning position of the ray is set to 0.0 meters in the horizontal direction and to the source height in the vertical. The topographic elevation (BOTZ) is set to zero. The up/down direction of the ray is set according to the following convention: rays propagating in the positive z direction receive a positive sign and conversely for the negative propagating rays. Also MYFLAG is set to either zero or one. The length of a differential arc (SL) is defined to be 30.0 meters. The last initialization is to

determine the variable SNEL. This variable is related to Snell's law; it is $\frac{\cos \theta}{c_i}$. SNEL is used to find the cosine of the transmitted angle into the next height:

$$\cos \theta_t = \text{SNEL} * c_t.$$

After initializing, CALRAY loops through 6000 differential arcs. Each arc is sufficiently small to be considered a straight line and is angled at θ_t. For each arc the x position (RAYX), the z position (RAYZ), the total path length (PATHLN), and the total travel time (TRAV) are calculated.

Each time these variables are revised for a new arc the boundaries are checked. If the ray reached either the top of the boundary layer or DMAX in the x direction, the subroutine then starts with the next ray. If it is still within those boundaries then the program checks to see if the ray has reached a vertex. Reaching a vertex means the ray will be heading in the opposite vertical direction for the successive arc calculations. The current angle is multiplied by negative one giving it the opposite direction. The next verification is whether or not the ray has hit or "passed" through the ground. If so and the ray is the first of the pair then the number of bounces (NBOU) is increased. A new x, z, path length, and travel time is recalculated for exactly where the ray hit the ground. Next a check is made as to whether or not the ray has passed the next target. If this has happened then the number of targets is increased. The variable for the number of targets for the first ray of the pair is NTARG1. For the second the variable is NTARG2. New values for the usual variables are then found at the target location. Additional

variables are recorded for later use in SOUNDP. They are ρc (RCPU), c_{air} (CAIR), and ρc_{air} (RCAIR) where c is the sound velocity due to temperature and wind at the height of the ray over the target, and c_{air} is the sound velocity due to only temperature of the air at the same height. Finally the position for the next target is increased by 100.0 meters.

After adjusting the variables for each special condition the program gets ready to begin the next arc. It uses the new information to redefine the incident angle and SNEL which are determined differently depending upon whether or not the ray had bounced. If the ray is at a vertex the new angle was previously determined. Thus, depending upon the previous boundary conditions the new calculations take place in different parts of the program.

The final task for one arc is to save the x and z positions but if and only if it has been specified that the ray traces are to be saved. The program now continues with the next arc, getting its new position, path length, and travel time just as explained above. This process is continued for 6000 arcs. Experience has established that 6000 arcs are usually enough to carry the ray either to its vertical or horizontal limit. This number can be changed but doing so requires recompilation of the program.

Upon completing the arcs for one ray, the next ray of the pair is traced. Upon completion of the pair enough information is available to call SOUNDP. Next a new ray pair is traced and sent to SOUNDP. When all the rays are finished then so is the subroutine CALRAY.

3.2.11. ZINT

ZINT has the simple purpose of finding the sound velocity due to temperature and wind (CPUSHT), the sound velocity due to temperature alone (CHT), and the temperature (TZHT) at a given height (ZHT). It uses the previously mentioned splined profiles. Basically, the subroutine finds the interval into which ZHT falls and then linearly interpolates for each profile.

3.2.12. SOUNDP

SOUNDP is the other subroutine besides CALRAY that performs the majority of the calculations and creates output files. SOUNDP determines the total sound pressure level at each target one ray at a time. It takes into account atmospheric absorption, ground reflection and transmission loss. These effects were discussed theoretically and mathematically in section 2.2.

SOUNDP begins by initializing parameters and variables. The frequencies are converted from Hertz to angular frequency. All pertinent information previously calculated in CALRAY is read in for each target and for each ray of the current pair. This information includes the height of the ray above the ground at the target, the path length to the target, the angle of the ray as it hits the target, ρc, and c_{air}. Next, information pertaining to the bounces for each ray is read in. This includes the x position and the angle of the ray at each reflection. Reflections were recorded only for the first ray

of each pair. This is because the paired information is only important for determining the transmission loss and not the reflection coefficient.

Additional initializations are performed for those variables that need only to be initialized the first time in SOUNDP. The variable XTARKM, the position of each of the targets is normally defined to be every 0.1 kilometers. The variables SPSUM and SPDSUM, the running totals of the SPLs from all rays at each target for each frequency is set to zero. In the successive calls to SOUNDP these tasks are skipped over.

After all this preliminary set up, the subroutine begins the following calculations using data from the first ray of the pair. The only exception is when the divergence of the two rays needs to be determined. The subroutine loops through all the chosen frequencies. And for each frequency it loops through the number of targets for the current ray pair. At each target the ray's height above the ground is measured. A ray falling within five meters is considered a hit. If the ray height is greater then five meters then the program continues to the next target.

Upon successfully reaching the target, calculations of the losses are started. First attenuation due to atmospheric absorption is computed (ATMOS). Since the absorption coefficient is in units of db/100.0 meters the path length of the ray to the target is divided by one hundred. This number is then multiplied by the coefficient for the current frequency.

The second loss is due to the sound ray reflecting off the ground. For each bounce up to the current target the loss due to the reflection coefficient is calculated, converted into dB, and summed (TREFCL).

The final loss is due to sound transmission in a refractive atmosphere. The basis for this attenuation was discussed in section 2.2. This loss in dB can be separated into four parts -- TM, TM1, TM2, and TM3.

$TM = -10 * \log \left(\frac{\rho c}{\rho_o c_o}\right)$.

TM1 = 10 * log (XTAR), where XTAR is the horizontal distance to the target.

$TM2 = -10 * \log \left(\frac{\text{Sin}\ \theta_o}{\text{Sin}\ \gamma}\right)$, where θ_o is the original launch angle and γ is the complement of the ray's angle at the target.

$TM3 = -10 * \log \left(\frac{\partial\theta}{ZL}\right)$, where $\partial\theta$ is the original angle separation between the two rays of a pair and ZL is the vertical separation between the two rays at the time they reach a target. The four parts are summed into the variable TSRED. These three losses due to the atmosphere, reflection, and transmission are necessary in determining the SPL at a particular target for the current ray pair.

Next the actual sound pressure level is calculated in dB at the target. Given the SPL at one meter from the source to be 100.0 dB then the SPL at the target for this ray becomes 100.0 - TOTLOSS. TOTLOSS is the sum of the three losses. This value (SPTAR) is also

converted into sound power (SPTARL) in order to sum up all the rays coming into this target (SPSUM). A variable representing the value of loss in dB due to the reflections and atmosphere only (SPLDIF) is also calculated. Similarly SPLDIF is converted into power (SPLDIFL). This value, as well, is kept as a running total (SPDSUM). All these variables are frequency dependent. In general, the subroutine computes a single SPL value for the current ray pair and adds this to a total value at each target for each frequency.

Upon calling SOUNDP for the last ray pair, it also converts each one of the power sums back into decibels. In order to accomplish this task, loops of frequencies and targets are set up. If the power is less than zero then the sound pressure level is set to zero; otherwise

SPSUML = 10 * log (SPSUM).

The same is done for SPDSUML. After the calculation is made the target, bearing, SPSUML, and SPDSUML are written out to a file specified by frequency and time. Also output in the form of a time series is created. Either a time series of the SPLs at the previously specified target and bearing (See section 3.2.2) or a time series at all the targets and all the bearings is written out into the file FORT59. This task is the last in the subroutine SOUNDP.

3.2.13. SUMMARY OF THE PROGRAM

The previous eleven sections described the subroutines and main program, as they were combined to form the original sound propagation prediction model. Each subroutine performs its own task or tasks to

help achieve the final results. Let us here recapitulate the most important components. The first is: sound pressure levels are parameterized by time, bearing, frequency, target, and ray pair. Ray traces are parameterized by all of those except frequency and targets. A second important point is that several subroutines are dedicated to the making of the different profiles. PROD, READDAT, SURF, WSWD, DATIN, SPDATA, and SPLINE are the subroutines used for the construction of workable temperature, wind along the propagation bearing direction, speed of sound due to temperature alone, and speed of sound due to the combined temperature and wind profiles. The subprogram ZINT determines from the profiles the value of the variables representing temperature and both speeds of sound at a given height. Finally CALRAY and SOUNDP produce the ray traces and SPL graphs, respectively. Together all these subroutines are managed from the main program RAYPS. Each of the above parts is an integral and essential part to the propagation model.

3.3. OUTPUT FILES

3.3.1. INTRODUCTION

The output files are created as permanent storage for the results from each run of the model. These files facilitate convenient presentation of the results and transformation of them into various graphical formats. The first version of the model produces two types of output files -- ray traces and SPLs. Time series of the sound

pressure levels, can also be produced; however, they consist simply of the SPLs being presented in an alternate format. Details of the output files include contents, nomenclature, location of production, format, graphical representation, and interpretation. All graphs are produced by programs written for a VAX 8200.

3.3.2. RAY TRACES

The ray traces are all the paths taken by the rays through the refracting atmosphere. A single file contains all the rays for one time and one bearing. The naming convention is the first four letters of the meteorological data file concatenated with an 'RT' for ray trace. Attached to this is the bearing. Only the first two numbers are necessary and sufficient. The time is annotated in the extension of the file name. The hour followed by a '0' for an on hour data set or by a '3' for a half hour data set. In other words, only the first three numbers of the time are necessary and sufficient. For example, JL17RT09.120 stands for a ray trace produced from data for 1200 on 17 July along the 90° bearing. And AU29RT19.043 is a ray trace for 0430 on 29 August along the 190° bearing. The creation of this file takes place in the main program RAYPS each time a new bearing is started.

Even though the file is opened in RAYPS, entering the results occurs in CALRAYP. The file contains two columns. The first column represents the horizontal position, the second the vertical. Both are in meters. The first fifty points are the topography. The traces for each ray are listed one right after another. Figure 3.1 shows part of

0.000	0.000
500.000	0.000
1000.000	12.190
1500.000	12.190
2000.000	24.380
.	
.	
.	
24500.000	512.070
25000.000	560.840
0.000	2.000
29.835	7.724
59.707	13.305
89.617	18.741
119.565	24.034
149.549	29.182
179.572	34.186
209.632	39.045
239.730	43.760
269.865	48.329
300.040	52.753
330.253	57.032
360.505	61.165
390.798	65.153
421.131	68.994
451.507	72.690
481.926	76.239
512.391	79.641
542.902	82.897
573.463	86.006
604.076	88.967
634.745	91.781
665.474	94.447
696.268	96.965
0.000	2.000
30.394	5.656
60.833	9.164
91.319	12.524
121.853	15.735
152.439	18.797
183.079	21.711
213.777	24.475

ETC.

Figure 3.1. Part of a Sample Ray Trace Output File

a ray trace output file. The final results for one file are two long columns representing the horizontal and vertical positions.

Each line of the file being the x and y coordinate of a single point, a ray trace can be formed by connecting these points with straight lines. Both the topography and rays are handled in this fashion. For the rays, however, the points are so close together that the connecting lines are not noticeable. Consequently, the consecutive points form curved paths. Figure 3.2 is an example of the graphical representation. On this graph the x-axis represents the distance away from the source in kilometers, ending at 25.0. The y-axis represents height in meters, ending at 3000.0. Located above the x-axis is information about the ray traces. The date is displayed on the left, the local time in the center, and the bearing on the right.

Individual ray traces are used to visualize two concepts. First of all, on any given ray trace, i.e. the results at a particular time, the refractive state of the atmosphere is displayed. The picture gives the sense of curvature of the rays both in magnitude and direction. Depending on the profile and the launch angle of the rays, the rays may be refracted in a general upward or downward direction. The graph also clearly indicates the presence of a critical angle. The critical angle is the launch angle at which all rays with angles less than this one are eventually refracted towards the ground. All greater angles are refracted towards and lost to the upper atmosphere. Figure 3.3 shows the case where there is no critical angle and Figure 3.4 shows the case where the critical angle is 8°. In both figures

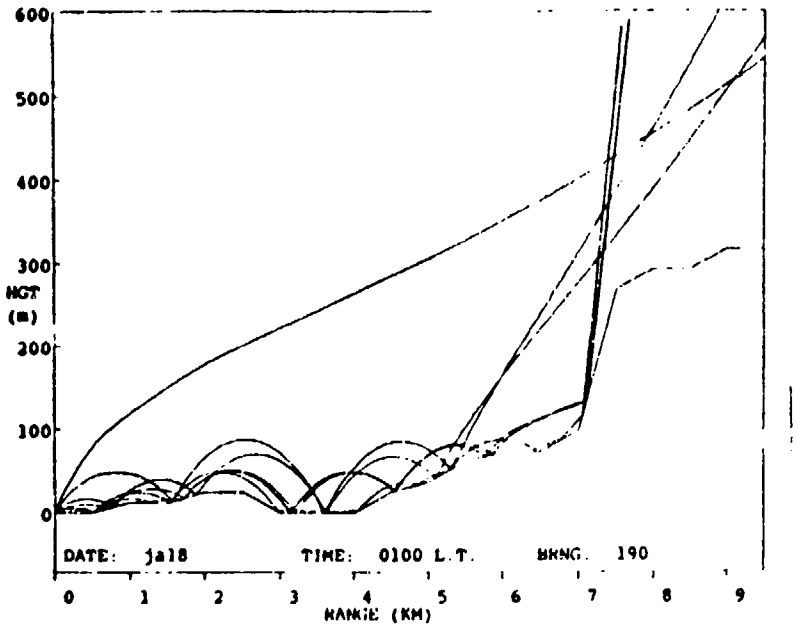

Figure 3.2. A Sample Ray Trace

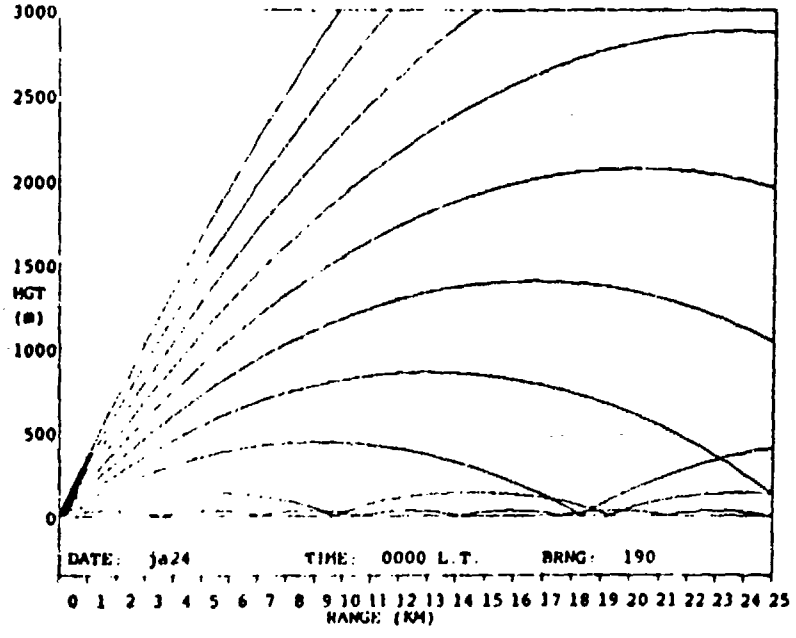

Figure 3.3. A Ray Trace with No Critical Angle

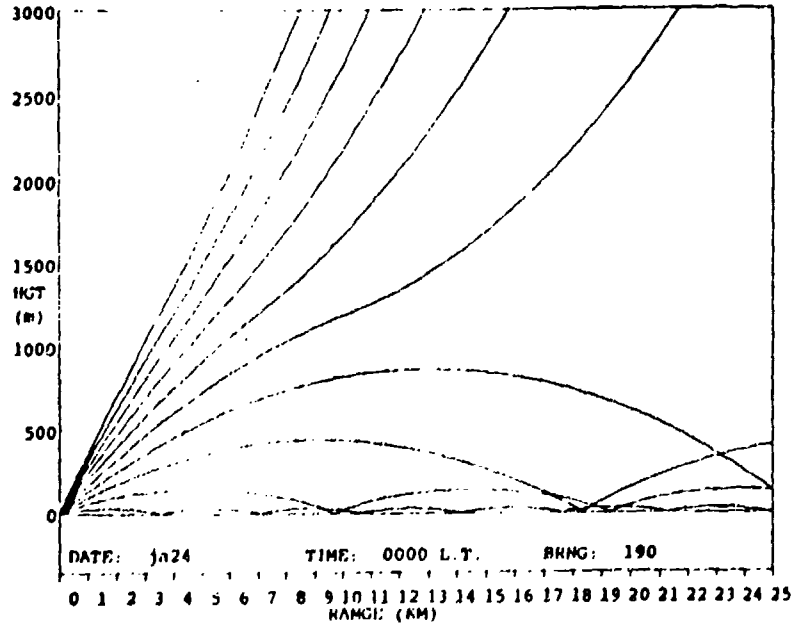

Figure 3.4. A Ray Trace with a Critical Angle at +8°

there are ten angles launched, each separated by two degrees. Besides the critical angle, a sound speed profile with a variable gradient, i.e. a gradient that changes with height, may also be detected. The changes in curvature of the rays are the key to observing this situation. A good example is seen in Figure 3.5. For comparison see Figures 3.6 and 3.7. They are ray traces with constant gradient and constant speed profiles, respectively. The profile of constant gradient gives rays that bend with the same curvature at all heights. With a constant speed profile curvature is absent and thus the rays are straight.

The graphical representation also gives an easy qualitative accounting of the rays. Both where along the horizontal the rays reflect off the ground and how many rays reflect can easily be seen on the graph. Each ray trace also represents a snapshot in time, and thus, supplies a quick sense of potentially important locations along a given bearing.

A set of ray traces may be used to visualize the change of the speed of sound profile with time. A developing inversion of the velocity profile can be seen when more rays are refracted downward with each new ray trace. Breakup of an inversion is evident when fewer and fewer rays are refracted down at each new time. In general, the ray traces are useful for quick qualitative interpretation of the effects of the atmosphere on sound propagation.

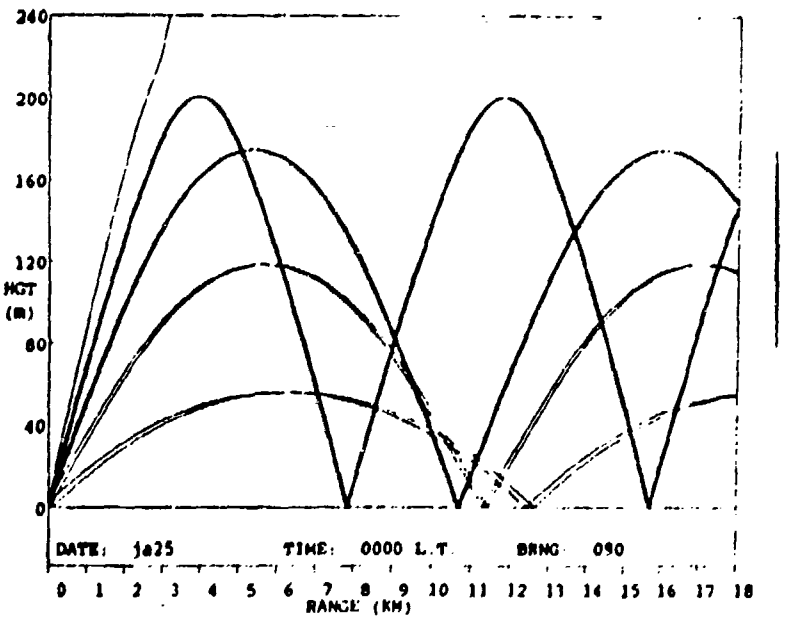

Figure 3.5. A Ray Trace from a Hypothetical Variable Gradient Speed of Sound Profile

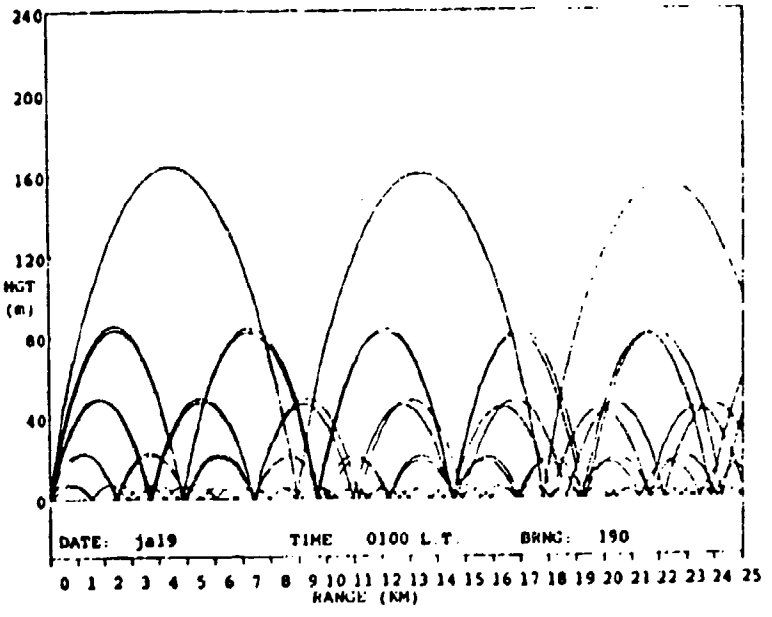

Figure 3.6. A Ray Trace from a Hypothetical Constant Gradient Speed of Sound Profile

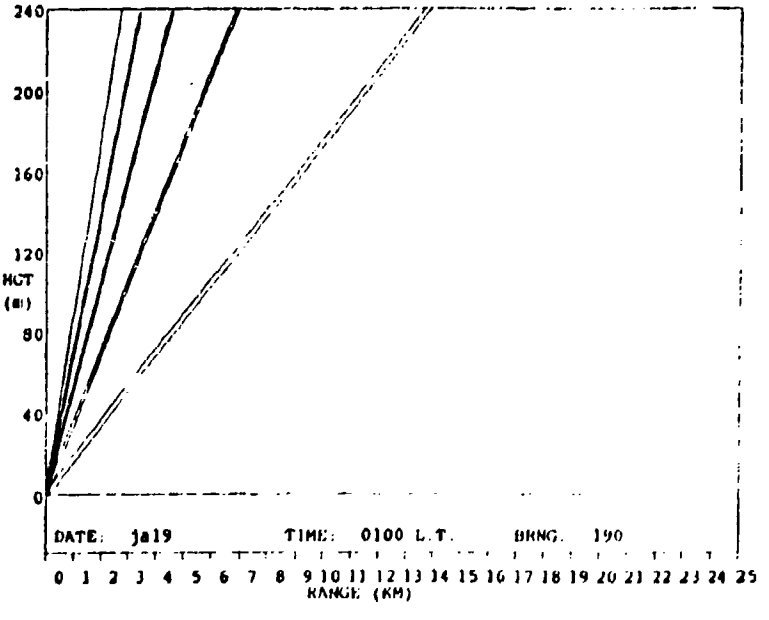

Figure 3.7. A Ray Trace from a Hypothetical Constant Speed of Sound Profile

3.3.3. SOUND PRESSURE LEVELS

While the ray traces show to where the individual rays travel, the sound pressure level output files store the predicted sound pressure levels at each time and location. At each target the sound pressure level from each ray coming into the target has been summed. In determining the SPL of one ray the losses due to atmospheric absorption, ground reflections, and refractive transportation have all been included. Since atmospheric absorption and ground reflection are frequency dependent, each output file contains the results for a particular frequency. The results from the different bearings are concatenated into one file. These files store both the calculated SPL and the value of the losses due to only the absorption and reflections.

The file naming convention was designed to take into account both the frequency and time dependence. Once again the first four letters are borrowed from the meteorological data file. The next character is "F", indicating the file's dependency upon frequency. The number that then follows is representative of the actual frequency associated with the data inside. Numbers 1 - 8 are assigned the frequencies 63, 125, 250, 500, 1000, 2000, 4000, 8000 Hz, respectively. As in the ray trace file, the extension denotes the time. An example name for an SPL file is JL17F2.033. The results, using the 0330 local time data set and a frequency of 125 Hz, from all the bearings are stored in this single file.

The SPL output files are created in RAYPS. Each time a new half hour is started all the files for the different frequencies are created. The SOUNDP subroutine enters the data into the necessary files.

The format of one of these files is as follows. There are four columns of data. The length of each column depends upon how many bearings are reported. The first column represents the horizontal position in kilometers of each and every target. It lists numbers from 0.1 to 25.0 incremented by 0.1. These numbers repeat for each new bearing. The second column represents the bearing. The third column contains the resultant SPL for each target. The forth column contains the data representing the total atmospheric and reflection losses in dB for each target. See Figure 3.8 for an example. The format of the sound pressure level output files is easy to follow.

The SPL data can also be expressed in a graphical form. Figure 3.9 is an example. On a single graph all eight frequencies are represented for a given bearing and time. The bearing is displayed on the right, the local time in the center, and the date on the left just above the x-axis. The frequency labels are just above each line graph on the right-hand side. A single line graph represents sound pressure level versus distance. Data exists for each discrete target. A line connecting all the target points forms the graph.

On the left-hand edge there is a scale for estimating the SPLs in dB. The range of the scale is from -80.0 dB to +80.0 dB. No alterations are made for values above +80.0 dB. They just appear above the top tic mark. Values less than -80.0 dB are forced to -80.0

0.10000	190.00000	62.06027	9.00257
0.20000	190.00000	50.85740	4.07942
0.30000	190.00000	43.84297	4.35943
0.40000	190.00000	46.76294	6.23722
0.50000	190.00000	40.69180	6.51729
0.60000	190.00000	32.92811	12.63926

ETC.

Figure 3.8. Part of a Sample Sound Pressure Level Output File

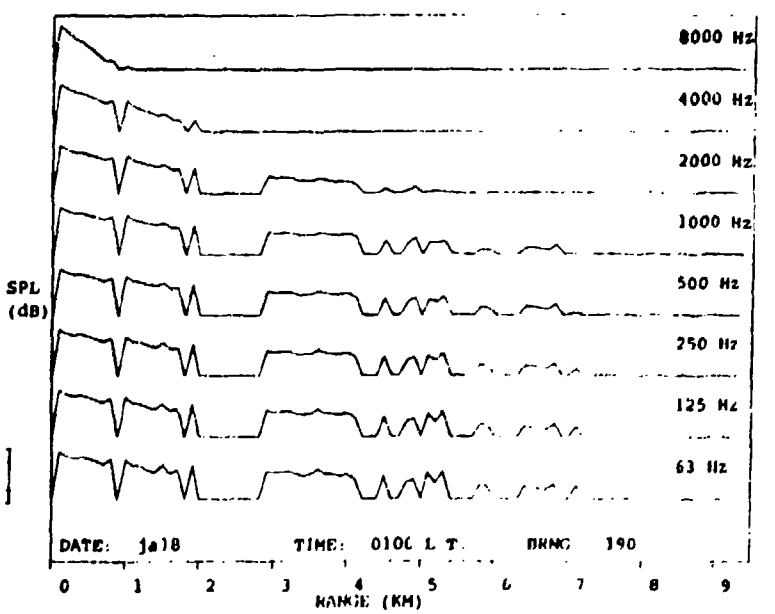

Figure 3.9. A Sample Sound Pressure Level Diagram

dB. Thus no data points will appear below the bottom tic mark. Targets in shadow zones for which values are nonexistent, but are recorded as zero decibels in the SPL output files, are also forced to -80.0 dB. In Figure 3.10 contrived data to aid in understanding the scale is presented. The values in order are: 80.0, 100.0, 67.0, 0.0, -67.0, and -80.0 dB.

An artifact of the graphing routine needs to be explained. The first data point is at 0.1 km and not at 0.0 km. The graphing routine sets the value at 0.0 km to either zero or the value found at 0.1 km. It is important to note that the value at 0.0 km is not the SPL at the source.

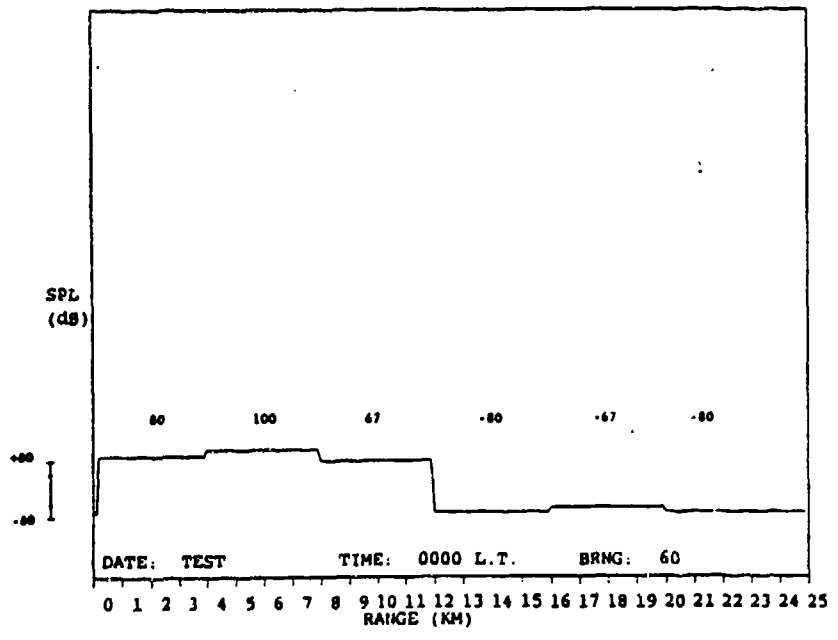

Figure 3.10. A Sample SPL Diagram to Demonstrate the Scaling

As with the ray traces, these graphs can be used to show both shadow zones and regions of enhanced sound. Not only do the SPLs show where the sound returns to the ground but also the magnitude of the sound at each of these targets. Another aspect of the propagation which is easily visualized in the SPLs is the dependence upon frequency. In Figure 3.9 the decrease in magnitude with an increase of frequency can be seen. This dependency is mostly due to the higher frequencies having greater atmospheric attenuation. Also just like the ray traces, a set of SPLs can be used to see the temporal variation. They will show as the day or night progresses the changing location and/or magnitude of the zones with sound levels.

3.3.4. TIME SERIES

Except for the different format the time series provide the same information as the sound pressure level output files. The SPLs of a specified target along a specified bearing are stored as time series for all of the frequencies. The name of the file is the date concatenated with "TS," time series. The extension is "PRN." For example, JLO3TS.PRN is the time series for 3 July. Opening of the file is done in RAYPS; entering its data occurs in SOUNDP each time the processing of a new half hour data set is completed.

The data is presented in the following format. See Figure 3.11. The bearing is acknowledged on the first line. A list of the frequencies appear on the second line. Following this heading are columns of data. The first column lists the times. The other columns

```
190.0
                500.00          4000.00
   0          0.00000          0.00000
  30          0.00000          0.00000
 100         39.97021         11.80949
 130         25.71843          0.99082
```

Figure 3.11. Part of a Sample Time Series Output File with the Gate and Bearing User Specified

are the SPLs of the specified target for the respective frequencies and times.

In this thesis study no attempt was made to design a graphical representation for the time series. A plausible graph might be similar to the SPL diagrams. A line graph would be used. However, instead of the SPL versus distance at a certain time it might be the SPL versus time at a certain target. All eight frequencies could be displayed on one graph. Such a representation would allow for visualization of the variability with time of the sound pressure

level.

3.4. SUMMARY OF THE MODEL

The ray traces and SPL output files produced by this model are simulations of the results of sound propagation through a refracting atmosphere which also varies temporally. The ray traces represent the predicted paths the sound will take through the refractive medium. The traces provide quick insight into the location of sound and shadow zones on the ground. The SPLs represent the sound's magnitude in each of these zones. A single ray trace or SPL shows the results at a given time; a set of results may be used to simulate the temporal variability of the propagation.

For any prediction model it is instructive to be able to apply it to as many different environmental situations as possible. The input files for RAYPS facilitate its application in this manner. Once assembled they contain data necessary to run the program. A single meteorological data file allows for processing many profiles for a given day. By assembling different meteorological files, many different days can be processed for the same location. For example, how does the sound propagation on one day with one type or evolution of atmospheric conditions compare to that of another? The input file for topography allows for "actual" land contours to be incorporated into the model. One single file provides access to different directions (bearings), while other files provide access to different locations. Each location requires its own topographic data file. One

disadvantage of the present version of RAYPS is that the name of the topography file is hard coded into the program. Sometimes it would be helpful if the user was prompted for the topography file. The final input file, the angles file, includes the answers to some "what if" questions. What if the top of the boundary layer has changed? What if the source is placed at a new height? And what if more or fewer angles were processed? All of these questions can be satisfied by changing a number or numbers in the ANGDAT.DAT file.

Thus, RAYPS in its entirety calculates the paths of sound and the sound level at different locations away from the source for different times. It takes into account actual meteorological parameters (temperature, wind, and relative humidity), actual ground conditions (topography and the reflection coefficient), and atmospheric sound absorption.

Chapter 4

DOCUMENTATION OF THE MODIFICATIONS

In its original form the ray tracing model was coded only for calculations of ray trajectories and computations of sound pressure level. For this thesis study the model was modified to also include calculations of the phase for each ray. Although it was not necessary for the phase calculations to make modifications to the format of the input files, alterations were required to two subroutines. Also a new subroutine, PHASE, was created to perform the calculations. Finally, to store the results three additional output files were created.

4.1. ROUTINES

4.1.1. RAYPS

Recall that RAYPS is the "manager" of the propagation model. In order to keep the run time as short as possible it was first necessary to reduce the size of the overall program. Efficiency was achieved by reducing the dimensions of certain arrays. Instead of looping through multiple frequencies, the user chooses a single frequency for each run. This eliminates one of the questions that organize a particular run. However, in order to organize the phase calculations several new questions had to be asked in RAYPS. First, the number and location of targets requiring the phase information is asked. If zero is entered

for the number of targets then phase is not recorded at any target. If negative one is entered then all targets are considered. In this case no specific targets need to be typed in by the user. There can be up to 249 targets. When there is a need to input specific targets the user must type in leading zeros because each target is read in as a character string of length three. For example, the second target is '002,' the twenty-nineth is '029,' and the two hundred and forty-nineth is '249.' The second additional question is, simply, whether or not the output file PDIS is to be saved. This file contains the same information as the PTIM file, except that it is in a different format. The former records the phase information as a function of distance at a particular time. The latter records the same information as a function of time at a particular target. PTIM is automatically saved. Choosing not to save PDIS will reduce both the run time and the required storage space. The purpose of these modifications has been to help define the parameters pertinent to a given run of the program.

All three output files -- PTIM, PDIS, and PCOM -- are written in the subroutine PHASE to a direct access file. It is also RAYPS' task to rewrite each file into a sequential file so that it is readable by the user. This is performed after all else is completed. If PDIS was not saved then only PTIM and PCOM are rewritten. Thus, rewriting and asking new questions were the modifications made to RAYPS.

4.1.2. CALRAY

Besides performing the ray tracing, CALRAY also has the function to call SOUNDP every time a new ray pair is completed. The new version of CALRAY calls PHASE immediately after the call to SOUNDP.

Other necessary procedures are also performed in CALRAY in preparation for this new subroutine. Instead of recording the travel time as a non-dimensional variable (TRAVT) it now is transferred into an array (TRVT) dimensioned by ray pair and target. Another addition to CALRAY is that for each ray pair the maximum number of targets between the two rays is saved. The final change is the saving of information to be read in and used by the PHASE subroutine.

Changes were also made to CALRAY to help keep the program from becoming too large. Instead of maintaining the option of being able to trace 310 rays, the number is now limited to only 60. In most cases this number is still adequate to cover a sufficient range of angles. This having been done, the dimensions of certain other arrays were reduced.

4.1.3. PHASE

Subroutine PHASE is the critical addition to the new version of the model. It performs all the calculations necessary to find the resultant signal phase at each target. The calculations for each ray include the time it takes each ray to travel to the target and the phase changes due to each ground reflection. PHASE also determines

and stores other variables such as phase and travel time differences. The phase of a ray allows for the coherent summation of the rays at a single target and time. Each ray can be represented as a vector (phasor) with an associated angle and magnitude. The angle is the signal phase and the magnitude is the linear power as it arrives at the target. The coherent sum of all the rays can also be expressed as a phasor. The resultant magnitude may either be kept as linear power or changed into decibels. An alternate representation of the total phasor are its real and imaginary components on the complex plane. The coordinates and both magnitudes are variables determined in the love subroutine PHASE.

PHASE begins by initializing parameters and variables. The frequency of concern is converted from Hertz into angular frequency. All information prepared by CALRAY is read in for each target for each ray of the current pair. This information includes the height of the ray above the ground at the target and the travel time to the target. Next the information pertaining to the bounces for each ray is read in. This includes the x position, and the angle of the ray at each bounce.

More initializations are performed. The power at each target, calculated in SOUNDP, is transferred from a one dimensional array depending upon target only (SPMAGN) to a two dimensional array (SPMAGNSAV) where the additional dimension is per ray. This variable is used later for the coherent summation. Next the variables that need to be initialized only once, not every time PHASE is called, are processed. PHMAGN, PHMAGNDB, PHX, and PHY are all set to 0.0. These

variables are the running totals for the rays arriving at each target.

Before beginning the calculations PHASE checks to see if either of the rays from the new pair travels to a greater number of targets than had any of the previous rays. This information is stored in MAXRAY and MAXTARG.

Completing this preliminary set up, the subroutine begins the greater part of the calculations. All of the values for the variables used in these calculations are from the first ray of each pair. The total phase (TOTPHSE) at each target of the current ray is calculated by summing the phase of the ray as it reaches the target (PHSE) with the total phase change due to the ground reflections (TOTBPHASE). The travel time and angular frequency are used to determine the phase of the ray. The expression for complex reflection coefficient is used to determine the phase changes due to the bounces. The total phase of a single ray is set to -8888.0, a nonsense number, unless it hits a target. Recall as was earlier defined that a hit means the ray comes within five meters above the ground at the target. With the true total phase the phasor is decomposed into the real (r) and imaginary (q) parts. The running total of the r and the q coordinates are updated for each new ray entering a particular target.

When PHASE is called for the last ray pair it performs the final calculations and writes the information to output files. The variables calculated are the minimum travel time (TTMIN), the travel time difference (TRAVTDIF), the minimum phase (PHMIN), the phase difference (PHSEDIF), the angle of the total phasor (PHSESUM), and the magnitudes of the phasor (PHMAGN and PHMAGNDB). A subroutine call to

GETTTMIN, discussed in the next section, retrieves the minimum travel time to each target. The travel time difference is calculated by subtracting the minimum from the actual travel time. The difference exists for each ray at each target. By using the travel time minimum and angular frequency the minimum phase can be determined; PHMIN = TTMIN * AFREQ. Once again for each ray at each target the phase difference between the minimum and actual phase is found. The angle associated with the sum of all the phasors coming into one target is the arctan (PHY/PHX). The magnitude of this phasor is $\sqrt{PHY^2 + PHX^2}$. In dB this magnitude is 10*log(PHMAGN). These last three variables use the running totals of the r (PHX) and q (PHY) coordinates and represent the coherent sum (PHMAGN) of the SPL entering a target.

Once all the variables are calculated, each is written to at least one of the three direct access output files. Written to PTIM is the phase difference, the travel time, the travel time difference, the magnitude, and the total phase of each ray at each target. Also written is the angle of the total phasor at each target. PCOM has the summed r and q components, and both magnitudes of the phasor for each target written to it. Finally, PDIS, only if selected to do so in RAYPS, has the total phase, the phase difference, the travel time, the travel time difference, and the angle of the phasor. Before closing each file, "filler" is added for each variable. Because some rays may not travel to as many targets as others zeros are placed in the "no-hit" targets for these rays.

4.1.4. GETTTMIN

The sole purpose of GETTTMIN is to find the minimum possible travel time to a given target. This travel time is representative of a ray launched at 0.0°, horizontal, traveling in an isothermal, no wind atmosphere. For this calculation the temperature of the atmosphere is set to that at the ground. ZINT is called to find the speed of sound at this height. With the speed of sound and the target to which the ray is traveling the minimum travel time is calculated. TMIN = XTG/c. The minimum travel time is a ray traveling in a straight line the distance from source to a particular target.

4.2. OUTPUT FILES

4.2.1. INTRODUCTION

The purpose of these new output files is the same as for the previous ones. They permanently store the results from the phase calculations and allow for easy and convenient presentation of the results as graphs. These files are referred to in the previous section as PTIM, PCOM, and PDIS. For all three files the information is calculated in a different order from what would be preferred. Consequently, each file is first written to a direct access file where each datum is given a record number and placed in a precise position.

Because these direct access files are not ASCII readable they are later read and rewritten to a sequential readable file. Details of these output files include contents, nomenclature, format, and graphical representation.

4.2.2. PTIM

The PTIM file stores the data as phase information versus time. The variables contained in this file are the phase difference, the actual and difference travel time, the magnitude, the phase for each ray, and the total phase. A definition of each was supplied in section 4.1.3. The naming convention for this file is similar to the other new files. The prefix works the same as the original output files, i.e. the date from the meteorological input file is used. Following the prefix is the type of file reference, in this case 'PTIM.' Following all this is the extension '.dat.' An example is MA09PTIM.DAT.

Several parameters, such as type of variable, bearing, frequency, and target, describe a set of results. A single PTIM file contains all the results from any parameter change that occurred during a single run of the model. Every time the value of a parameter is changed, a line ascribing its value is written to the file. For this file, type can have a value of one of six character strings: 'dif,' 'tim,' 'tdf,' 'mag,' 'phs,' and 'sum.' Bearing and frequency are set equal to their specific values. For example 190.0 could be for bearing and 500.0 for frequency. The target represents the number

assigned to the target. In order to find the distance in meters from the source this number is multiplied by one hundred. For example 'targ = 012' represents information recorded at 1200 meters from the source. Under each target subsection the results are then listed for each time. A list from a single time contains the results from each of the rays. The first number in the list is the 24 hour clock time. An exception to this format is the variable representing the angle of the total phasor (type = sum). This variable has only one value for each time. Only the first number after the time is valid. All others are simply repeats of previous values and are to be disregarded for this subsection. Figure 4.1 is an example of the beginning of a PTIM file. Recall that PTIM is the file displaying phase information versus time.

The graphical representation uses only the total phase coming into one target for a particular frequency and bearing. Essentially, the line graph is a time series showing the phase fluctuation. Figure 4.2 is an example of how the phase changes from 0200 to 1200 every half hour on July 1 at target 22 (2200 meters) along bearing 60 for 125 Hz frequency. All the essential information describing the graph is located at the bottom near the x axis The ordinate is in units of degrees. The sum fluctuates between zero and 360°. The missing points correspond to times when no sound was present at this target. PTIM stores and graphs the temporal variations of phase.

```
type = dif
bear = 190.0
freq = 500.0
targ = 001
100 .0 .0 .0 .0 -6.424430776545591 -5.912761343840657
130 .0 .0 .0 .0 -4.924690994829575 -4.252666231141347
200 .0 .0 .0 .0 -3.401592364944349 -2.712861861782699
targ = 002
100 .0 .0 .0 .0 -13.024527253962106 .0
130 .0 .0 .0 .0 -9.634531331333882 .0
200 .0 .0 .0 .0 -6.591611825478140 .0
targ = 006
100 .0 .0 .0 .0 .0 .0
130 .0 .0 .0 .0 -29.577558775941725 .0
200 .0 .0 .0 .0 -20.508266405038739 .0
type = tim
bear = 190.0
freq = 500.0
targ = 001
100 .288432143793023 .285232971752555 .283778933547894 .283247458442908
.283099105728177 .283446991153668
130 .291835188884861 .288742431236141 .287376885913414 .286909148747104
.286862126301456 .287194554146273

                                ETC.
```

Figure 4.1. Part of a Sample PTIM Output File

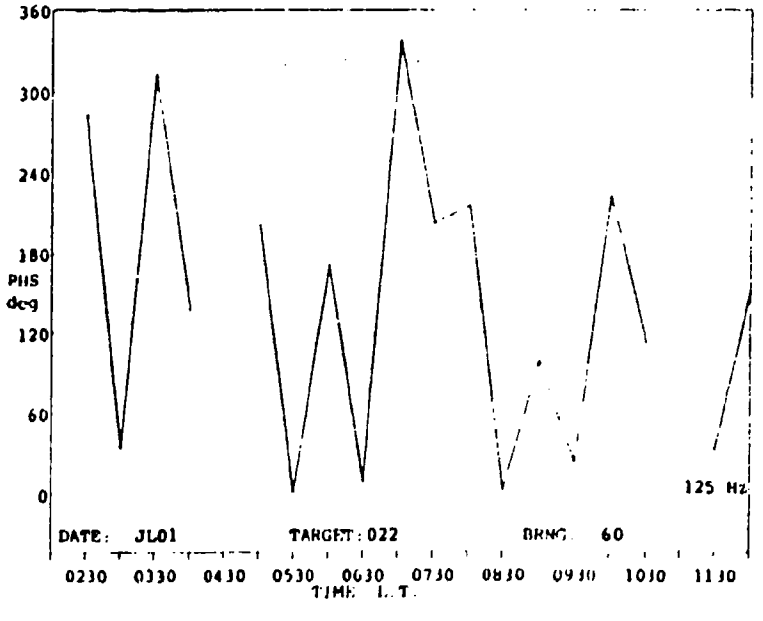

Figure 4.2. A Sample Phase versus Time Graph

```
type = dif
bear = 190.0
freq = 500.0
targ = 001
100 .0 .0 .0 .0 -6.424430776545591 -5.912761343840657
130 .0 .0 .0 .0 -4.924690994829575 -4.252666231141347
200 .0 .0 .0 .0 -3.401592364944349 -2.712861861782699
targ = 002
100 .0 .0 .0 .0 -13.024527253962106 .0
130 .0 .0 .0 .0 -9.634531331333882 .0
200 .0 .0 .0 .0 -6.591611825478140 .0
targ = 006
100 .0 .0 .0 .0 .0 .0
130 .0 .0 .0 .0 -29.577558775941725 .0
200 .0 .0 .0 .0 -20.508266405038739 .0
type = tim
bear = 190.0
freq = 500.0
targ = 001
100 .288432143793023 .285232971752555 .283778933547894 .283247458442908
.283099105728177 .283446991153668
130 .291835188884861 .288742431236141 .287376885913414 .286909148747104
.286862126301456 .287194554146273

                                ETC.
```

Figure 4.1. Part of a Sample PTIM Output File

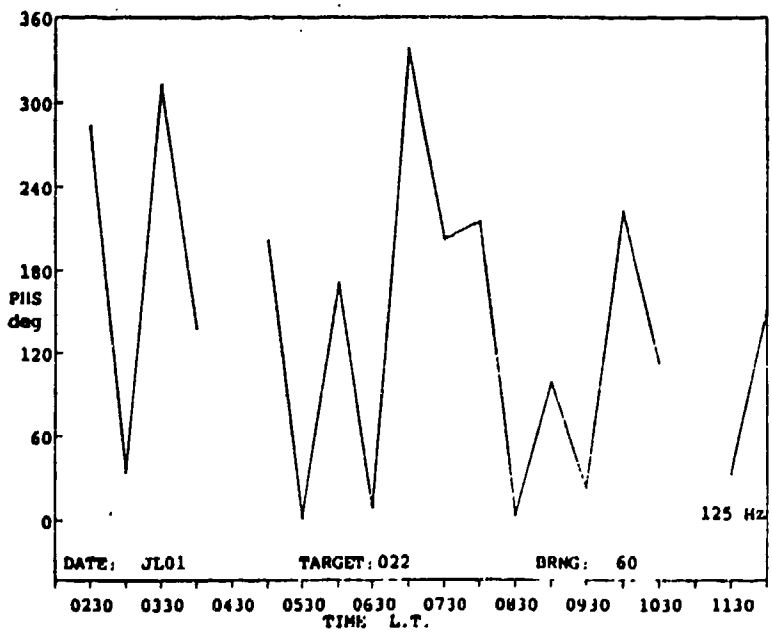

Figure 4.2. A Sample Phase versus Time Graph

4.2.3. PCOM

The PCOM file contains information necessary to describe the phasor as it moves about the complex plane. This file contains the real and imaginary component, and the magnitude of the phasor (linear and logarithmic) as it changes with time. The nomenclature follows the PTIM output file's convention: date followed by the type of the file followed by '.dat.' An example is NO27PCOM.DAT.

This file also is separated into subsections with header information separating each. Bearing, frequency and target are the parameters to describe a single section. Under each target is a list of five numbers. Once again the first is the clock time. The second is the real part of the phasor. Following this, respectively, are the imaginary part, the linear magnitude, and the decibel representation of the magnitude of the phasor. All times are displayed for each target. If sound did not reach a particular target at a particular time, then these variables are assigned the value of zero.

Two different graphs can be extracted from this file. The first displays the phasor position on the complex plane, Figure 4.3. Using the r and q coordinates a dot is mapped onto the plane. A line then connects the points at consecutive times. However, if sound is absent at a particular time the line is stopped at the preceding point and started again at the next time sound is predicted. The date, target, bearing and frequency for which the time series was generated are displayed below the graph. The length of each axis is determined by

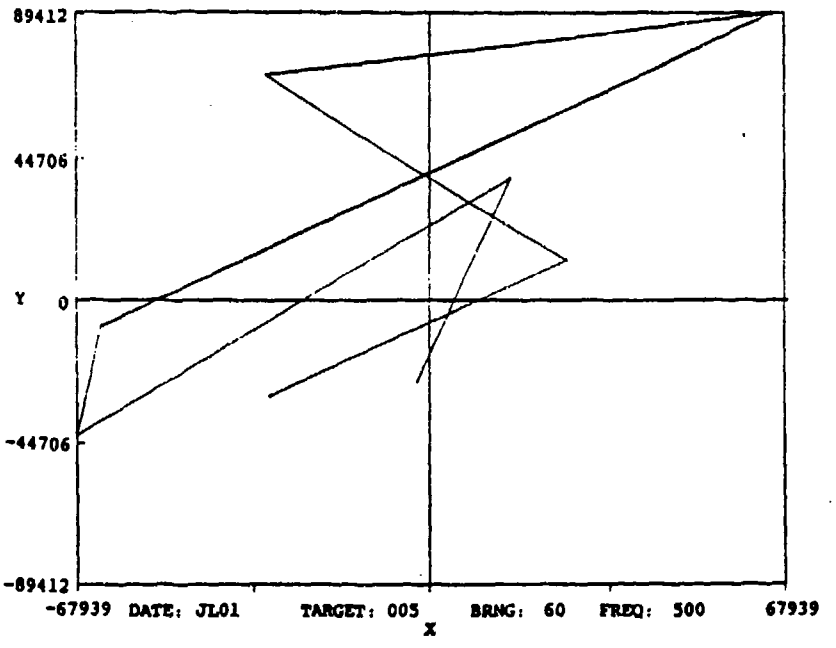

Figure 4.3. A Sample of the Phase Displayed on the Complex Plane

the maximum value of the r and q data points for the particular target. A general idea of how the angle and magnitude of the phasor changes with time can thus be obtained from this graph.

The second graph is a time series of the magnitude (dB). This simplifies viewing the amplitude fluctuations. A simple line graph similar to the graphical representation of the phase fluctuations is used. Figure 4.4 is an example. The abscissa denotes the time intervals; the ordinate represents the magnitude. All pertinent reference information is displayed at the bottom of each graph.

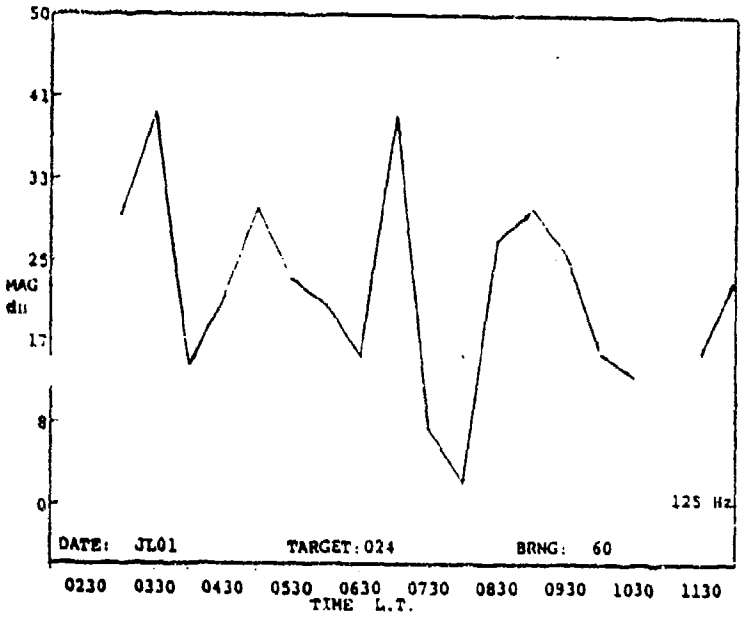

Figure 4.4. A Sample Coherent Sum versus Time Graph

4.2.4. PDIS

PDIS, the final of the three output files, contains the same information found in PTIM but in an alternate order. This file allows the information to be easily accessed for presentation of phase versus distance instead of time. The results stored include the phase of each ray, the phase difference, the travel time, the travel time difference, and the total phase from all the rays. Following the regular naming convention an example file would be called FE15PDIS.DAT.

The format of this file is similar to a PTIM file. PDIS is parameterized by type of data, bearing, and frequency. The exception is that PTIM has target as its last subdivision classification and

PDIS has time. Under each time are multiple lists of the results from the different targets. A single list begins with the number of the target and then follows with the particular variable values for all the rays. Figure 4.5 is an example.

The graphical representation is similar to the SPL graphs from the original version of the model. Distance along a single bearing is represented on the x axis and phase on the y axis. Data exists for each target; a line connecting the points is drawn to form the graph. The bearing, time, date, and frequency are displayed just above the x axis. The PDIS graph presents the spatial variability of the phase.

```
type = phs
freq = 500.0
bear = 190.0
time = 100
.1000000000000000 -8888.0 -8888.0 -8888.0 -8888.0 889.382095542791600
889.8937649745965400
.2000000000000000 -8888.0 -8888.0 -8888.0 -8888.0 1778.588525384712300
-8888.0
.3000000000000000 -8888.0 -8888.0 -8888.0 -8888.0 2668.000255981437000
-8888.0
.4000000000000000 -8888.0 -8888.0 -8888.0 -8888.0 -8888.0 -8888.0
.5000000000000000 -8888.0 -8888.0 -8888.0 -8888.0 -8888.0 -8888.0
.6000000000000000 -8888.0 -8888.0 -8888.0 -8888.0 -8888.0 -8888.0
time = 130
.1000000000000000 -8888.0 -8888.0 -8888.0 -8888.0 900.975851101692110
901.6478758653503420
.2000000000000000 -8888.0 -8888.0 -8888.0 -8888.0 1802.166521861709500
-8888.0
.3000000000000000 -8888.0 -8888.0 -8888.0 -8888.0 2703.193935160799100
-8888.0
.4000000000000000 -8888.0 -8888.0 -8888.0 -8888.0 3604.111252014200100
-8888.0

                                ETC.
```

Figure 4.5. Part of a Sample PDIS Output File

4.3. SUMMARY OF THE NEW ADDITIONS

In summary, only a few modifications had to be made to the old subroutines, RAYPS and CALRAY. These changes modified the program so that the new main addition subroutine PHASE, could be called. PHASE performs the majority of the calculations. The phase of a ray at any target is calculated by using the travel time and the reflection coefficient. The resultant phase from the contributing multipath signals at the target is also calculated. Initially within PHASE the results are written to either the PTIM, PCOM, or PDIS as direct access files. Then at the end of RAYPS each of these files are rewritten into sequential files. PTIM displays the phase as a time series. PCOM displays the phase parameterized by time on the complex plane. Finally, PDIS stores the phase vers

Chapter 5

VALIDATION OF THE MODEL

For test and validation purposes the revised model was run successfully in a series of tests using artificial environmental conditions. The artificial environments differed from one another in that each sound speed profile was constructed to have a particular height dependence. For each test the terrain was set to be flat and the same humidity values were used.

5.1. CONSTANT SOUND SPEED

The first artificial situation used a profile with constant sound speed. The speed of sound, set to 339 m/s, neither varied with height nor time. None of the profiles normally created by RAYPS from real or model (meteorological) output databases were used. Instead of calculating the sound speed at each height it was set within the program to 339.0 m/s. This speed corresponded to a windless, isothermal atmosphere with T = 287.6 °K (58.0 °F). The same sound velocity profile could have been achieved by setting the temperature at each height to 287.6 °K and the wind to zero. In this case the profile would have been created through the model's normal calculation processes.

As expected for the rays travelling through such a constant speed atmosphere no refraction was evident. Rays emitted from the source

traveled in straight lines and the travel time between any two consecutive targets, again as expected, remained constant. The phase along each ray increased linearly with radial distance. Figure 5.1 illustrates this phase change. The model output was graphed for one ray with a small launch angle of 0.005° so that the ray would remain within five meters of the ground even out to the maximum distance.

5.2. CONSTANT GRADIENT

The next test was for a sound speed profile with a constant speed gradient. The speed of sound was forced to increase linearly with height. As in the previous test the profile did not change with time. In order to easily achieve the constant gradient sound speed profile winds were again set to zero. The input temperature was calculated using the formula, $T(i) = (c(i)/20.05)^2$. The speed at the surface was set to 339.0 m/s and increased by 2.5 m/s / km. This artificial situation might occur on a calm evening with a strong surface-based temperature inversion.

As expected refraction was in the downward direction. Since the gradient of the sound speed was constant, the curvature of the ray was likewise. Using Snell's law, the radius of the circular path can be defined as $1/ab$ where $a = \sin\theta/c(z)$ and b is the gradient of the speed (Cl[illegible] and Medwin 1977, p. 97). Figure 5.2 illustrates a ray launched at an initial angle of 0.005°. As previously mentioned the small angle was used to keep the height of the ray all along the radial bearing under the target height of five meters. Starting at the

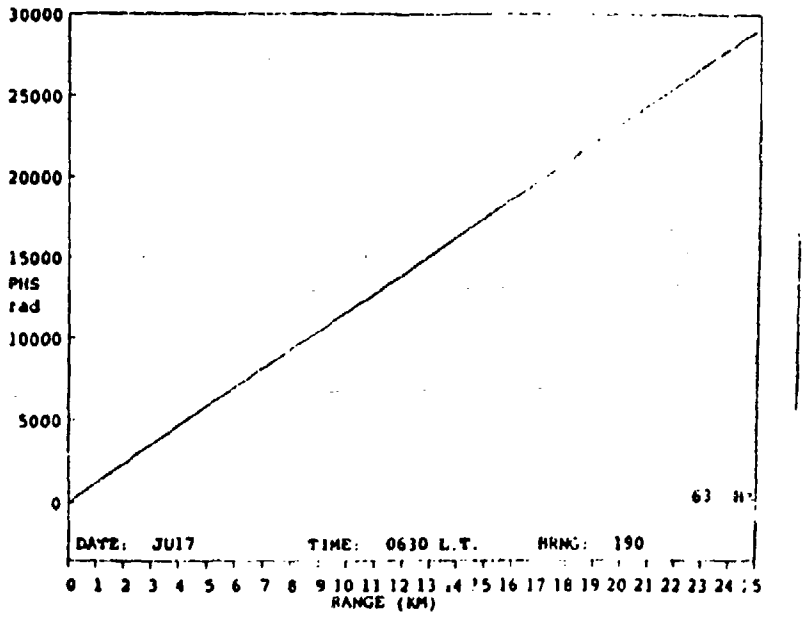

Figure 5.1. Phase versus Distance, Hypothetical Constant Speed of Sound Profile

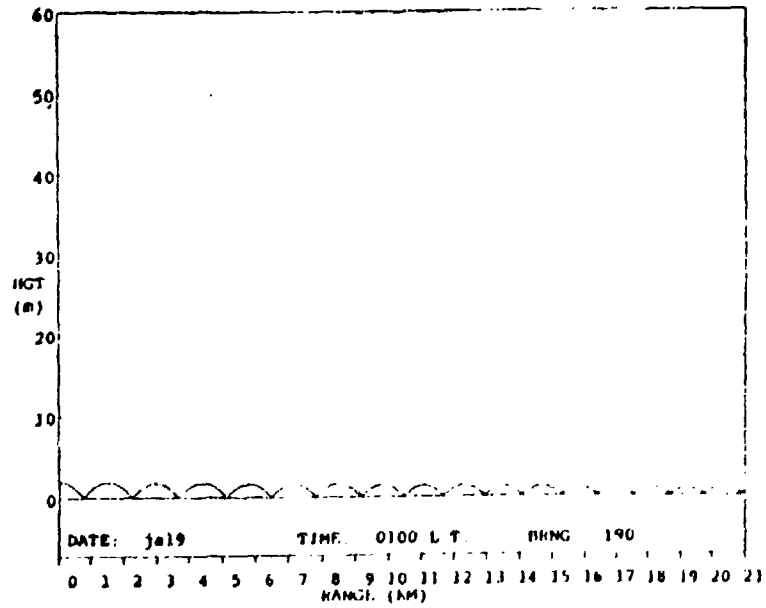

Figure 5.2. A Ray Trace from a Hypothetical Constant Gradient Speed of Sound Profile. A Single Ray With Initial Angle of 0.005° is Used.

source, it can be seen easily in Figure 5.3 that on the "down" side of the ray trajectory with each consecutive horizontal interval the arc length becomes longer until the ray bounces. Also, the speed of sound decreases with each interval. However, on the "up" side of the curve the arc length becomes shorter with each consecutive horizontal interval and the speed of sound increases. These horizontal intervals remained constant over the entire propagation path; they correspond to the distance between targets, one hundred meters. The time it takes the ray to travel within each range interval first becomes longer and longer and after the bounce becomes shorter and shorter until the vertex. The phase follows suit. In calculating the phase versus distance, terms were successively added to each previous phase, first increasing in value each time and then decreasing. Graphically, these changes would show in principle as a slight convex curve followed by a slight concave curve superimposed on the generally increasing trend. However, the magnitude of the difference between each term added is much smaller than the magnitude of the actual phase. In comparison to the phase which had a magnitude of 10^3 to 10^4 the difference had a magnitude of about 10^{-3}. On a graph such as the one used for the constant speed environment, such small curvatures are undetectable. Table 5.1 gives the actual data and displays the changes. The tabulated data corresponds to the constant gradient environment described above. The large change in phase added at 0.7 kilometers is the result of a reflection at the surface. Figure 5.4 shows the "phase added" versus distance. In order to emphasize the changes the value at 0.0 km is subtracted from all the terms.

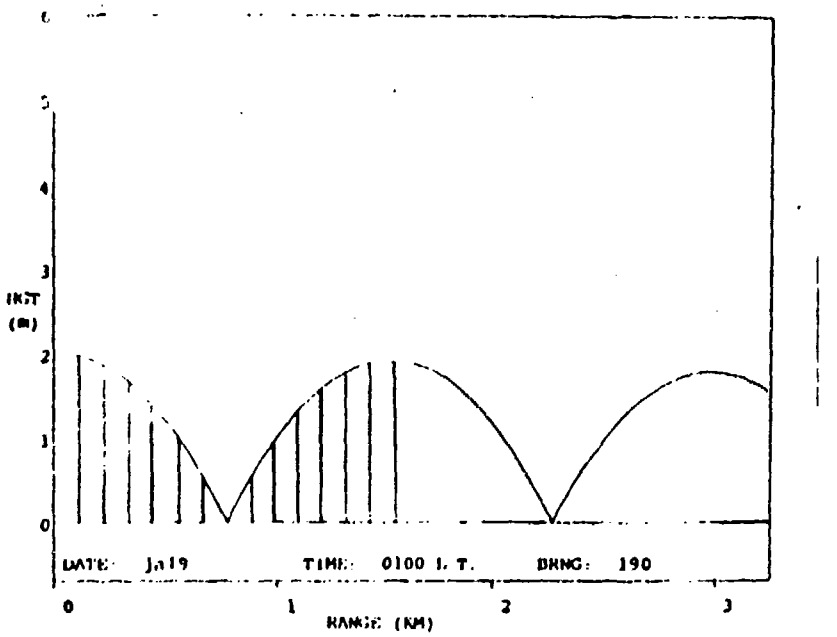

Figure 5.3. Figure 5.2 Expanded to Aid in Demonstrating How the Phase Changes with Distance in a Constant Gradient Speed of Sound Atmosphere

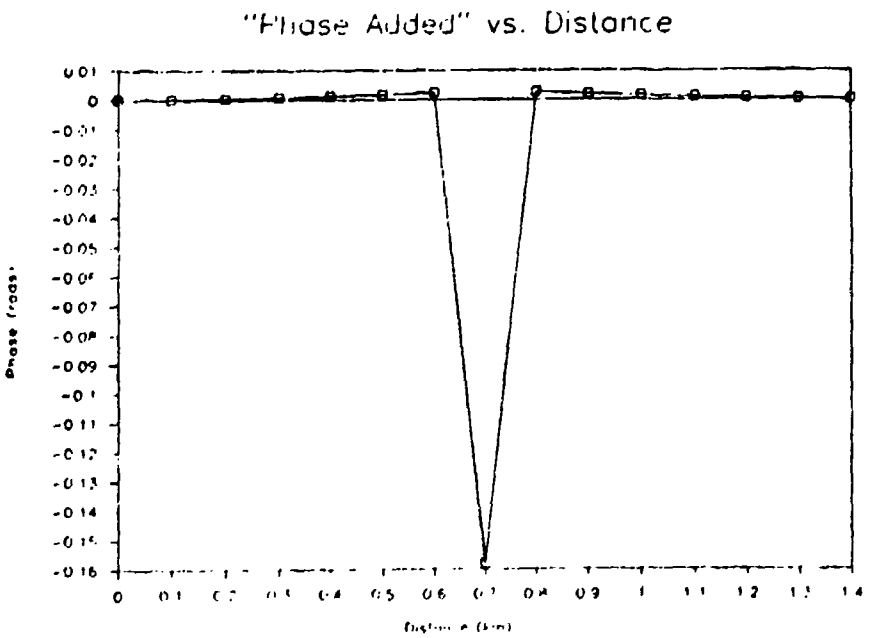

Figure 5.4. "Phase Added" versus Distance with the Initial Value Subtracted Out

Table 5.1. An Example of Changes in Phase with Distance for a Single Ray in a Constant Gradient Speed of Sound Atmosphere

Distance (km)	Phase (rads)	Phase Added
0.0	0.0000000	116.5076712
0.1	116.5076712	116.5077558
0.2	233.0154271	116.5079666
0.3	349.5233937	116.5082924
0.4	466.0316861	116.5087639
0.5	582.5404500	116.5093374
0.6	699.0497874	116.5100601
0.7	815.5598475	116.3494875
0.8	931.9093350	116.5103399
0.9	1048.4196749	116.5095356
1.0	1164.9292846	116.5089913
1.1	1281.4382759	116.5084962
1.2	1397.9467721	116.5081250
1.3	1514.4548971	116.5078785
1.4	1630.9627756	116.5077617

5.3. TIME SERIES

Before running the model for variable gradient situations, a final test involving a set of temporally changing profiles was performed. For each successive time a new isothermal, no wind environment was created. At each time the magnitude of the temperature was increased by 0.6 °K. Only one ray at a small launch angle was emitted from the source.

In this situation at each time the ray would travel in a straight line to a particular target. However, at each new time as the propagation speed increased the travel time to the target proportionally decreased as would the phase. By viewing the signal "coherently," that is as a phasor, the temporal change could be seen. Only the speed was changed; there was no change in refractive

gradients, in the number of bounces, in path length, or in humidity. Thus only changes in the phasor angle occurred; the magnitude remained constant. A constant magnitude phasor is shown in Figure 5.5. It monotonically circumvents the complex plane (the elliptical shape is due only to aspect in the graphing). This figure was produced from a run with the following parameters: one ray launched at a 0.005° angle, a frequency of 63 Hz, eleven different time sets, and the target at 700 m. Clearly if the complex signal is tracked it is in principle possible to monitor temporal changes in the atmospheric sound speed profile.

5.4. SUMMARY OF THE VALIDATION TESTS

The above three tests were performed to ensure that the model was running correctly. The first established that the model's basic procedures for calculating the signal phase were correct. The second test, the constant gradient situation, provided validation of model's refractive calculations. The final test confirmed the propagation model's handling of sequential profiles. These evaluations serve to validate the performance of the model.

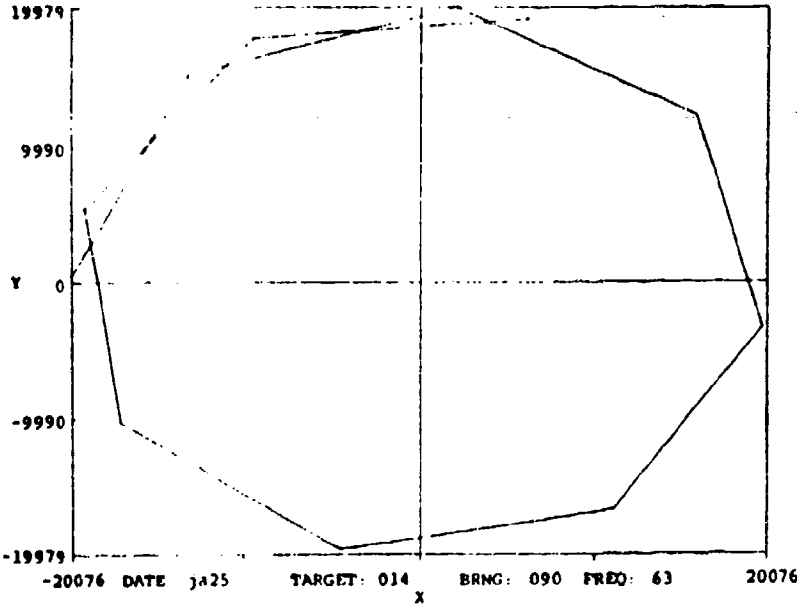

Figure 5.5. Phase on the Complex Plane from a Temporally Changing, Isothermal, No wind, Atmosphere. The Temperature is Increased by 0.6° Each Time.

Chapter 6

CASE STUDY - I

Using real topographical and atmospheric data from a mountainous region in southwestern Utah a case study was performed to examine the temporal variability of sound propagation. Investigation of temporal variability also provided additional insight regarding the horizontal variability of sound pressure levels and signal phase. Heuristic plots of the raw data as well as the statistics were used for both the temporal and horizontal variations. The surrounding topography at a given site strongly influences the horizontal variations and the classifications of them. In the following sections the processing of the data and the results from the model are further explained.

6.1. PREPARATION

For this study the model was applied to a mountainous region located in southwestern Utah. Computations were made for only one bearing -- 58.87°. It defined a line from a hypothetical noise source to a scenic point (Yovimpa) in Bryce Canyon National Park. From a USGS map, the elevation at five hundred meter intervals up to twenty-five kilometers was interpolated and recorded. The irregularities in the resulting terrain cross section with a general upslope can be seen in Figure 6.1. The hypothetical source was placed at the zero kilometer point at a height of 2 m. The receivers were

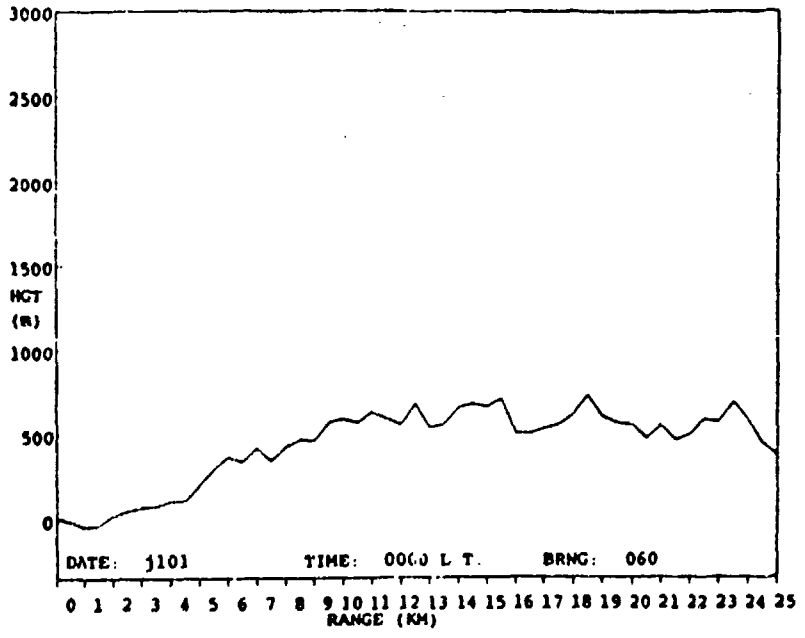

Figure 6.1. Topography Used in the Bryce Canyon National Park Study

placed at 100 m intervals.

Two days, one designated as being "extreme" and the other "typical," were chosen for analysis. The extreme day, 1 July, 1971, was selected as such because the sound velocity profile showed a strong sound channel (Thomson, 1987) along the 58° bearing. The typical day, 22 July, 1971, was representative of days with similar profiles, days with typical summer weather conditions. For both days, beginning with the available temperature and wind data at twelve hour intervals, a state-of-the-art boundary layer model was used to reconstruct profiles with a temporal resolution of three hours. Since calculations for 1 July at the three hour intervals displayed interesting downward refractive propagation of the sound, we thought it would be useful to generate plots of even higher temporal resolution between the local times 0200 and 1200. Rather than rerunning the boundary layer model, splining was used to produce half hour intervals from the three hour interval boundary model output. Relative humidity data was also available at only twelve hour intervals. Thus linear interpolation was performed to achieve both the three hour and half hour profiles. All four profiles -- temperature, wind (u and v components), and relative humidity were compiled into the formatted files named JL01BC.DAT and JL22BC.DAT.

Finally preliminary runs were made to address the question as to which initial angles would be necessary for the rays. Rays that most of the time refract upwards and never reach the ground do not contribute to the received sound pressure levels. For the extreme day, angles above +10° did refract upwards most of the time; angles

below +10° refracted downwards most of the time. Therefore, the angle data file consisted of pairs of rays launched from +10° to -10° at 0.5° intervals. The negative angles added symmetry to the angles about the horizontal line from the source.

6.2. SPEED OF SOUND PROFILES

Some of the temperature and wind profiles, for the extreme day, used to make up the speed profiles are shown in Figures 6.2 - 6.6 and Figures 6.7 - 6.11. In general, all the temperature profiles show a ground based inversion and a positive lapse rate aloft above the inversion. The top of the inversion is at 400.0 meters above the ground for each time. The only difference among the profiles, although slight, is the surface temperature and the temperature at the top of the inversion. If the speed of sound profiles were determined solely from the temperature their slopes would change in time causing either elongation or compression of the path length and travel time. The gradients at 0230, 0300, 0330, 0430, and 0730 are found to be 10.0, 10.1, 10.2, 10.3, and 5.9 °K/km respectively. The gradients for the first four times appear to have insignificant differences.

Contributions by the wind profiles, however, alter the sound speed profiles so that they do differ significantly from each other. For the times 0230, 0300, and 0330 the wind profiles have much more variation. There are many more relative minima and maxima. These profiles even include negative wind speeds which signify a reverse in wind direction along the source-receiver bearing. Each profile is

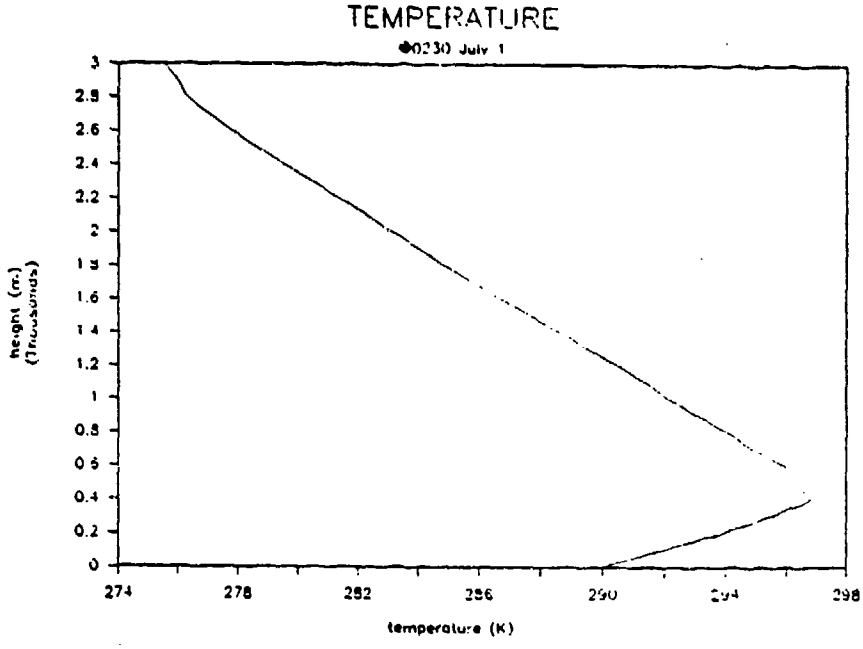

Figure 6.2. Temperature Profile, 0230 L.T., 1 July, 1971

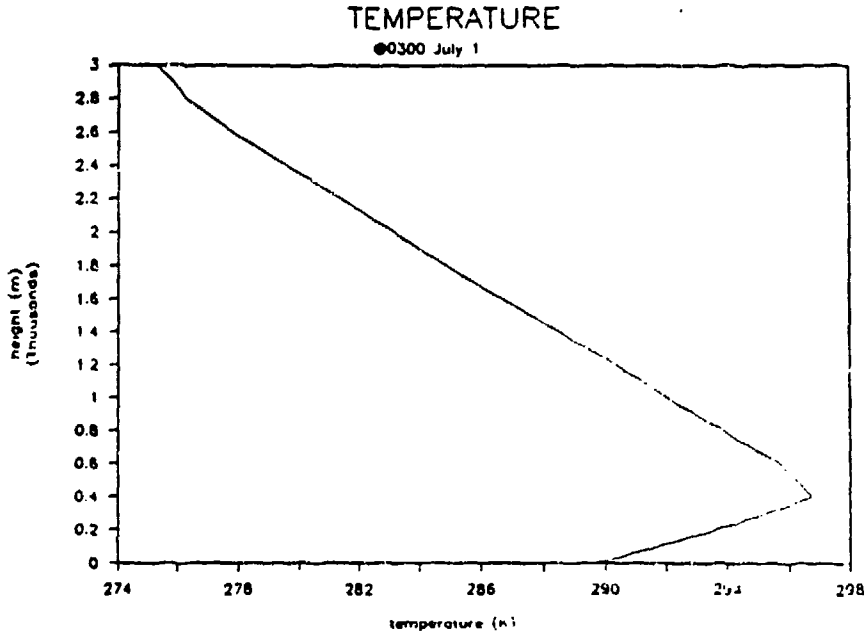

Figure 6.3. Temperature Profile, 0300 L.T., 1 July, 1971

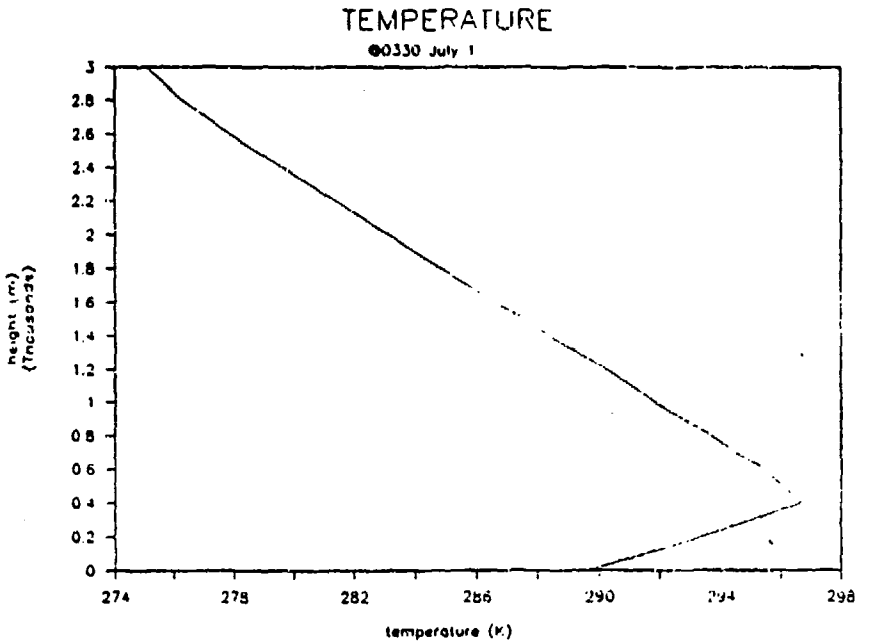

Figure 6.4. Temperature Profile, 0330 L.T., 1 July, 1971

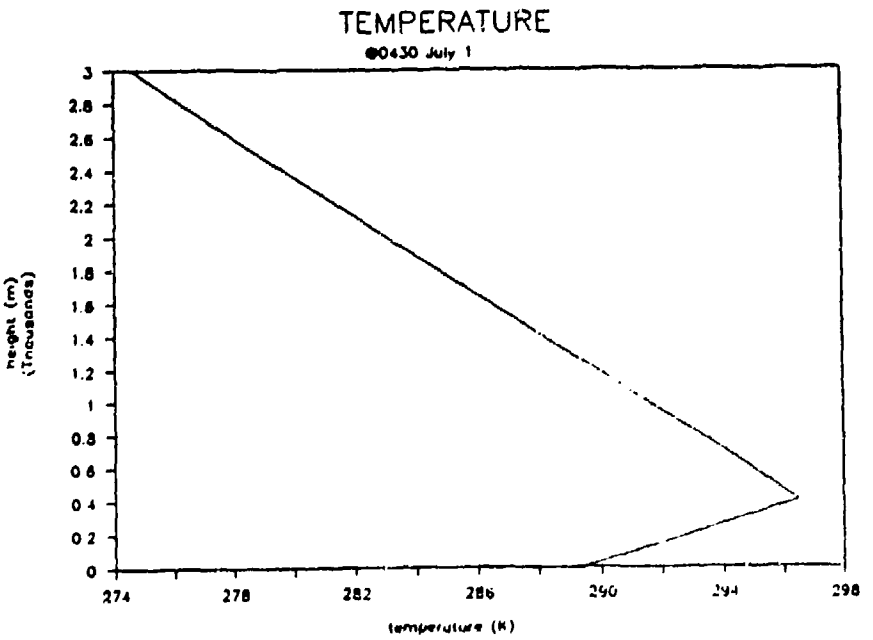

Figure 6.5. Temperature Profile, 0430 L.T., 1 July, 1971

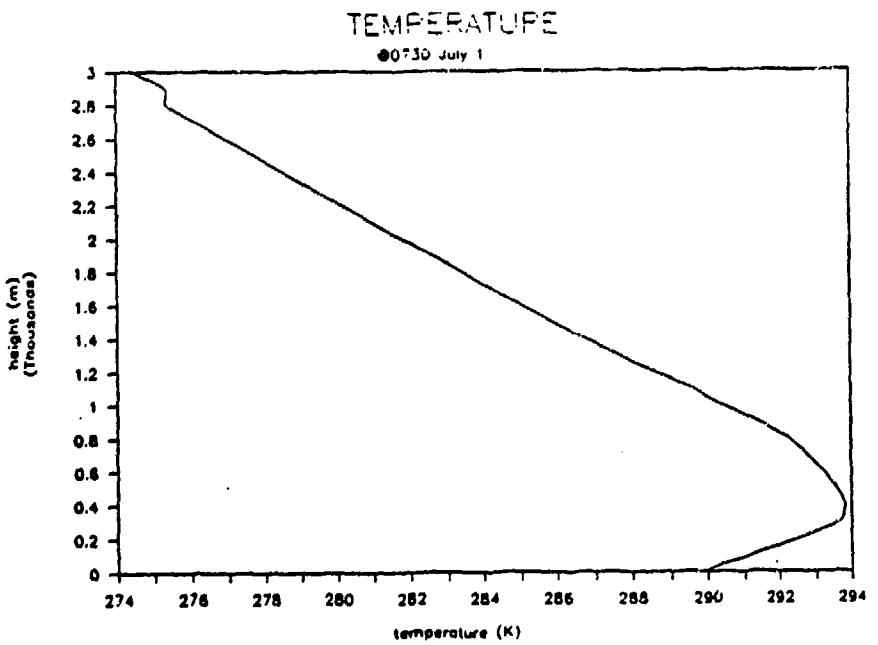

Figure 6.6. Temperature Profile, 0730 L.T., 1 July, 1971

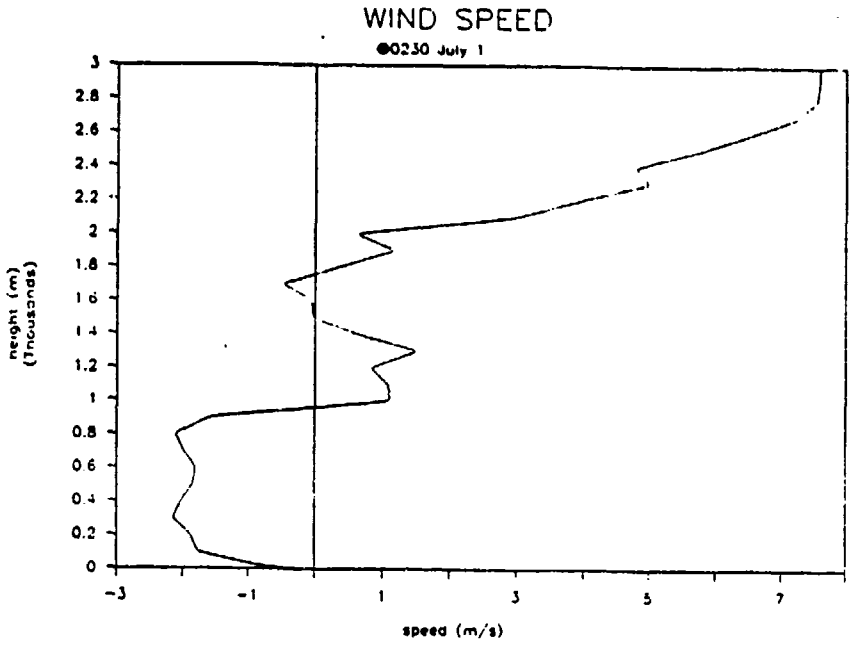

Figure 6.7. Wind Profile, 0230 L.T., 1 July, 1971

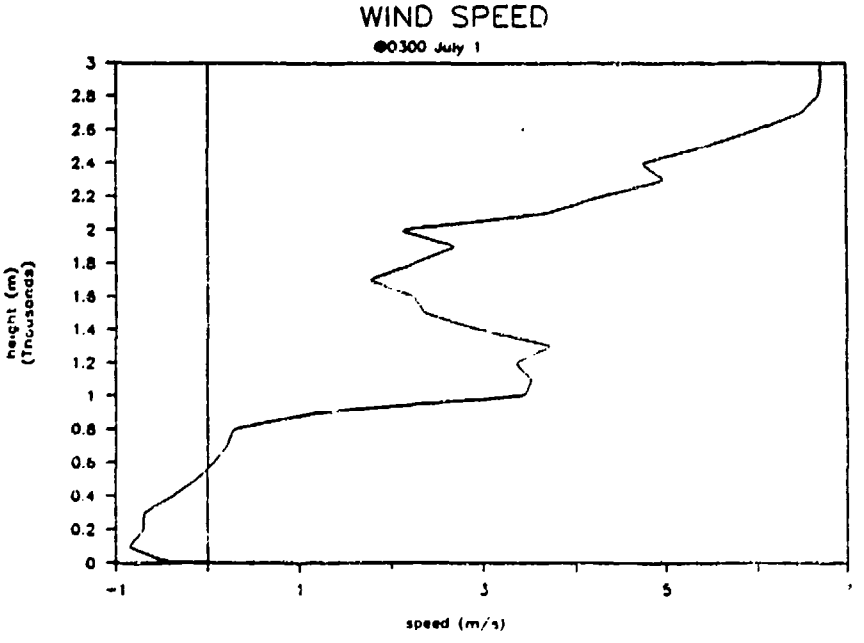

Figure 6.8. Wind Profile, 0300 L.T., 1 July, 1971

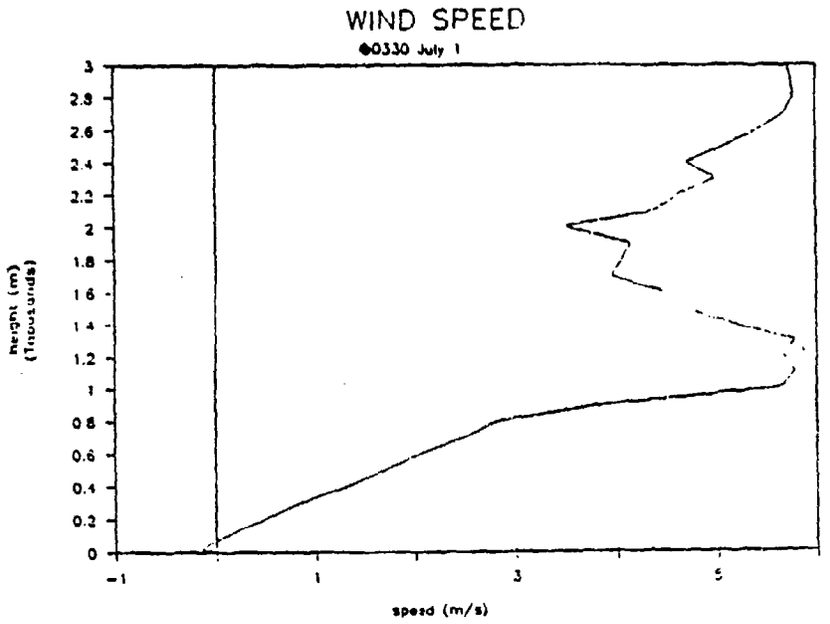

Figure 6.9. Wind Profile, 0330 L.T., 1 July, 1971

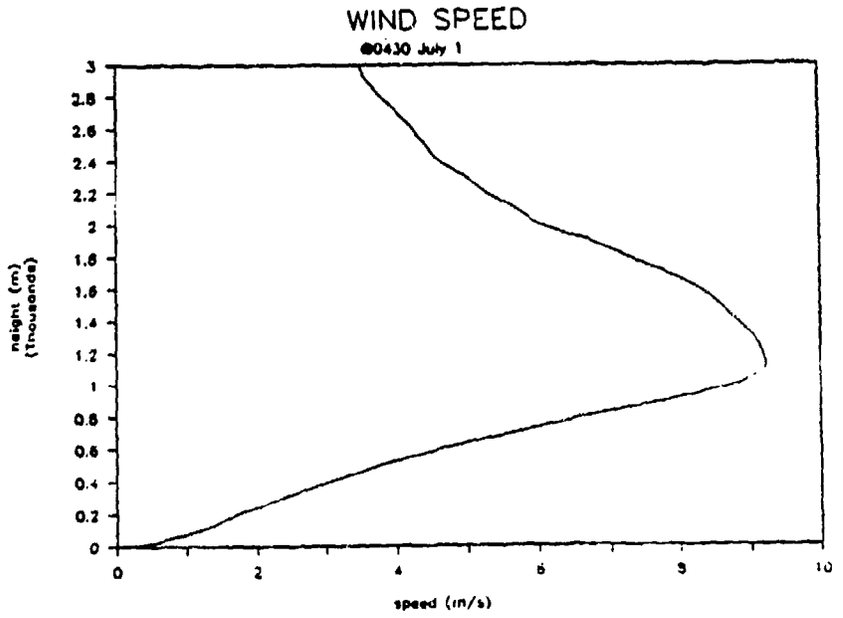

Figure 6.10. Wind Profile, 0430 L.T., 1 July, 1971

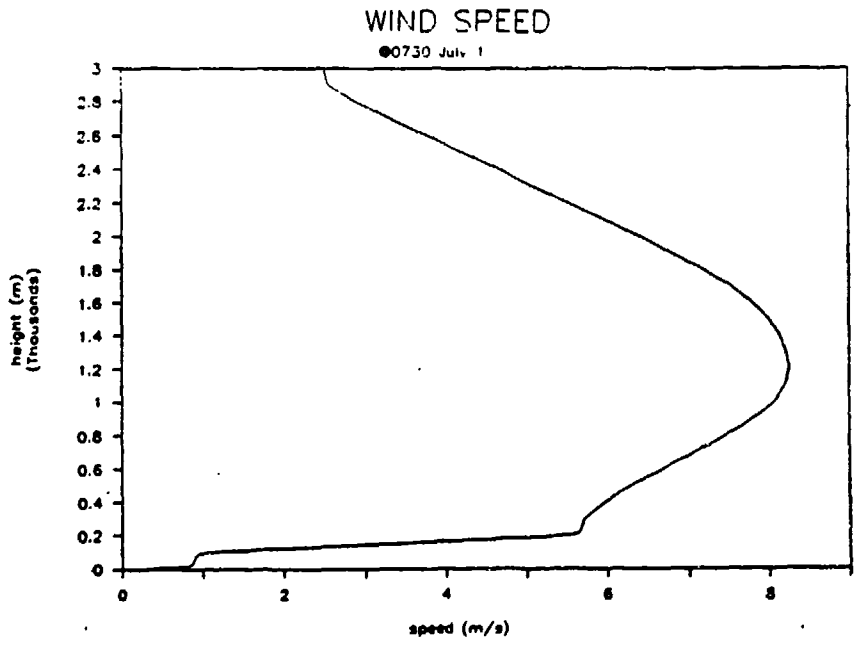

Figure 6.11. Wind Profile, 0.[illegible] L.T., 1 July, 1971

significantly different from the times before and after it. Even for the times 0430 and 0730, where there are apparently few changes in the gradients, a dissimilarity is evident. In using these wind profiles to calculate the speed of sound profiles, the resulting profiles also differed significantly from one time to the next. See Figures 6.12 - 6.16. For the earlier times, 0230 - 0330, some of the "randomness" in the gradients is evident. More than one inversion existed. The first inversion might be above a small positive lapse rate. Other inversions are separated from the first by a larger lapse rate. Both the top and slope of the first inversion changed significantly from time to time. Values were not constant at 400 meters and around 10 °K/km, respectively. For the later times, 0430 and 0730, the ground based inversion consisted of two distinct slopes. The ranges of distinct slopes are referred to as different inversions. A sense of the variability in the speed profiles is evident in Table 6.1.

Table 6.1. Characteristics of the Speed of Sound Profiles, 1 July, 1971

Time	Initial Lapse or Inversion	First Inversion		Second Inversion	
		Range (m)	Slope (°K/km)	Range (m)	Slope (°K/km)
0230	lapse	80-420	7.7	---	---
0300	lapse	20-420	10.0	---	---
0330	lapse	10-410	13.6	---	---
0430	inversion	0-380	18.0	380-1010	5.1
0730	inversion	0-180	34.2	180-800	4.4

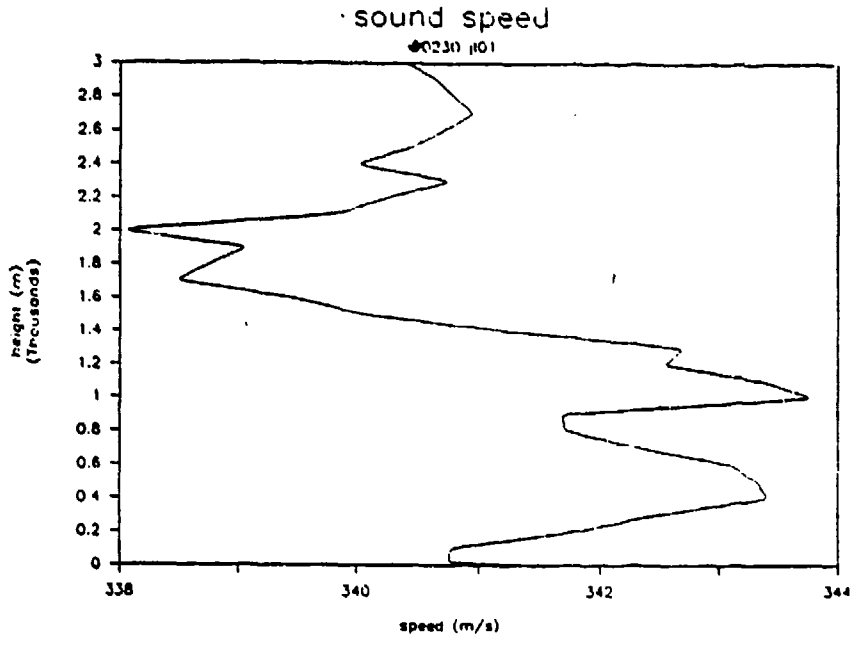

Figure 6.12. The Speed of Sound Profile Calculated from the Temperature and Wind Profiles, 0230 L.T., 1 July, 1971

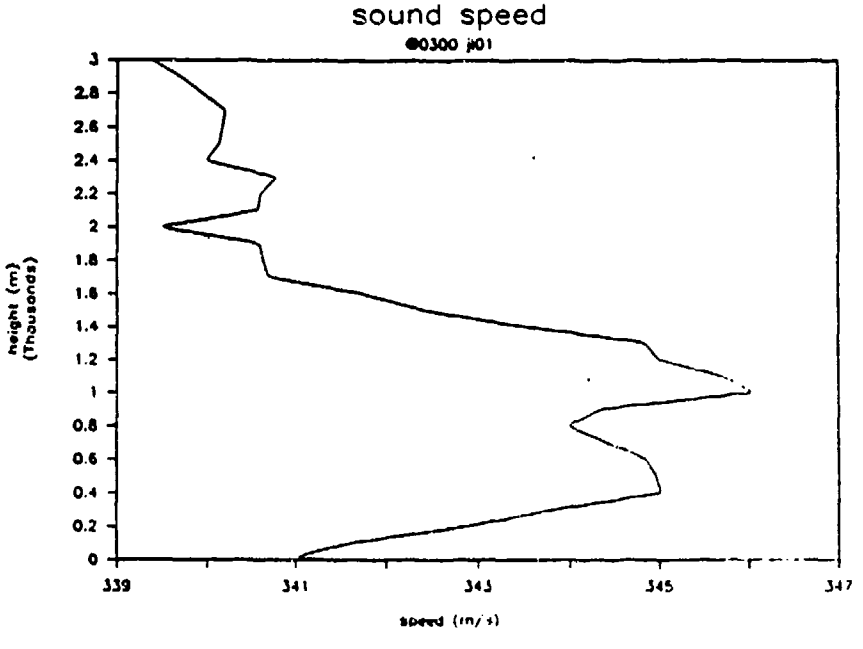

Figure 6.13. The Speed of Sound Profile Calculated from the Temperature and Wind Profiles, 0300 L.T., 1 July, 1971

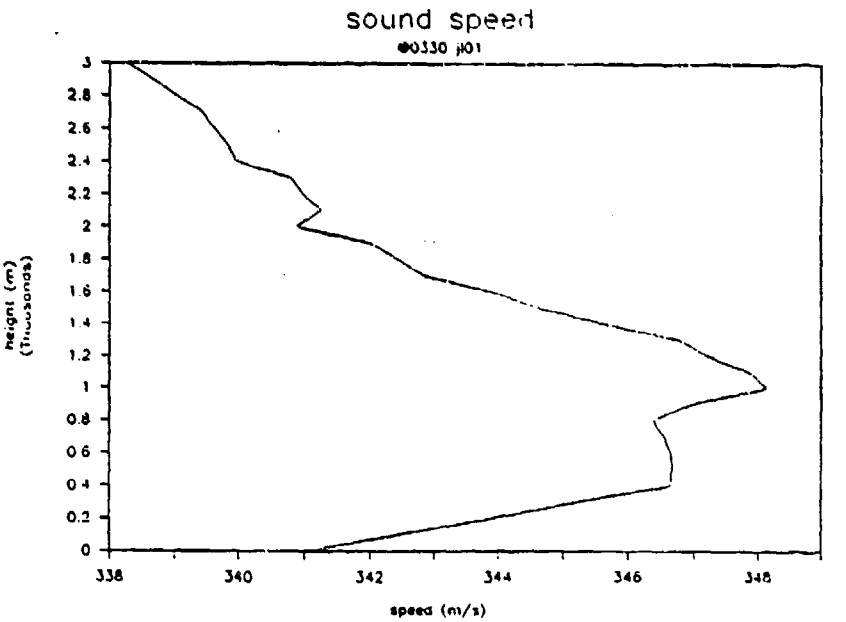

Figure 6.14. The Speed of Sound Profile Calculated from the Temperature and Wind Profiles, 0330 L.T., 1 July, 1971

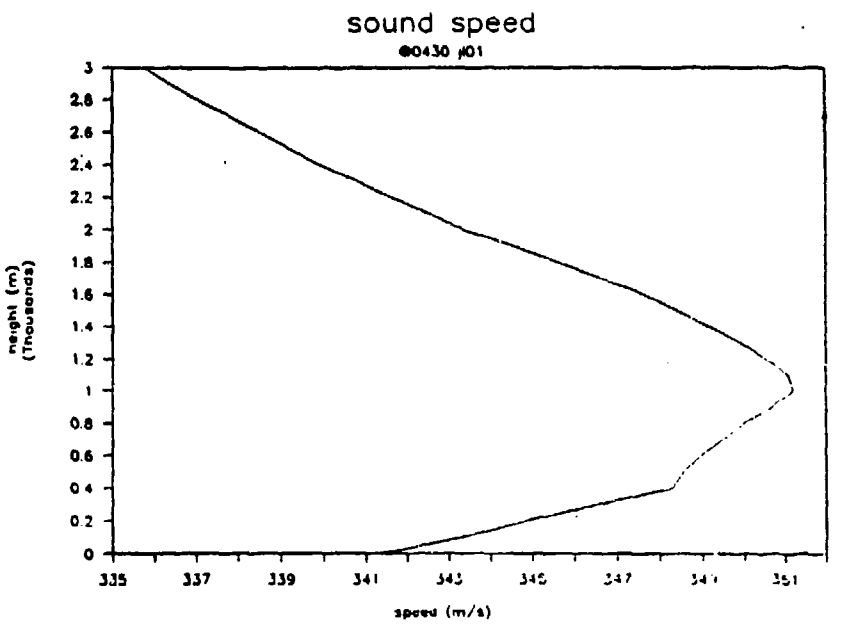

Figure 6.15. The Speed of Sound Profile Calculated from the Temperature and Wind Profiles, 0430 L.T., 1 July, 1971

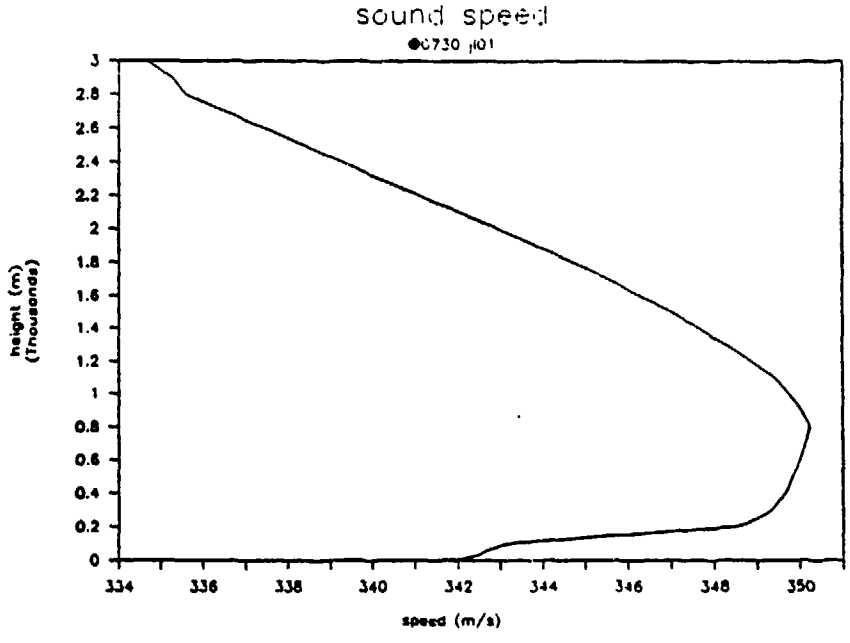

Figure 6.16. The Speed of Sound Profile Calculated from the Temperature and Wind Profiles, 0730 L.T., 1 July, 1971

6.3. RESULTS

6.3.1. RAW DATA

6.3.1.1. RAY TRACES

After readying the input files the model was run for the two case days. The results, i.e. the ray traces, sound level diagrams, and phase graphs clearly show the existence of temporal variability. The evolution of the speed of sound profile throughout the day causes the variety in the ray traces. From the ray traces (Figures 6.17 - 6.24 for the typical day and Figures 6.25 - 6.32 for the extreme day) it is apparent how the sound propagation varied throughout each day. For instance, on 22 July at 2000 local time, only a few rays intersected the ground at about two kilometers. But at 0500 local time, only a few rays were initially refracted upwards. The majority of the rays were directed towards the ground and "bounced" once or twice before being refracted upwards. At this time sound could propagate out to about seven kilometers. Unique ray traces are shown for each of the three hour intervals. On the extreme day traces also varied significantly throughout the day. Even during the half hour intervals, changes in the ray traces were apparent. Compare 1 July, 0430 to 0500, and those to 0530 (Figures 6.33 - 6.35).

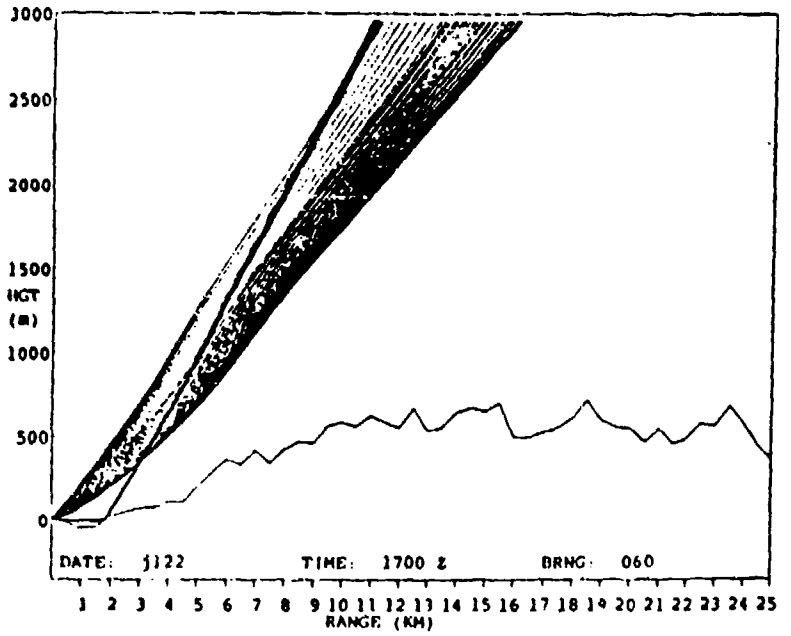

Figure 6.17. Ray Trace, 1700 L.T., 22 July, 1971 (Typical Day)

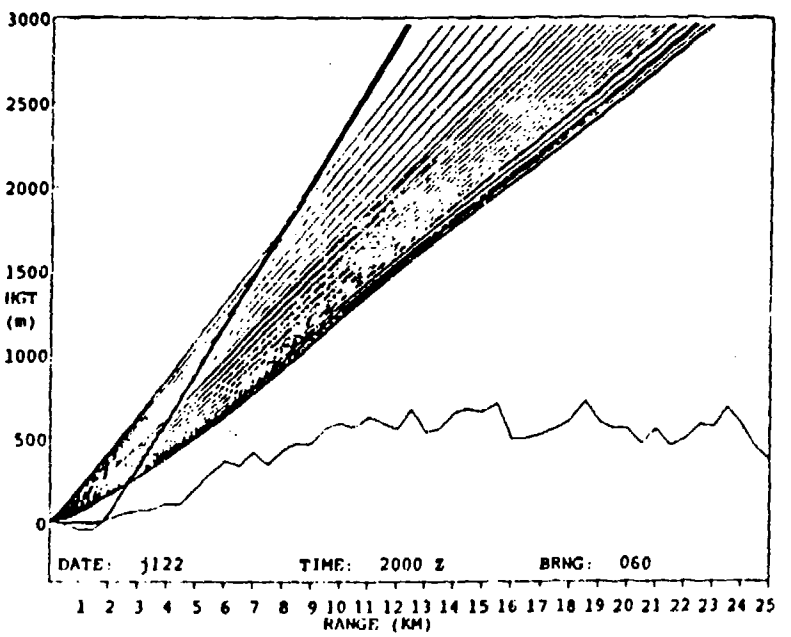

Figure 6.18. Ray Trace, 2000 L.T., 22 July, 1971 (Typical Day)

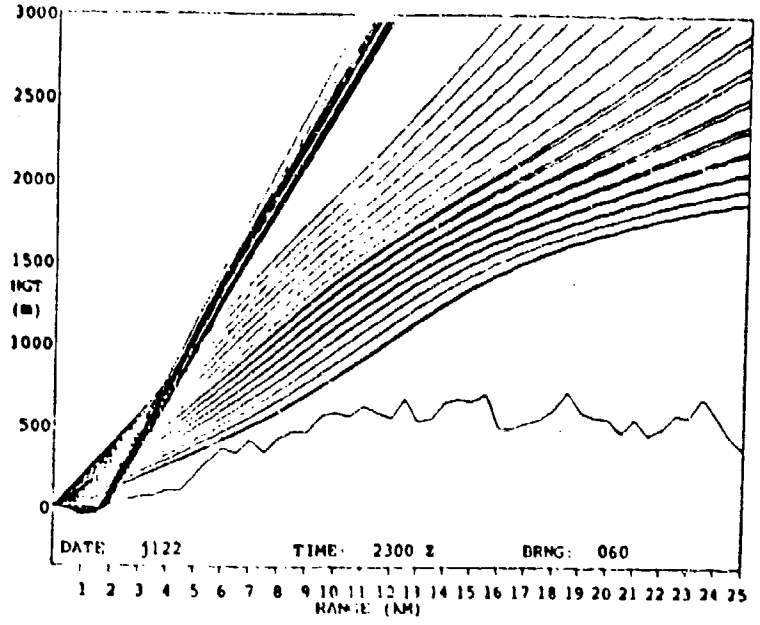

Figure 6.19. Ray Trace, 2300 L.T., 22 July, 1971 (Typical Day)

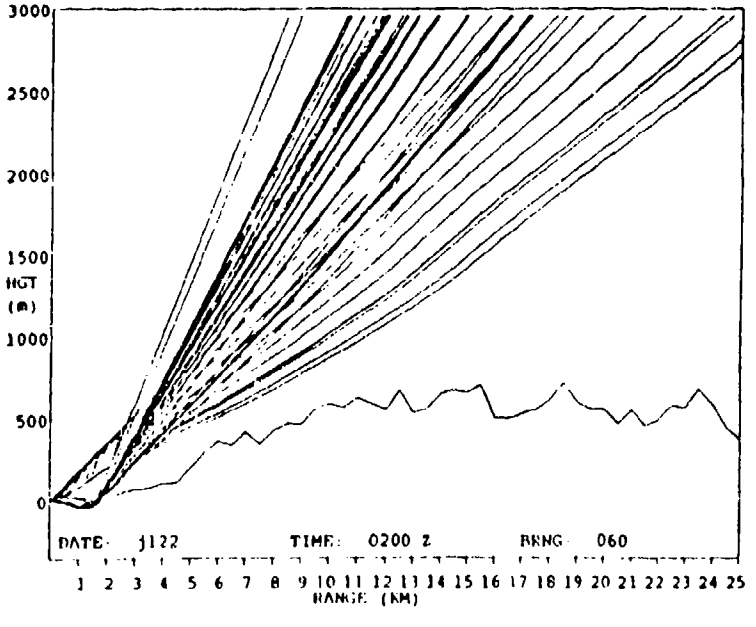

Figure 6.20. Ray Trace, 0200 L.T., 22 July, 1971 (Typical Day)

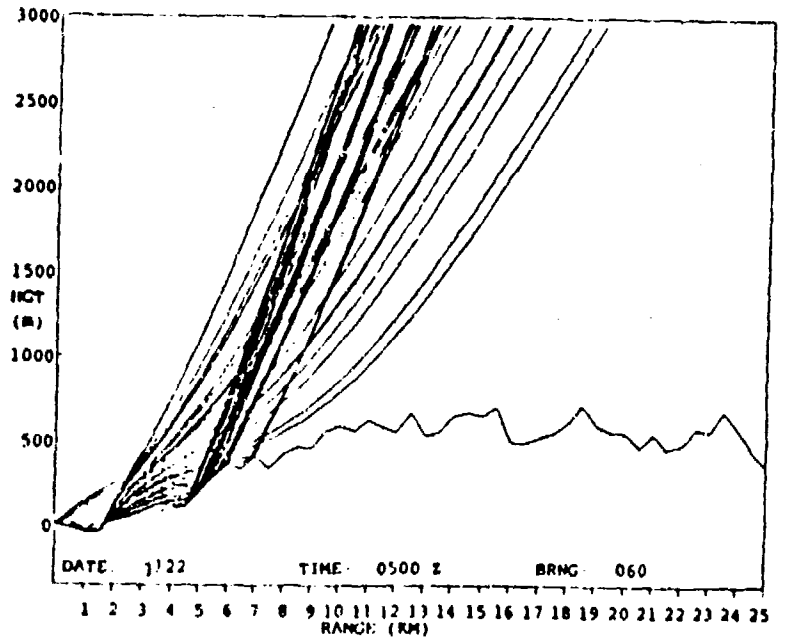

Figure 6.21. Ray Trace, 0500 L.T., 22 July, 1971 (Typical Day)

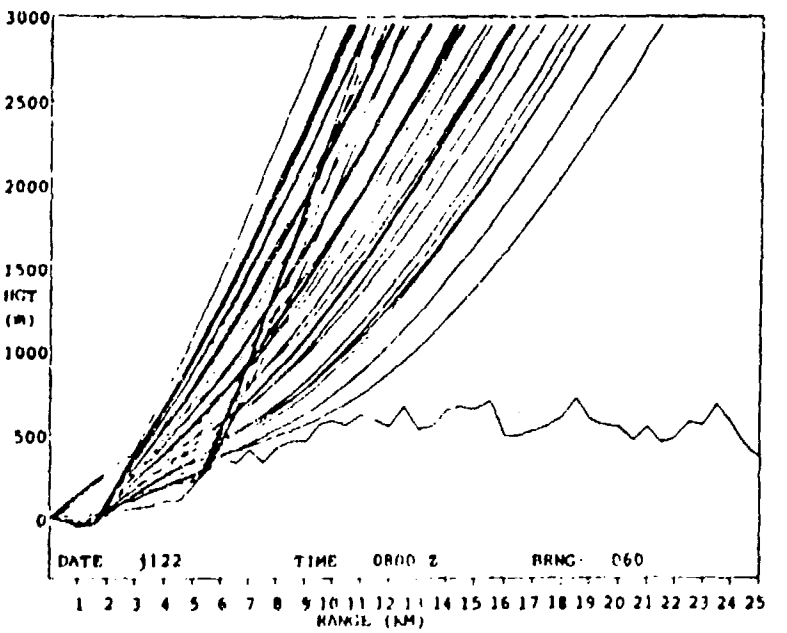

Figure 6.22. Ray Trace, 0800 L.T., 22 July, 1971 (Typical Day)

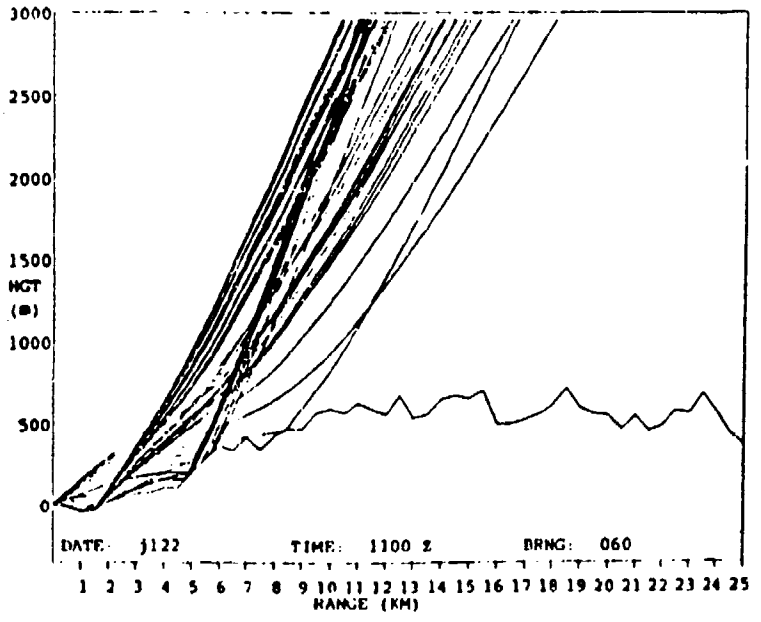

Figure 6.23. Ray Trace, 1100 L.T., 22 July, 1971 (Typical Day)

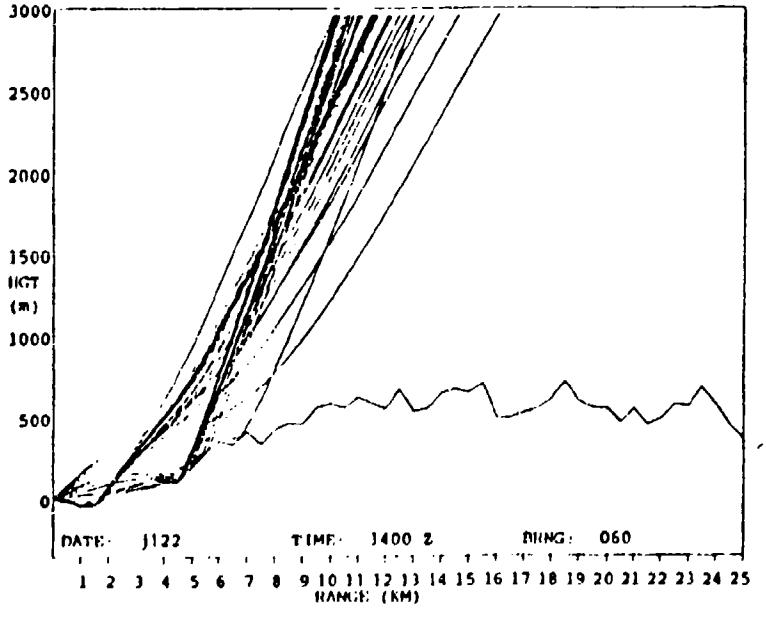

Figure 6.24. Ray Trace, 1400 L.T., 22 July, 1971 (Typical Day)

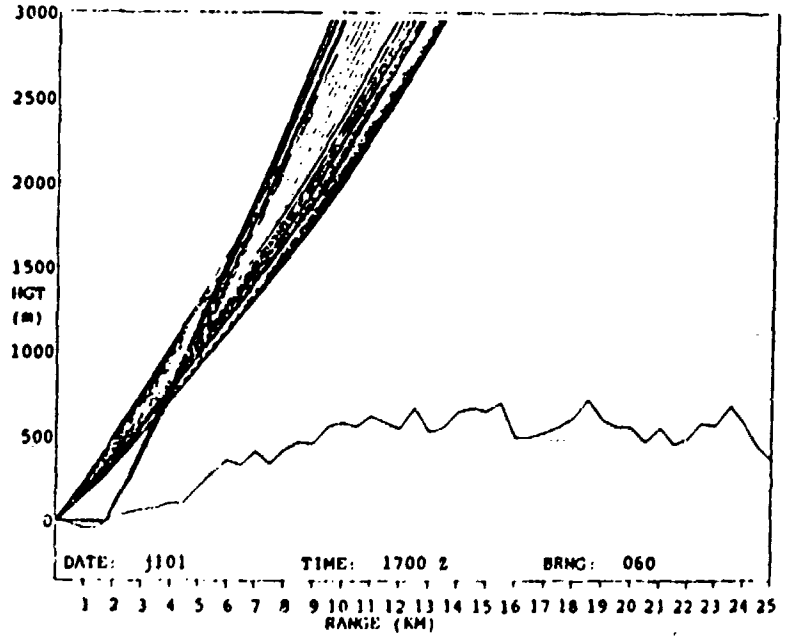

Figure 6.25. Ray Trace, 1700 L.T., 1 July, 1971 (Extreme Day)

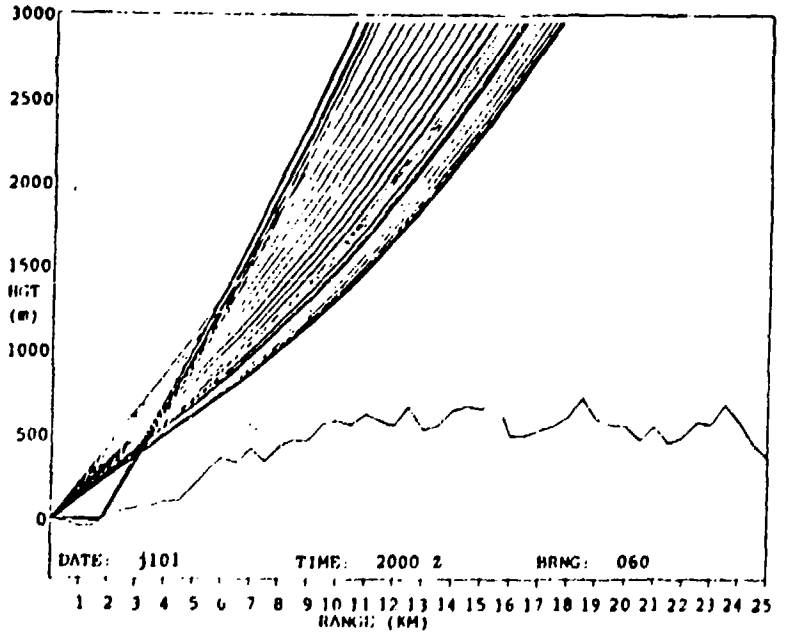

Figure 6.26. Ray Trace, 2000 L.T., 1 July, 1971 (Extreme Day)

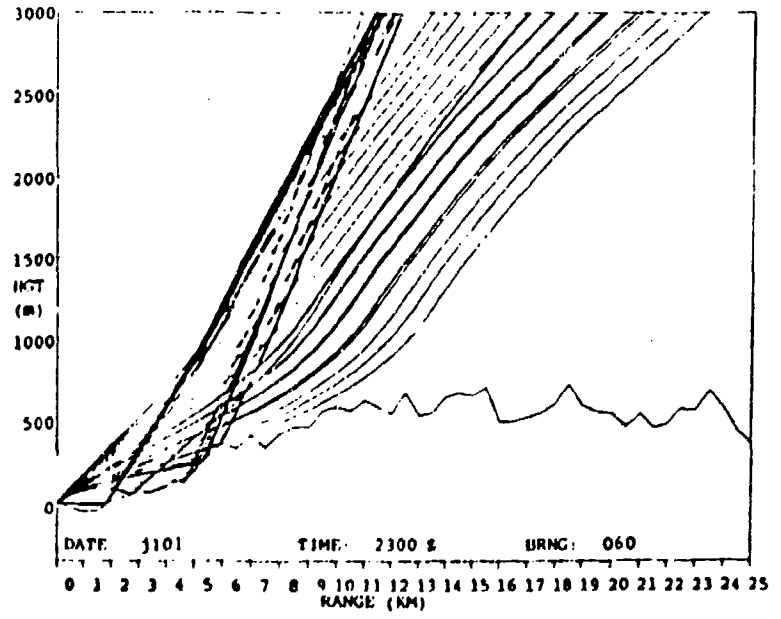

Figure 6.27. Ray Trace, 2300 L.T., 1 July, 1971 (Extreme Day)

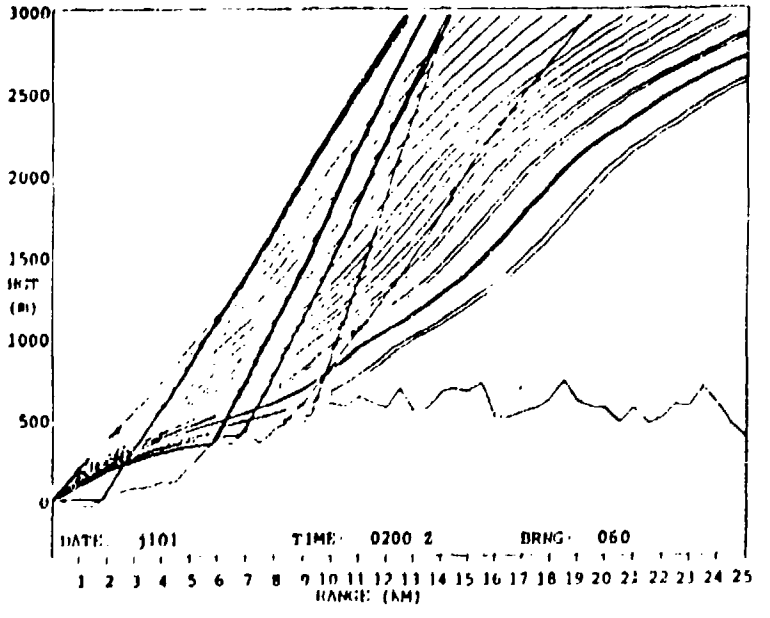

Figure 6.28. Ray Trace, 0200 L.T., 1 July, 1971 (Extreme Day)

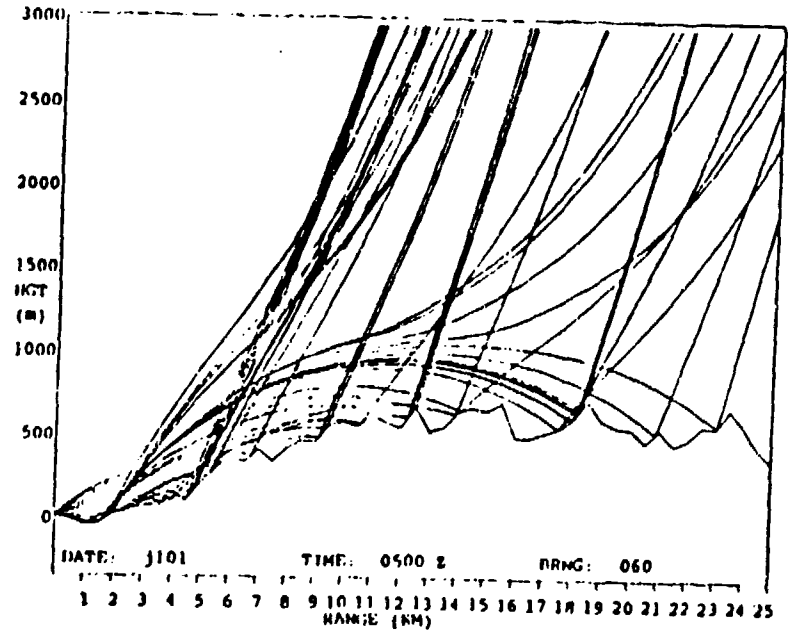

Figure 6.29. Ray Trace, 0500 L.T., 1 July, 1971 (Extreme Day)

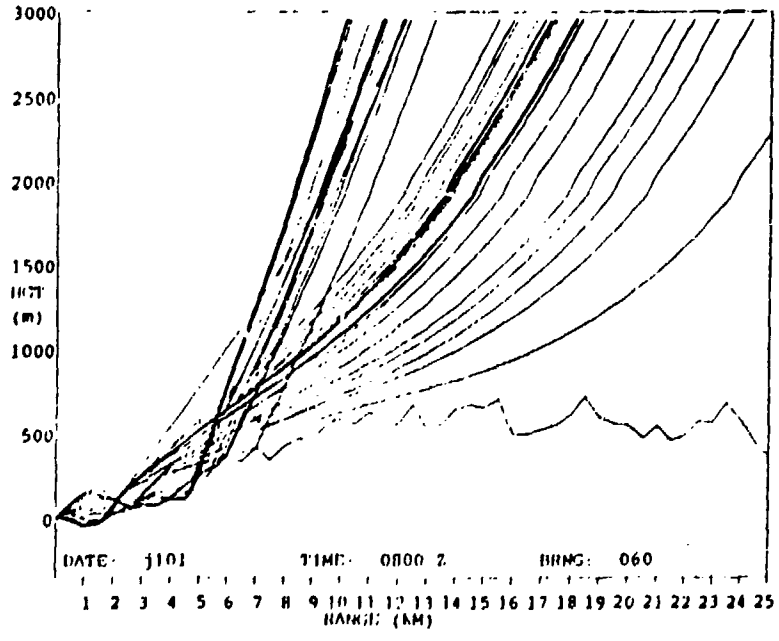

Figure 6.30. Ray Trace, 0800 L.T., 1 July, 1971 (Extreme Day)

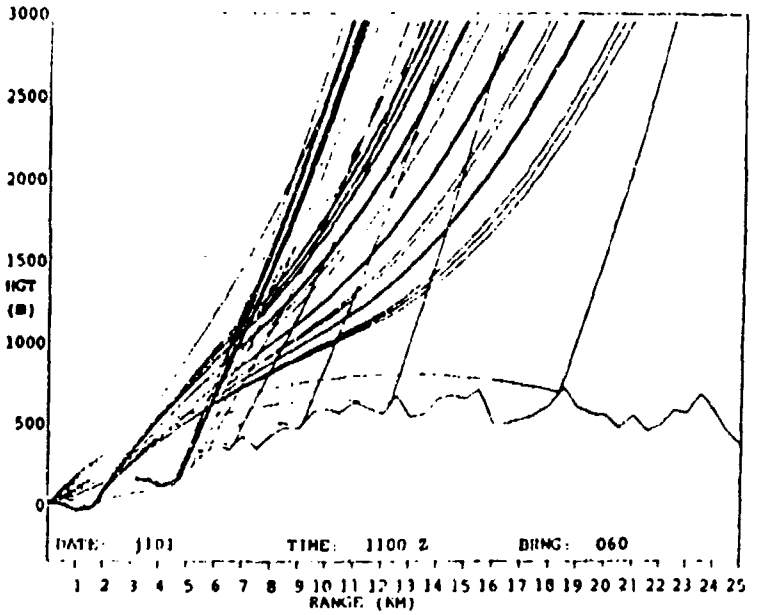

Figure 6.31. Ray Trace, 1100 L.T., 1 July, 1971 (Extreme Day)

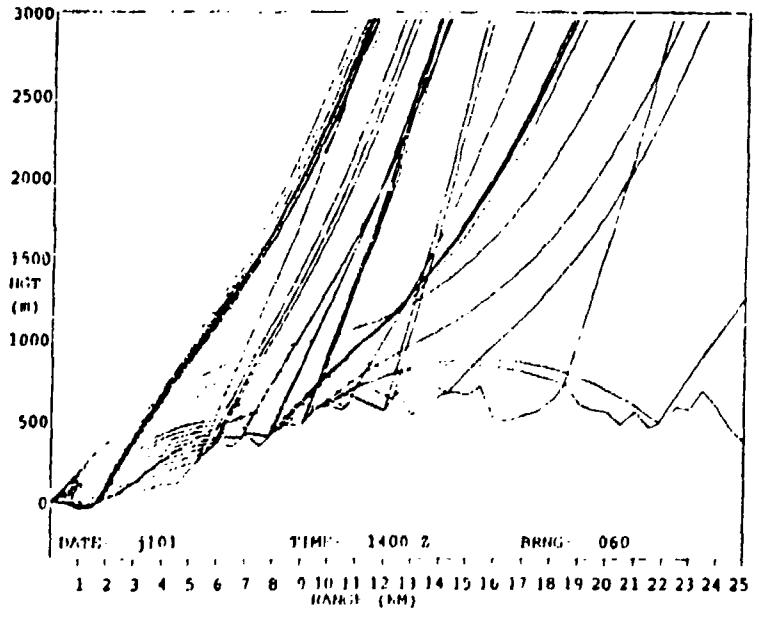

Figure 6.32. Ray Trace, 1400 L.T., 1 July, 1971 (Extreme Day)

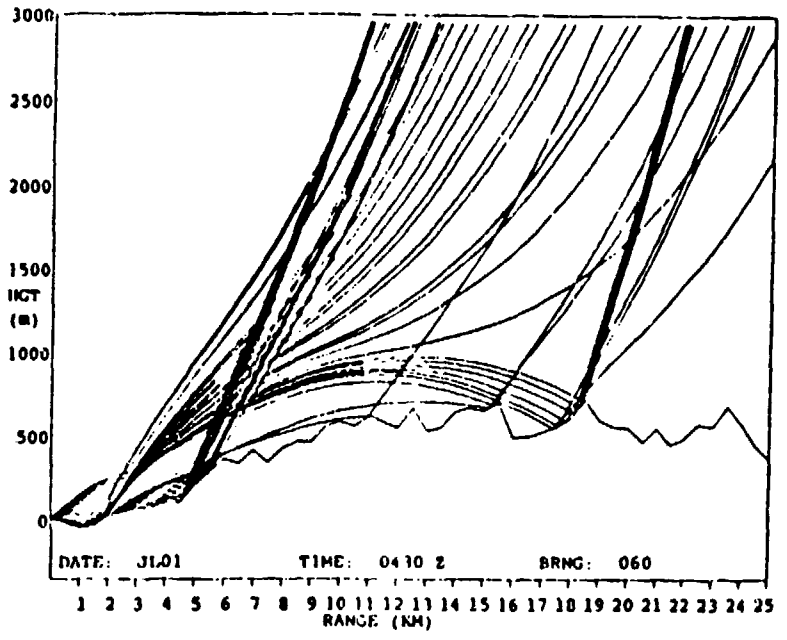

Figure 6.33. Ray Trace, 0430 L.T., 1 July, 1971 (Extreme Day)

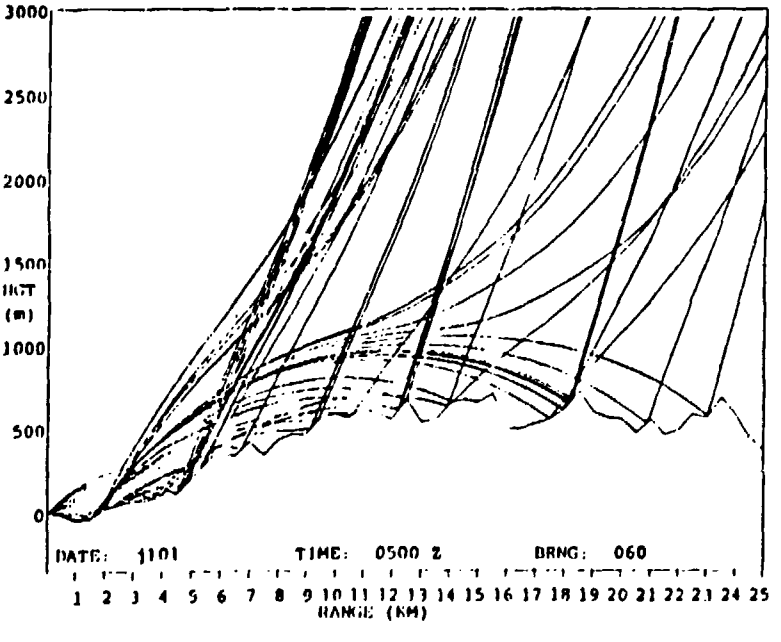

Figure 6.34. Ray Trace, 0500 L.T., 1 July, 1971 (Extreme Day)

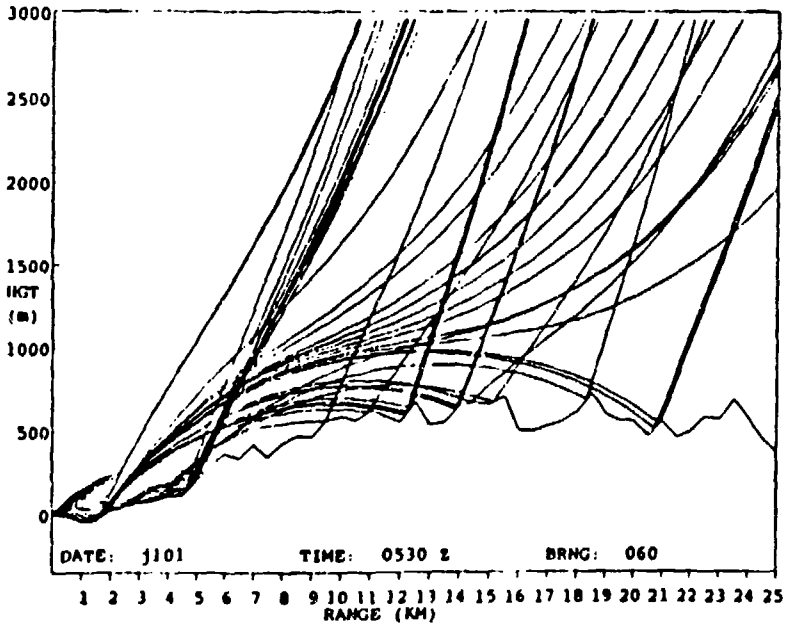

Figure 6.35. Ray Trace, 0530 L.T., 1 July, 1971 (Extreme Day)

6.3.1.2. AMPLITUDE

Using the sound pressure level graphs from 1 July, Figures 6.36 - 6.38, it is easier to distinguish one time from another as well as one horizontal range from another. Consider the 63 Hertz data, having the lower atmospheric attenuation, for 0430. The nearest range to which sound would be detected at a continuous set of targets stops at a close distance of 1.3 kilometers; for 0500 this range extends out to 2.5 kilometers; and for 0530 out to 1.8 kilometers. A second range is defined where notable sound levels are no longer continuously present with distance but rather occur only intermittently. This range is includes the appearance of sound at some targets and its absence at others. In general in this range interval at a given time there are about as many locations with sound as without. For 0430 this range begins around 1.3 kilometers and ends around 5.6 kilometers; for 0500 the range is from 2.5 kilometers to 5.6 kilometers; and for 0530 1.8 kilometers to 5.0 kilometers cover the intermittent range. For these intermediate distances not only is the extent of the range variable but also the apparent signature of the sound. It is evident that at all three times the rays hit at different targets. Table 6.2 shows the sound pressure level for the three times in a small section of this range. Note how the SPL at the various targets changes with time.

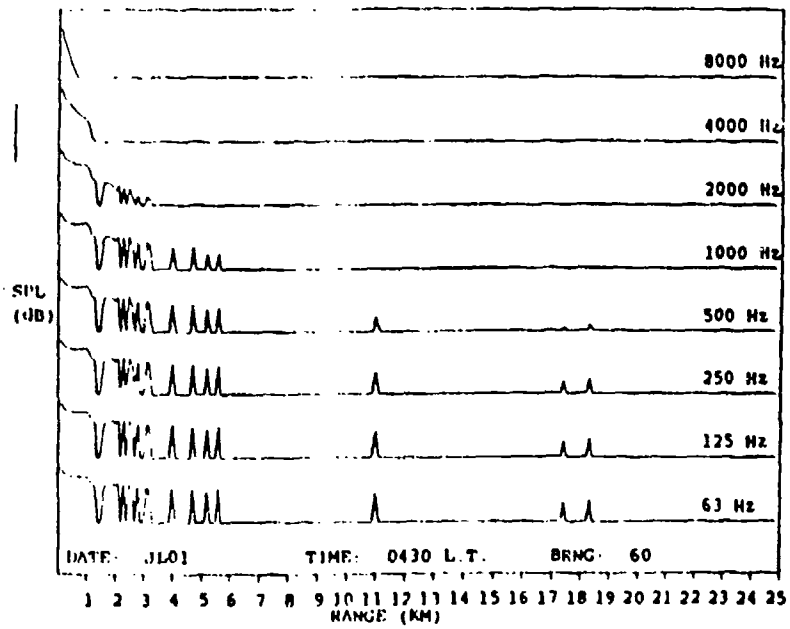

Figure 6.36. Sound Pressure Level Diagram, 0430 L.T., 1 July, 1971 (Extreme Day)

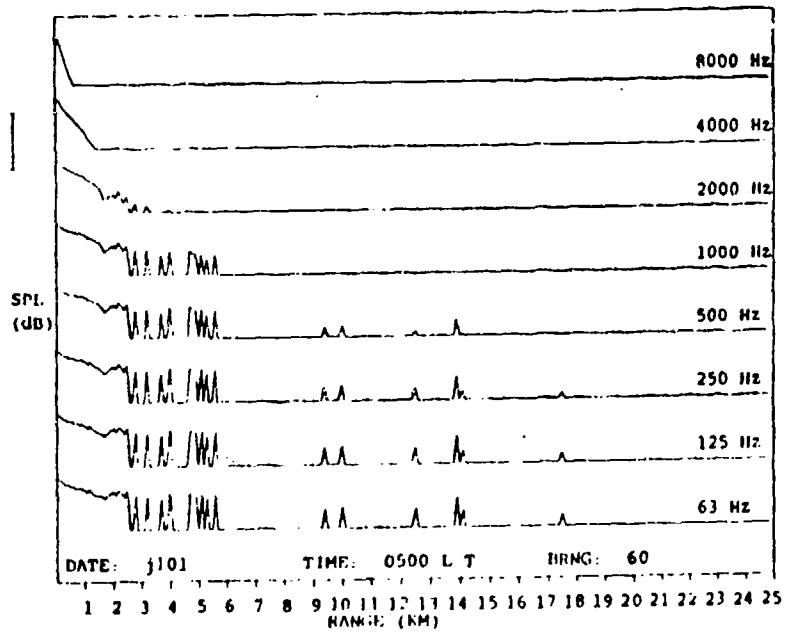

Figure 6.37. Sound Pressure Level Diagram, 0500 L.T., 1 July, 1971 (Extreme Day)

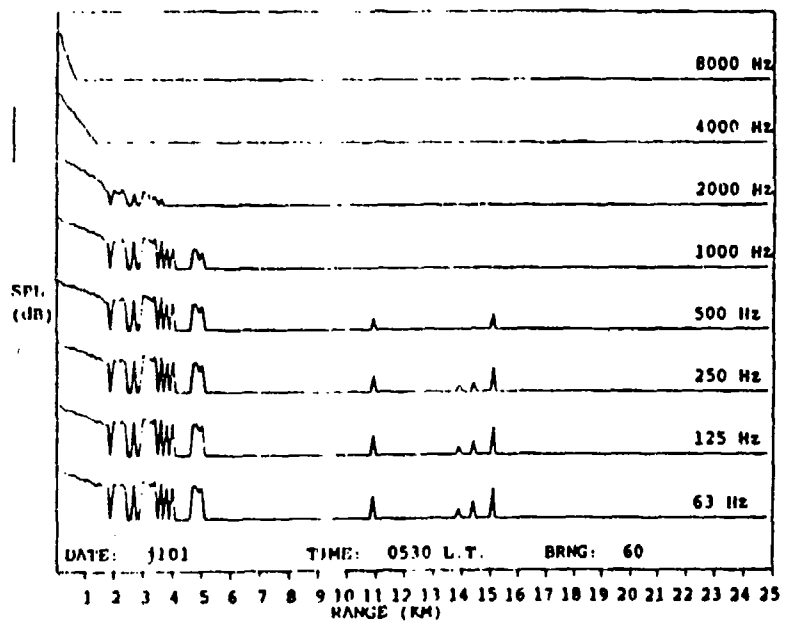

Figure 6.38. Sound Pressure Level Diagram, 0530 L.T., 1 July, 1971 (Extreme Day)

Table 6.2. Sound Pressure Level versus Time and Location

	target	3.0	3.1	3.2	3.3
time	0430	---	20.8	13.0	---
	0500	---	---	16.2	---
	0530	31.7	28.7	23.1	14.1

A third and final range interval can be defined as one with "sporadic" occurrence of sound. Once again, as shown in the diagrams, this range is quite different at each of the three times. Characteristics such as the location, number, and magnitude of hits are highly time dependent. From this comparison it is clear that each sound velocity profile results in a particular distribution of SPL. In using the SPL graphs to describe sound propagation it is important to identify the time associated with each graph. A new profile is needed to describe propagation at a new time.

Not only will the propagation of sound change throughout any given day, it will also change from day to day. Comparing Figures 6.17 - 6.24 to Figures 6.25 - 6.32, the persistent sound channel of the extreme day is evident in the evolution of the ray traces. In general, for 1 July, more rays are refracted downwards as well as refracted to larger ranges. This is especially apparent from the times 0200 to 1100. Comparing the ray trace from one time on the extreme to the ray trace from the same time on the typical day, the differences are obvious.

6.3.1.3. THE EFFECTS OF TOPOGRAPHY

To this point we have explicitly addressed only the effects of the meteorological parameters on sound propagation. The particular topography along the sound propagation path also is extremely important. Sloping ground will have a different angle of incidence and reflection from that of flat ground. A ray with a reflection angle that normally causes the ray to refract downwards on flat ground may be changed in such a way that the new angle is above the critical angle and thus will cause the ray to refract upwards. Or following a reflection the new angle may still be below critical; however, the ray may travel a longer distance before again reaching the ground. Sloping ground may also "cut off" the ray, causing it to travel a shorter distance between bounces. To illustrate the importance of topography, the results from a run with topography will be compared to a run with only a flat surface. For this purpose the meteorological profiles from 1 July, at 0500 were used. Figures 6.39 and 6.40 show the ray trace and SPL graphs, respectively, for flat ground. On the ray trace all the rays are refracted continuously towards the ground. The ray with the highest launch angle extends to a horizontal distance of about seven kilometers between each bounce. The +10° ray, however in Figure 6.34, travels a horizontal distance of 5.2 kilometers before it is intercepted by the ground and then is sent upwards never to return. Also evident in this figure is that some of the other rays after their second bounce travel horizontal distances of up to twenty-three kilometers.

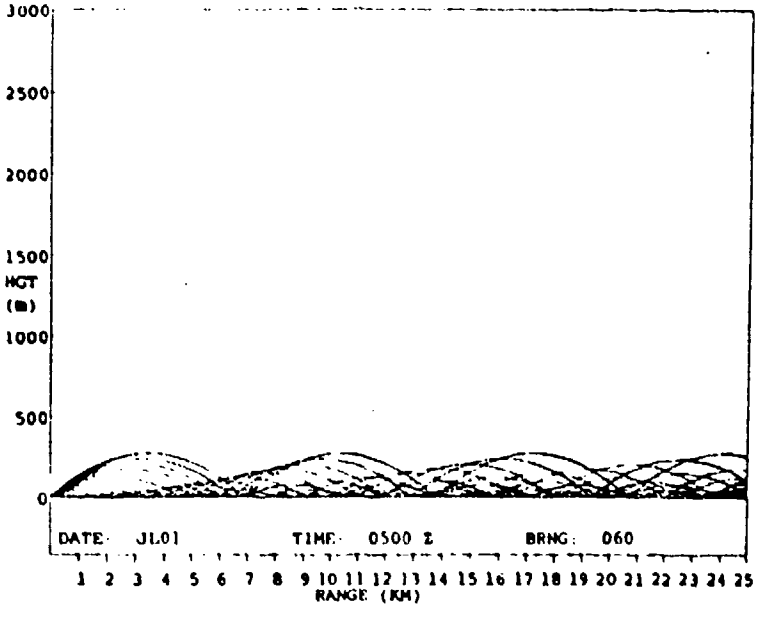

Figure 6.39. Ray Trace, 0500 L.T., 1 July, 1971, Flat Terrain

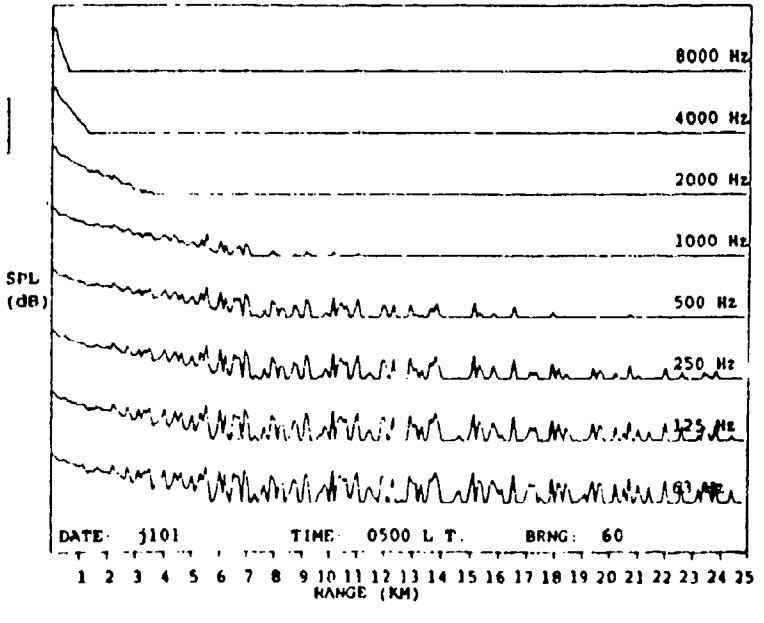

Figure 6.40. Sound Pressure Level Diagram, 0500 L.T., 1 July, 1971, Flat Terrain

Clearly the topography thus also modifies the nature of the SPL diagrams. Compare Figure 6.37 to Figure 6.40, topography to no topography. All three classifications of sound ranges -- continuous, intermittent, and sporadic are evident in the topography run. The length of the intermittent range along with the absence of the sporadic range distinguishes the SPL with no topography from that of the SPL with topography. For no topography the continuous range ends around 5.5 kilometers and the intermittent range continues all the way to the twenty-fifth target. Also evident are the effects of shielding due to the sloping ground.

Even without topography interesting features do show up in Figure 6.40 -- fluctuations out to twenty-five kilometers. The continual downward refraction and reflection of all the rays sets up a complicated multipath propagation situation to most of the targets. This means that even out to the large distances many rays may tend to converge at one target and produce a significant sound pressure level. It is quite obvious from the fluctuations that there is no constant six decibel decrease per doubling of distance, a common assumption which is mistakenly used in environmental noise impact studies.

5.3.1.4. PHASE

In section 5 discussing the validity of the program it was shown what happens to phase in simple artificial environments. The case study demonstrates the effects that temporally active variable gradient sound speed profiles have on phase. In fact, it is possible

to use the signal phase to examine the temporal changes in the atmospheric sound speed profile. This principle is applied over short paths using ultrasonic frequencies in the sonic anemometers which are widely used for atmospheric surface layer wind velocity measurements (Fleagle, 1963, p. 294). Reviewing the profiles described in Section 6.2, the temperature causes slight and smooth changes in the phase, while the wind exaggerates the temporal variability.

In Figures 6.41 and 6.42, phase versus time graphs of the three hour and half hour intervals for a target 500 meters from the source are displayed. Two precautions are necessary if one is using this type of graph. The first deals with the "problem" of the phase being the sum of all the phases from each ray coming into the named target. This sum is modulated over 2π, i.e. 360 degrees. In principle the increase of 340 degrees between the times 0530 and 0600 in Figure 6.42 could actually be a decrease of 20 degrees. The other admonition is to consider the temporal resolution of the data before analyzing the signal fluctuations. A change in signal that appears small on a low resolution graph may have actually included many fluctuations of that signal over a greater range of values and would be evident on a graph of higher resolution. This limitation can be demonstrated by using the three hour and half-hour results at target 27. The graphs are shown in Figures 6.43 and 6.44. First of all, it is evident from the three hour graph that there is a small phase change between the hours of 0500 and 0800. However, between the same hours on the half hour resolution graph the phase fluctuate over a range of 150 degrees. It is also interesting to note that on the first graph it appears as if

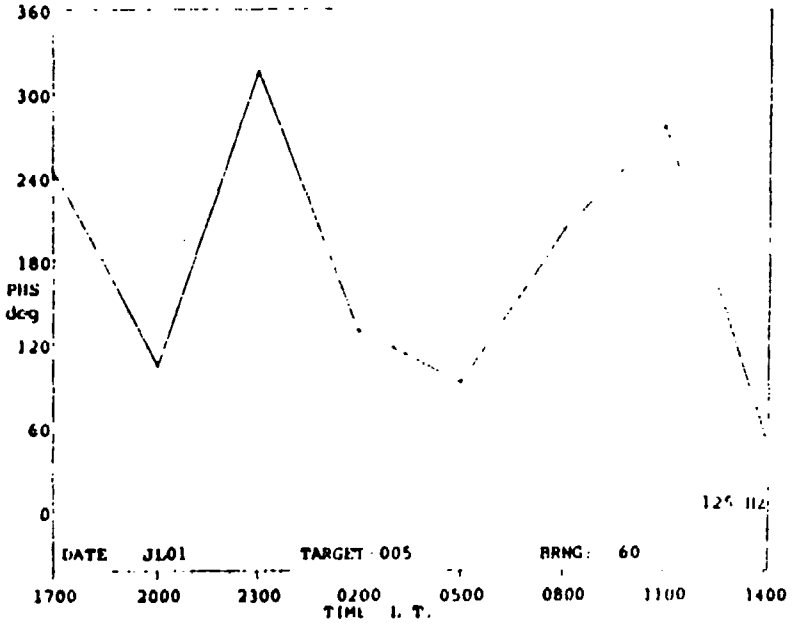

Figure 6.41. Phase versus Time, 1 July, 1971, 500 Meters from the Source, 3 Hour Intervals

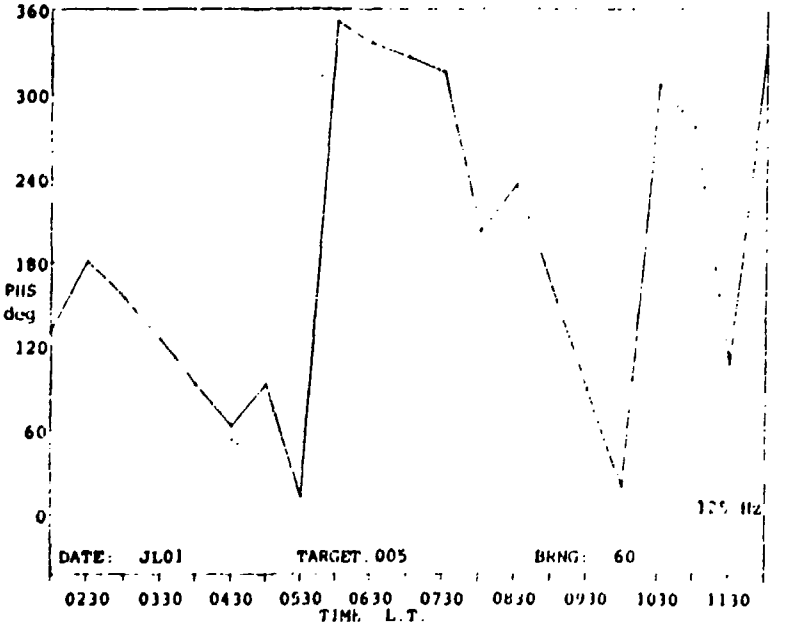

Figure 6.42. Phase versus Time, 1 July, 1971, 500 Meters from the Source, 1/2 Hour Intervals

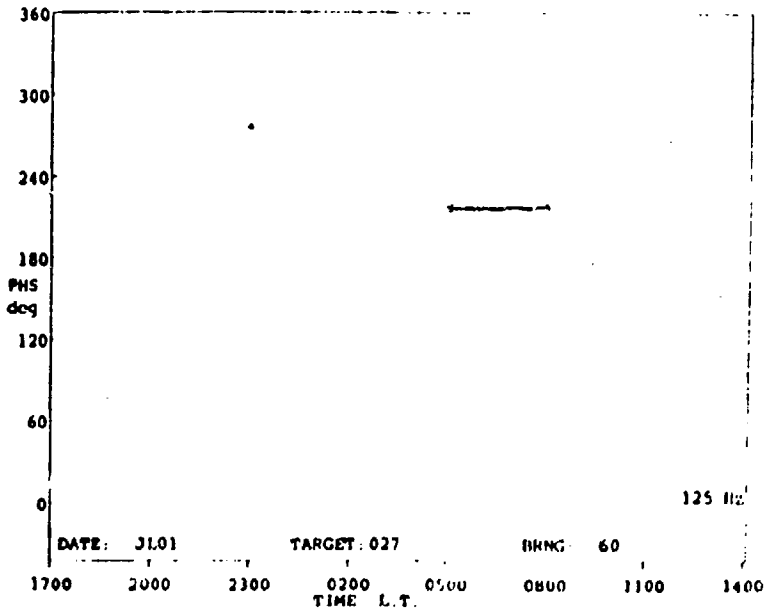

Figure 6.43. Phase versus Time, 1 July, 1971, 2700 Meters from the Source, 3 Hour Intervals

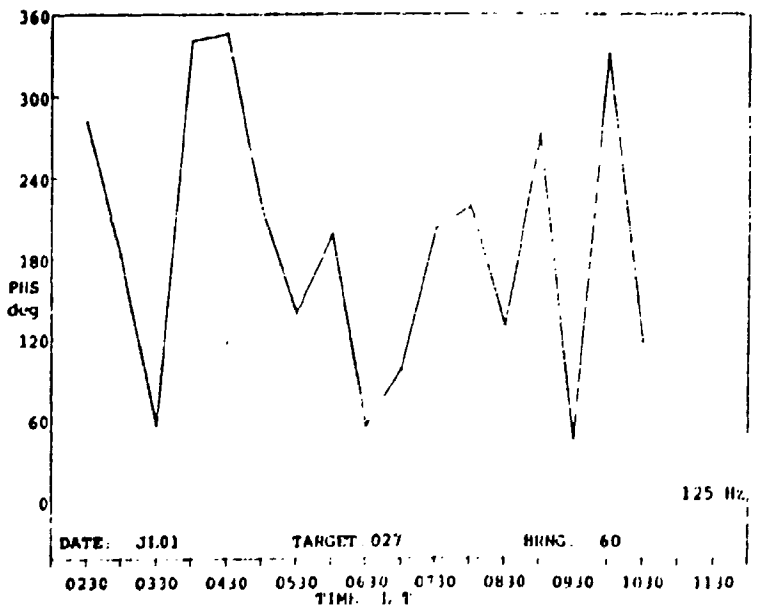

Figure 6.44. Phase versus Time, 1 July, 1971, 2700 Meters from the Source, 1/2 Hour Intervals

no rays managed to reach this target before 0500 or after 0800. But the second graph indicates that much activity existed on either side of those times.

Due to the fluctuating speed of sound profile three "events" could happen which would result in a difference in total phase at a single location from one time to the next. 1) Even though the same rays, in number and launch angle, reached the target the travel times due to the new profile might be shortened slightly causing the respective phases to sum up to a new total. See Table 6.3 for a listing of the rays entering different targets at different times. At the 500 m target at the times 0230, 0300, and 0330 the same three rays came into the target, each with a different phase from the previous time. Figure 6.42 shows that the total phase decreased continually by about 50°. 2) With the new profile a different number of rays could reach the target. The same rays plus one or two more will guarantee a change in the resultant phase. This kind of event occurred between the times 0330 and 0400 at the 500 m target. Again the phase decreased by 50°. 3) The same number of rays but with all together different launch angles could reach the target. The different launch angles coincide with different path lengths and thus travel times. At the 2800 m distance this occurred between 0730 and 0800, and between 0800 and 0830. At each time a different set of four rays reached the target. Changes in the total phase are shown in Figure 6.45 to be decreases of 130°. It has been shown in these examples how easily the atmosphere can change signal phase at a given target. The changes can be produced by shortening or stretching the path of a particular ray

Table 6.3. The Phase of Rays Entering Various Targets at Various Times

Location (m)	Time	Launch Angle (°)	Phase (rads)
500	0230	-2.0	1153.08
		-2.5	1153.07
		-3.0	1152.79
	0300	-2.0	1152.68
		-2.5	1152.52
		-3.0	1152.27
	0330	-2.0	1152.21
		-2.5	1151.94
		-3.0	1151.73
	0400	-1.5	1151.34
		-2.0	1151.72
		-2.5	1151.39
		-3.0	1151.17
2800	0730	+5.5	6423.52
		+4.0	6423.80
		-9.5	6425.81
		-10.0	6425.68
	0800	+10.0	6413.84
		+9.5	6415.97
		+5.0	6422.52
		-7.0	6418.14
	0830	+10.0	6411.77
		-8.0	6417.69
		-9.5	6419.53
		+10.0	6422.17

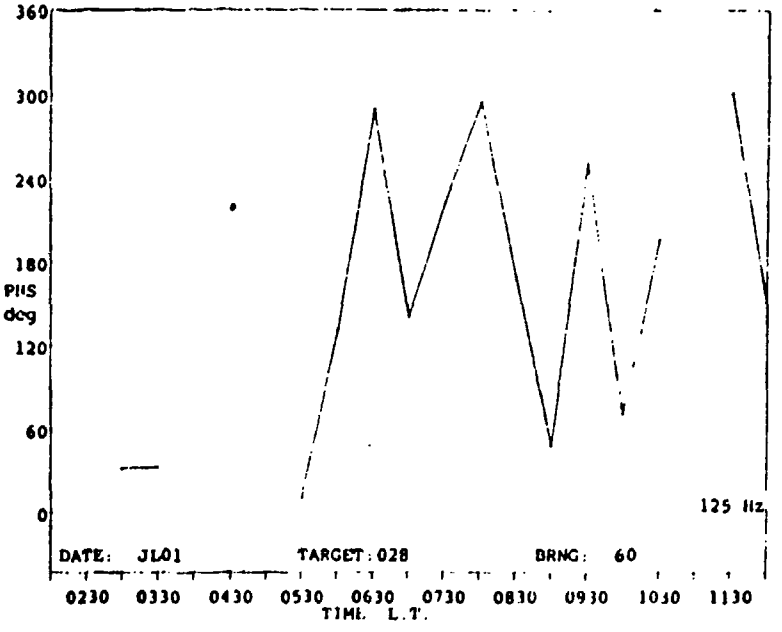

Figure 6.45. Phase versus Time, 1 July, 1971, 2800 Meters from the Source, 1/2 Hour Intervals

or by changing the number of rays contributing to the signal at the location of interest. It sometimes appears that the phase of the signal can be a better monitor of the atmosphere than signal amplitude or power. Stretching or shortening the path length will cause the phase to change by an amount proportional to the number of wavelengths in this path change. Changes in path length will also cause changes in the atmospheric absorption loss which in turn effects the sound pressure level. Differences in SPL from reductions or increases in absorption are usually small by comparison to changes in phase. Consider a path length increase of $\lambda/2$ which will increase the phase by π radians or 180°. The absorption loss, say for 125 Hz signal, in an isothermal atmosphere of 20 °C and relative humidity at 15%, would be only about 9.6×10^{-4} dB for the same path length change. Either graphically or in actuality such changes would be imperceptible. An example in which the magnitude has a very small change and the phase has a large change is at the 500 m target at the times 0230, 0300, and 0330. Compare Figure 6.42 to Figure 6.46. The phase changes by 50° whereas the magnitude is essentially constant.

6.3.2. STATISTICS

With time varying signals such as the amplitude and phase fluctuations it is useful to explore their statistical properties. For a study of sound propagation the mean and standard deviation, the cumulative relative frequencies (CRF), and the frequency histogram are all appropriate methods to parameterize the fluctuations. The mean

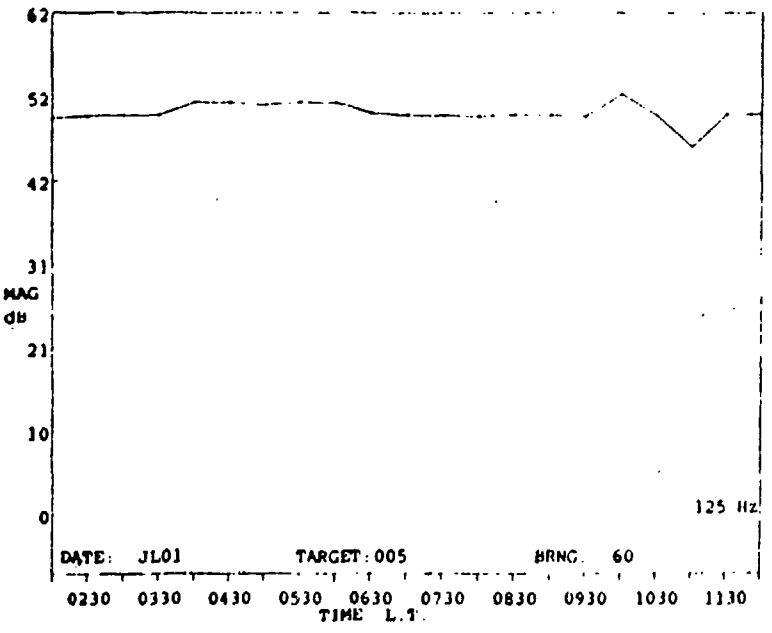

Figure 6.46. Coherent Sum versus Time, 1 July, 1971, 500 Meters from the Source, 1/2 Hour Intervals

and standard deviation give a quantitative rather than a qualitative description. The latter was supplied by the graphs. Means with percentile standard deviations provide another alternative description of the data. Since neither the amplitude nor the phase remain constant but have continuously changing values, the percent of time the amplitude or phase is at or below specified levels may also be useful. The CRFs are plots of such data. The distribution of the predicted SPLs or phases can also be displayed in a histogram format. The range of predicted values is divided up into equal increments called bins. The number of times the data is equal to a level within an increment is the said size or value of this bin.

For these statistical summaries, the data are separated by frequency and horizontal range. The case study focused on the frequencies: 125, 500, and 2000 Hz. Table 6.4 in Section 6.3.2.2. shows the location of each of the six horizontal ranges. By further stratifying the statistical properties by range one can evaluate the spatial variability of the sound propagation.

6.3.2.1. AMPLITUDE

Environmental noise impact studies are an area which could profit from wider use of statistical evaluation of amplitude variations. Every environmental study is unique. A change in any input parameter such as a different day's meteorological data or a variation in the terrain, will yield a change in the results which can best be shown using a statistical summary. The following discussion

using statistical summaries pertains only to this case study. But it is a general example of how environmental studies could benefit from such analyses.

For this study examples of the mean and standard deviations, and the mean and percentile standard deviations at each range for each frequency are shown in Figures 6.47 - 6.52. In general, the mean values decrease rapidly within the first three ranges. At larger ranges for both 125 and 500 Hz the mean values remain nearly constant. At these distances each range contains an abundance of shadow zone values, values of 0.0 dB. These keep the means about the same. The frequency histograms, Figures 6.53 - 6.58, show how much larger in number the shadow zone values are from any other predicted value in these ranges. For 2000 Hz the mean value actually increases from the fourth to the fifth range and again from the fifth to the sixth. This "increase" is fictitious in that it is a result of the predominance of shadow zone values. Even though mathematically a zero value is greater than a negative value, in this study a zero SPL is the absence of sound while a negative SPL is the presence of a very low level signal. Thus, this increase does not necessarily imply an increase in "loudness." One question to ask in comparing these means is why the values for the 2000 Hz signal are less than the other frequencies, range for range? This is the result of the greater attenuation at the higher frequencies. For all three frequencies it is clear that the SPLs and the means do not decrease at a rate of six decibels per doubling of distance, the distribution which is predicted on the basis of spherical spreading. Both shadowing and multiple ray paths

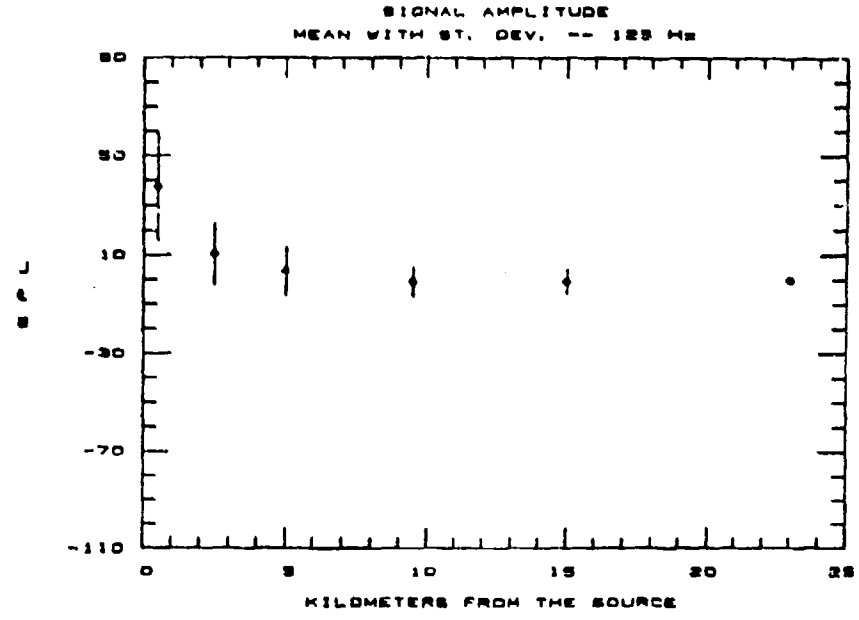

Figure 6.47. Mean and Standard Deviation of the Signal Amplitude by Range, 1 July, 125 Hz

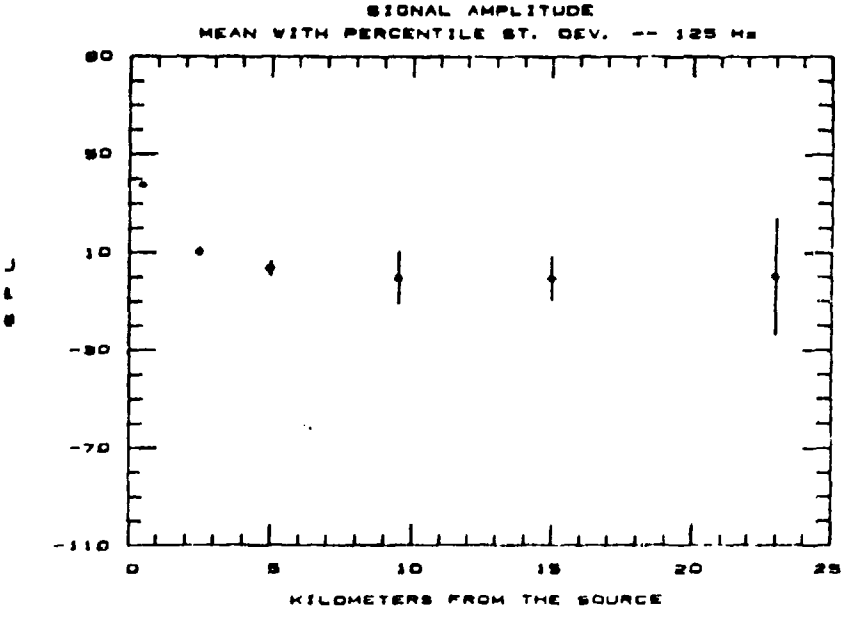

Figure 6.48. Mean and Percentile Standard Deviation of the Signal Amplitude by Range, 1 July, 125 Hz

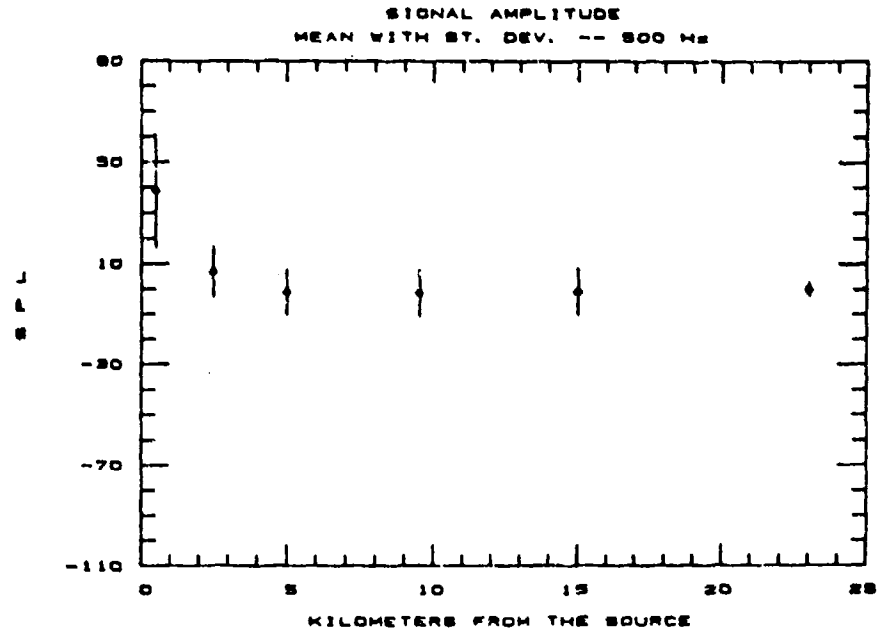

Figure 6.49. Mean and Standard Deviation of the Signal Amplitude by Range, 1 July, 500 Hz

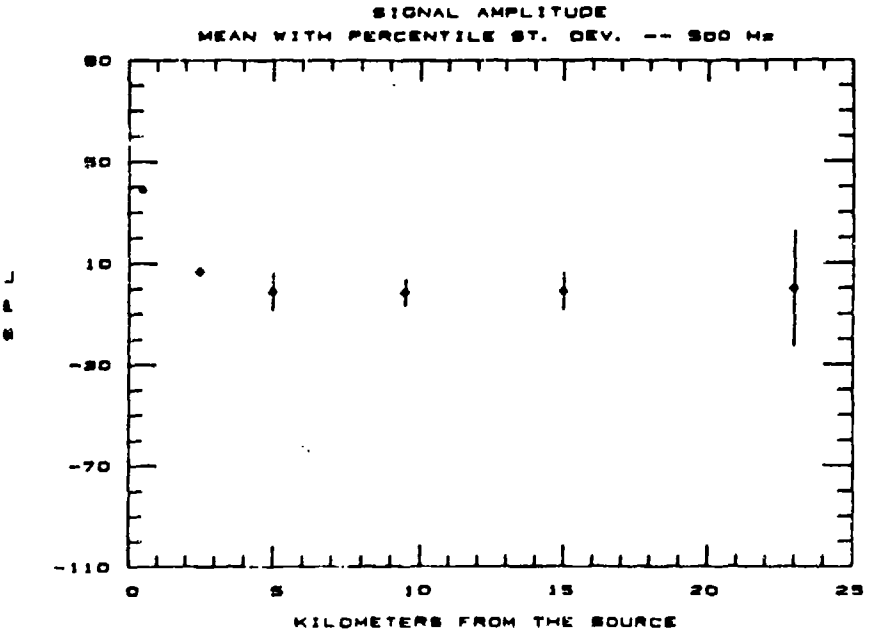

Figure 6.50. Mean and Percentile Standard Deviation of the Signal Amplitude by Range, 1 July, 500 Hz

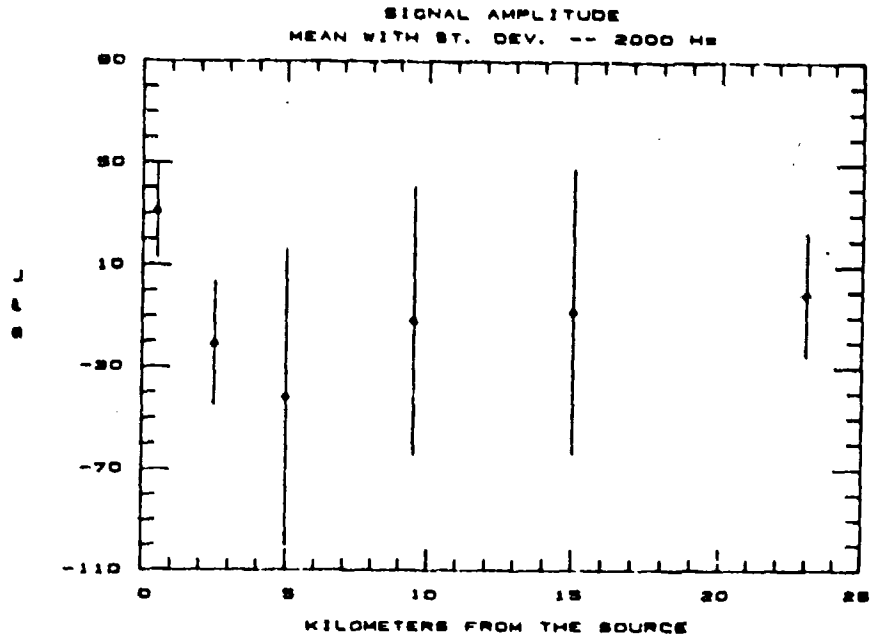

Figure 6.51. Mean and Standard Deviation of the Signal Amplitude by Range, 1 July, 2000 Hz

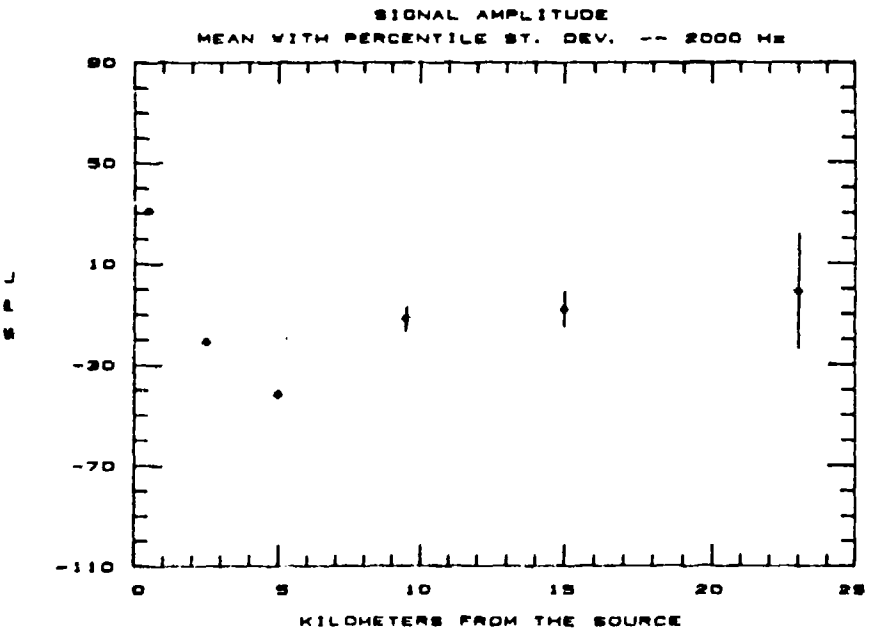

Figure 6.52. Mean and Percentile Standard Deviation of the Signal Amplitude by Range, 1 July, 2000 Hz

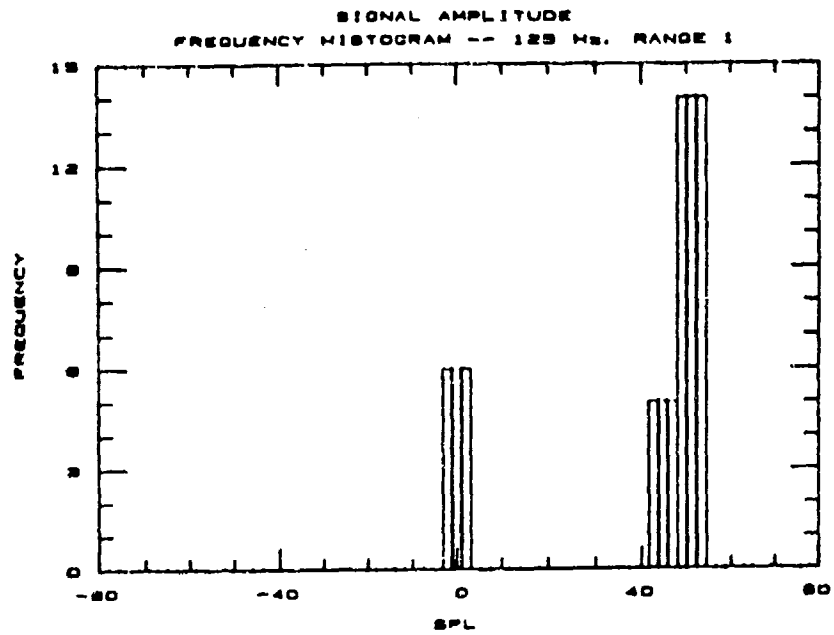

Figure 6.53. Frequency Histogram of the Signal Amplitude, Range 1, 1 July, 125 Hz

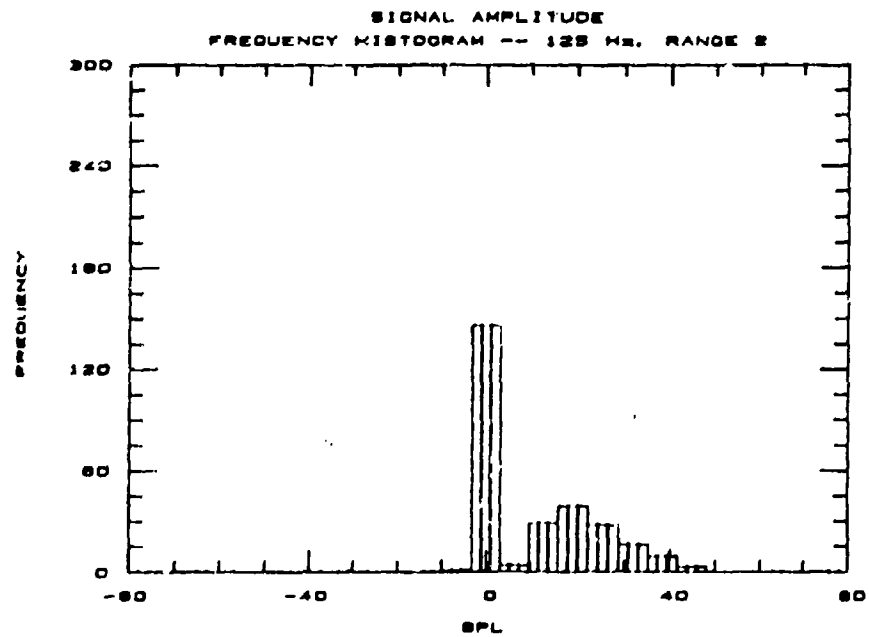

Figure 6.54. Frequency Histogram of the Signal Amplitude, Range 2, 1 July, 125 Hz

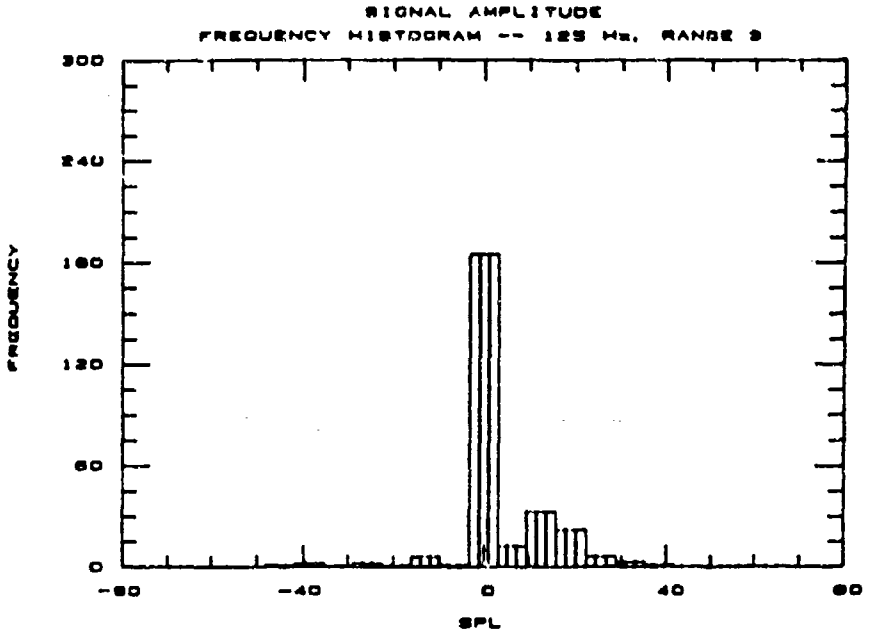

Figure 6.55. Frequency Histogram of the Signal Amplitude, Range 3, 1 July, 125 Hz

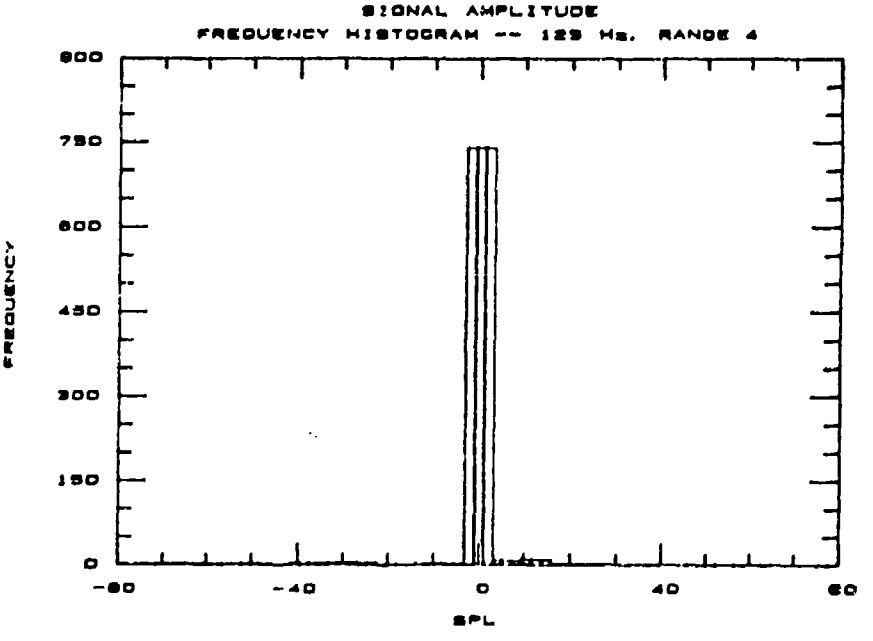

Figure 6.56. Frequency Histogram of the Signal Amplitude, Range 4, 1 July, 125 Hz

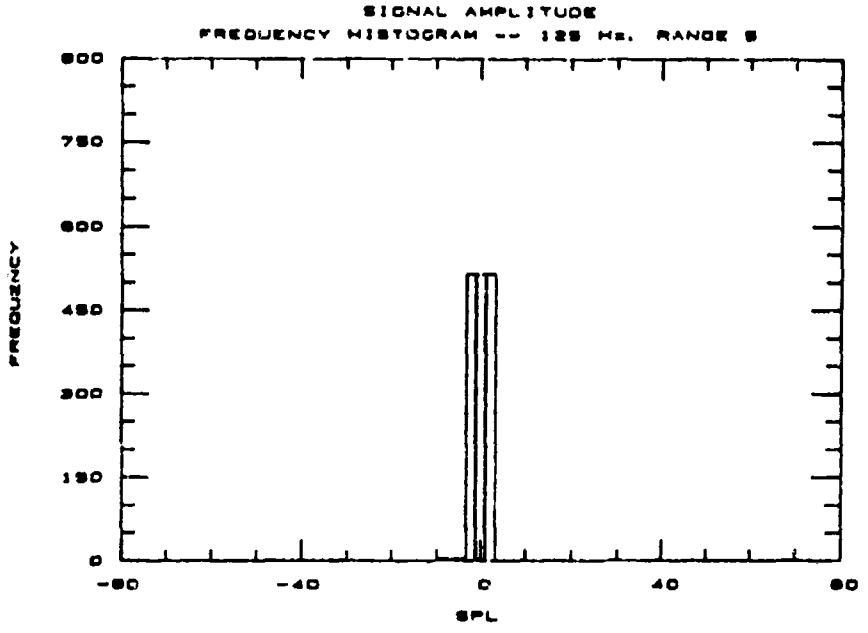

Figure 6.57. Frequency Histogram of the Signal Amplitude, Range 5, 1 July, 125 Hz

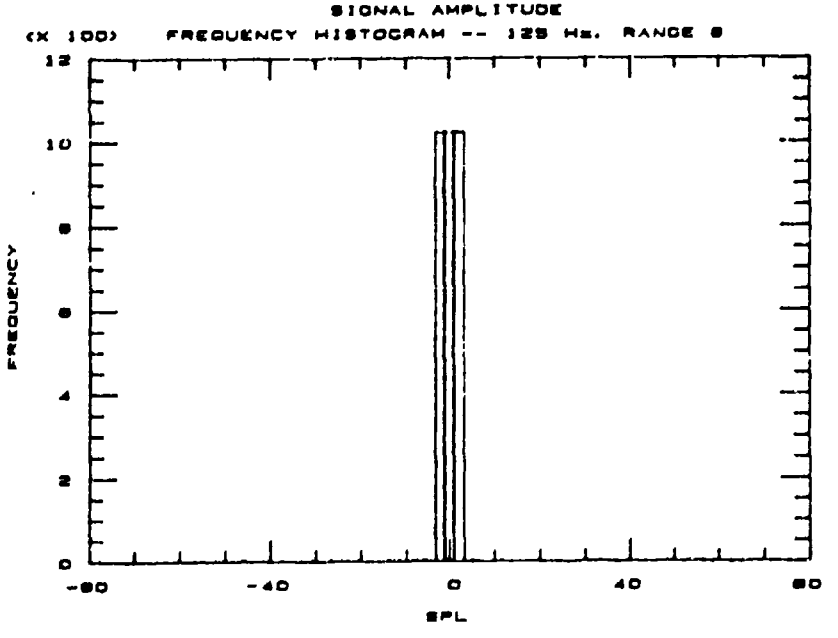

Figure 6.58. Frequency Histogram of the Signal Amplitude, Range 6, 1 July, 125 Hz

contribute to the departures from classical spherical spreading.

As for the variation of the SPLs, the percentile standard deviation actually increases with distance from the source. This deviation is computed by dividing the unaltered standard deviation by the mean for each range. The larger the percentile standard deviation the more noticeable one sound pressure level may be from another. These means and standard deviations are good indicators of the limits of the SPLs at different distances.

Knowing the limits of the SPL values in a single horizontal range is not sufficient for a noise impact study. The CRFs add a sense of relativity to each value inside the limits. The graphs displayed in Figures 6.59 - 6.64 show the fraction of time that the SPL is at or below a given value. The graphs could just as easily be interpreted as the percentage of time the SPL is at or above a given value. For example, for 125 Hz the noise in Range 2 is 23 dB or lower eighty percent of the time. The results could also have been expressed as "twenty percent of the time the noise level exceeds 23 dB." These types of statistics are more useful in the near and intermediate ranges than in the far. As is evident in Figure 6.63 the prediction to be noted is that the values are all below zero and that the percent of time that there are non-zero values is exceedingly small. However, Figure 6.61 shows variations of 40 dB (0.0 to 40.0 dB) spread over thirty percent of the time. Starting with the 0 dB value, the graph shows that twenty-eight percent of the time the level exceeds 0 dB, twenty-three percent of the time it exceeds 10 dB, twelve percent 15 dB and so on until for just two percent of the time

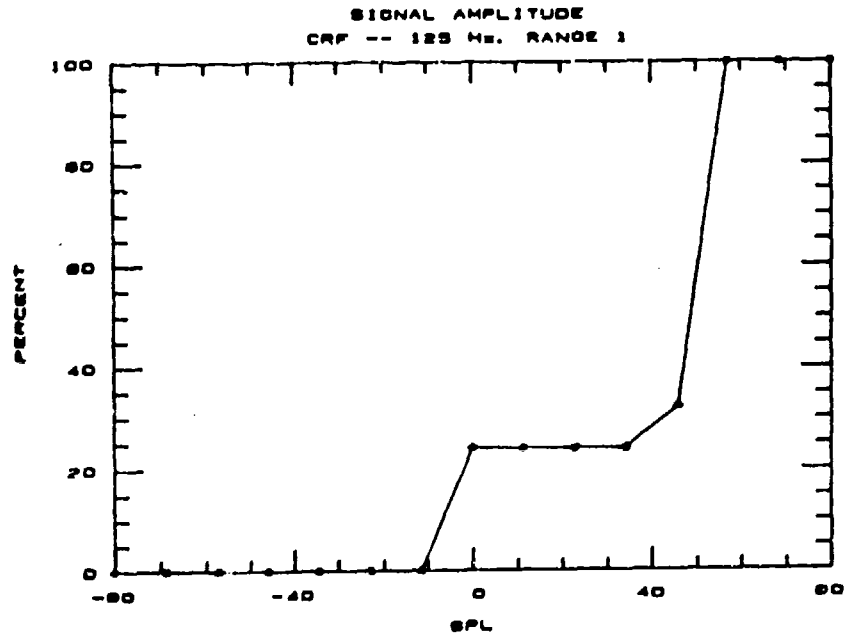

Figure 6.59. Cumulative Relative Frequencies of the Signal Amplitude, Range 1, 1 July, 125 Hz

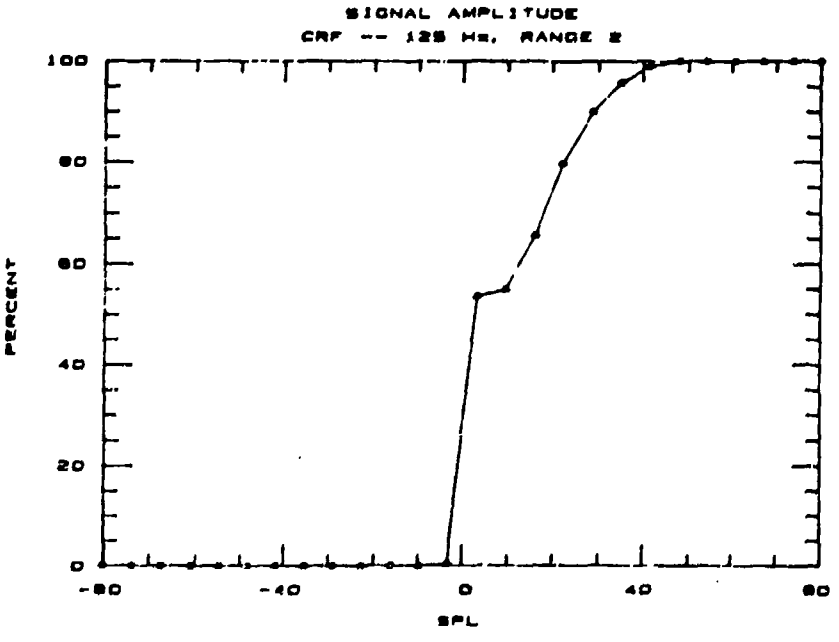

Figure 6.60. Cumulative Relative Frequencies of the Signal Amplitude, Range 2, 1 July, 125 Hz

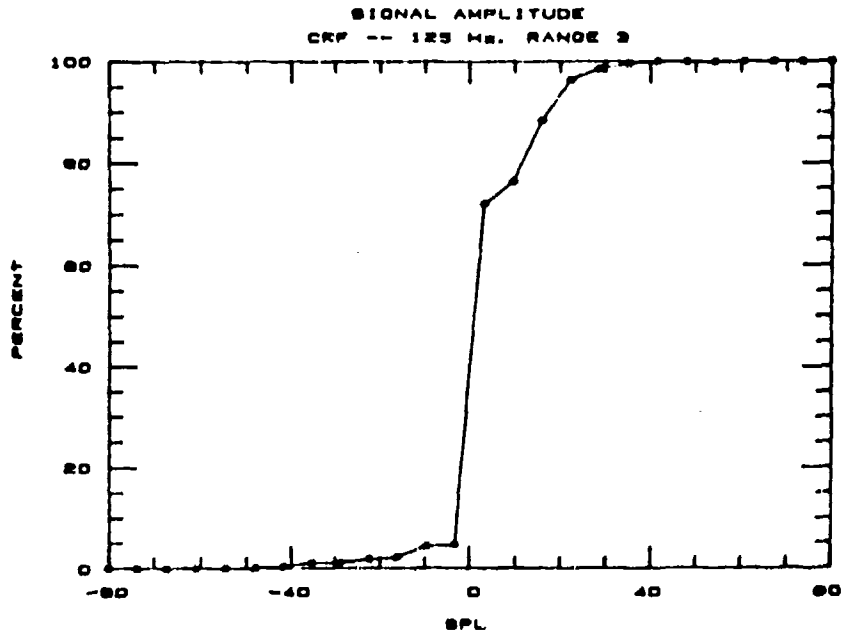

Figure 6.61. Cumulative Relative Frequencies of the Signal Amplitude, Range 3, 1 July, 125 Hz

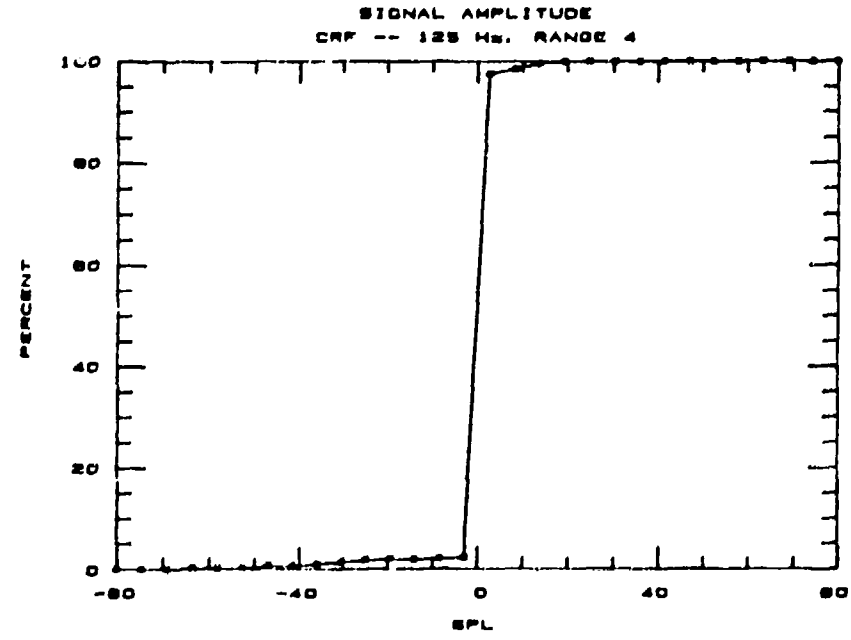

Figure 6.62. Cumulative Relative Frequencies of the Signal Amplitude, Range 4, 1 July, 125 Hz

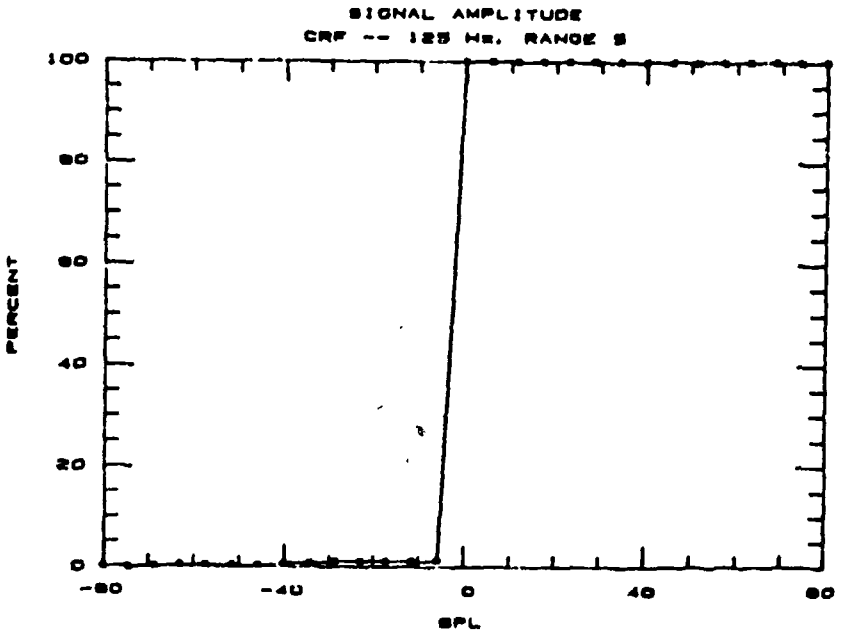

Figure 6.63. Cumulative Relative Frequencies of the Signal Amplitude, Range 5, 1 July, 125 Hz

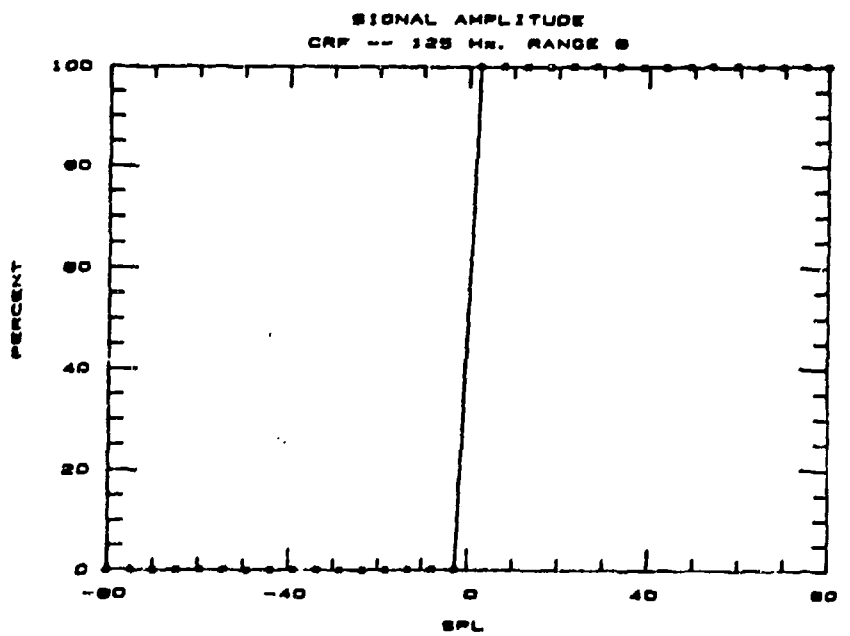

Figure 6.64. Cumulative Relative Frequencies of the Signal Amplitude, Range 6, 1 July, 125 Hz

the level exceeds 29 dB. But note that a high level for a short period of time might psychologically have quite a different impact from the same level for extended periods of time.

Comparatively, the ranges closest to the source have significant noise levels, i.e. positive non-zero levels, a greater percent of time. Once again, zero decibel values refer to the shadow zones and negative numbers indicate very low levels. At the furthest ranges, as is shown on the graphs, most of the time the sound is either absent or at very low levels. All the CRFs show a definite increase in percent of time at the zero decibel level.

The final set of graphs, the frequency histograms, Figures 6.53 - 6.58, simply show the distribution of the sound pressure levels within each range. In these graphs, it is easy to see the "size" of the shadow zone. In the 125 Hz histograms, a shadow zone exists in the first range but it is small compared to the other ranges. The other levels in Range 1 are all located within a narrow set of continuous bins. The bin containing the largest number of values falls within this distribution. In the second range the bin with the largest number of values corresponds to the shadow zone. It is not within the distribution. At this range the distribution is more spread out than in the first range -- seven bins instead of two. Range 3 is similar to Range 2 except that the size of the shadow zone is larger. This is significant considering the fact that the same number of targets is contained in both of these ranges. Also in Range 3 the distribution is no longer continuous and it contains a few more negative values. A significant change appears in the fourth range.

It is primarily a shadow zone. There are no outstanding values like those found especially in Range 1 and to a lesser extent in Ranges 2 and 3. Ranges 5 can be described in the same way as Range 4. Finally, Range 6 is basically all shadow zone. A spatial variation of the SPLs is clearly evident from this comparison of the frequency histograms.

Model output displayed in the form of a histogram, CRF, or mean and standard deviation shows both the temporal and spatial variations. While a graph of predicted signals at a single range can express the temporal fluctuations, a comparison of all the ranges is necessary to describe the spatial variations. Specific results are all highly dependent upon input parameters. Changing the topography, any aspect of the meteorological data or the source-receptor bearing may alter the statistics of the signal behavior.

6.3.2.2. THE EFFECTS OF TOPOGRAPHY

The effects of topography on a set of raw data (a ray trace and an SPL diagram) at a single time were discussed in the previous Section 6.3.1.3. The following is a review of these effects illustrated using the statistical summaries. Basically, the prior conclusions indicated the existence of significant sound pressure levels out to intermediate and far distances and the non-existence of the applied six decibel decrease per doubling of distance. Statistics were also computed of the signal amplitude using the Bryce Canyon meteorological data but without the actual topography. Hereafter this

no topography, flat environment will be referred to as "NT." Frequency histograms with only occasional input from the CRFs demonstrate the former conclusion. Means and standard deviations for the flat topography case clearly show that the signal can be altered by changes in topography.

Recall from the ray traces that the old topography often obstructed some rays from traveling to and beyond the intermediate distances. Thus, in comparison to NT the number and distribution of non-zero SPLs were reduced in the farther regions. The classification of the sound pressure levels and the details of the frequency histograms, range by range, are compared in Table 6.4 for both the topography and NT results.

Table 6.4. Classification of the Sound Pressure Levels, the Shadow Zone, and the Distribution of the Frequency Histogram

				Frequency Histogram (125 Hz)			
Range	Location	SPL Classification*		Size of the Shadow Zone (%)		Limits of the Distribution	
		Top.	No Top.	Top.	No Top.	Top.	No Top.
1	0.5	C**	C	24	32	0/55	0/68
2	2.0-3.0	C/I**	C	54	38	-10/48	-35/42
3	4.5-5.5	I	C	67	29	-48/42	-80/48
4	8.0-11.0	S	I	97	28	-40/15	-80/35
5	14.0-16.0	S	I	97	23	-10/0	-80/35
6	21.0-25.0	S	I	100	28	0/0	-80/10

*C = Continuous, I = Intermittent, S = Sporadic

**Continuous during the times 0330, 0700, 0730, and 0830

First of all in discussing Table 6.4, at no time nor location were the SPLs for the flat topography sparse enough to produce a sporadic classification. Only continuous and intermittent zones are predicted. The continuous region for no topography includes Ranges 1 - 3, whereas with topography the continuous region includes Range 1 and sometimes Range 2. To further emphasize the classification differences it is important to note that the intermittent zones end with Range 6 and Range ? for no topography and topography, respectively. Also the rest of the topography ranges are sporadic.

A comparison of the 125 Hz frequency histograms between selected ranges is presented to reinforce the importance of topographic shielding. First a comparison is made on Range 1, a range considered to be continuous for both the flat topography and the actual topographical environments. From Figures 6.65 and 6.53 it can be seen that in both cases the majority of the values are distributed well above the shadow zone. That is they fall above +40 dB. In the case of no terrain the values are spread out over a wider range of values -- a range from 35 - 68 compared with 42 - 55 dB. In fact comparing the two environments range by range (see Table 6.4, and Figures 6.65 - 6.70 and 6.53 - 6.58) NT always shows a broader distribution of values. Returning to Range 1, also in common with both cases, it is evident that the shadow zone bin does not have the most values. The increase in percentage at zero decibels in the CRFs shows the relative sizes of the shadow zones. For Range 1, no terrain (Figure 6.71) this jump covers 32%, and for terrain (Figure 6.59) about 24%. Even though both environments consider Range 1 to be continuous, similarities as

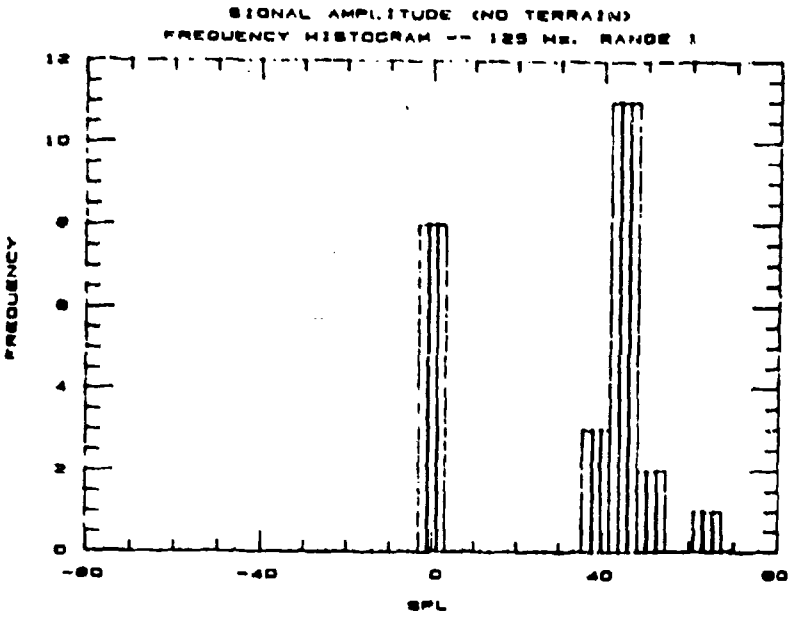

Figure 6.65. Frequency Histogram of the Signal Amplitude, Range 1, 1 July, 125 Hz, Flat Terrain

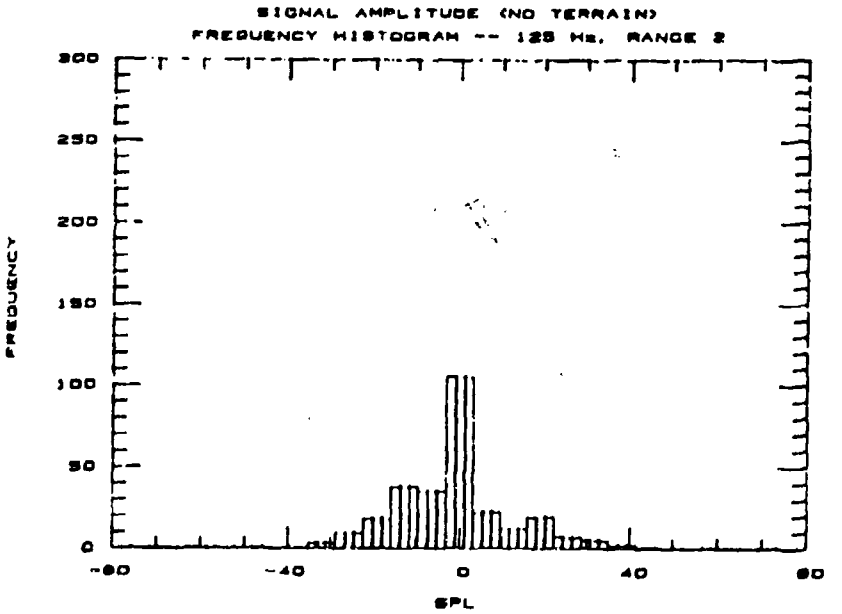

Figure 6.66. Frequency Histogram of the Signal Amplitude, Range 2, 1 July, 125 Hz, Flat Terrain

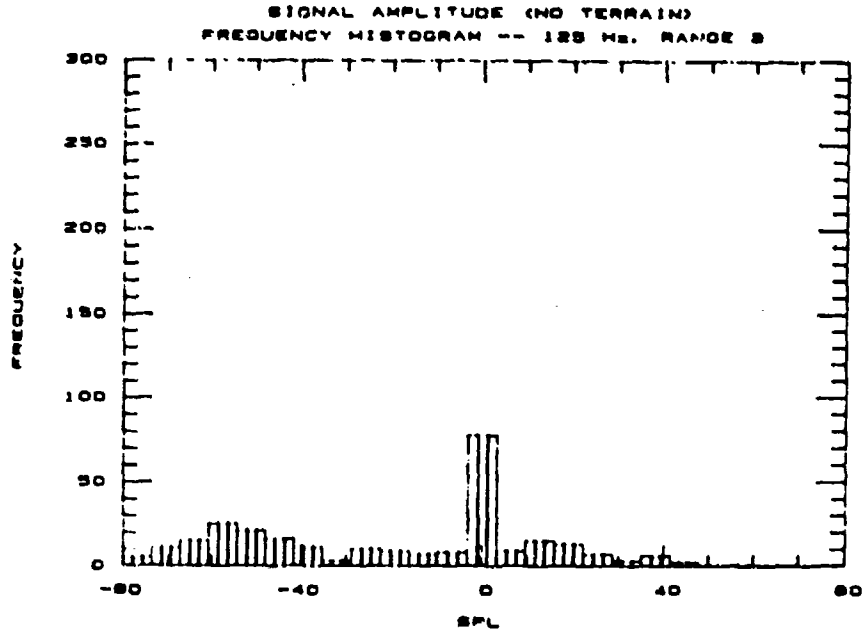

Figure 6.67. Frequency Histogram of the Signal Amplitude, Range 3, 1 July, 125 Hz, Flat Terrain

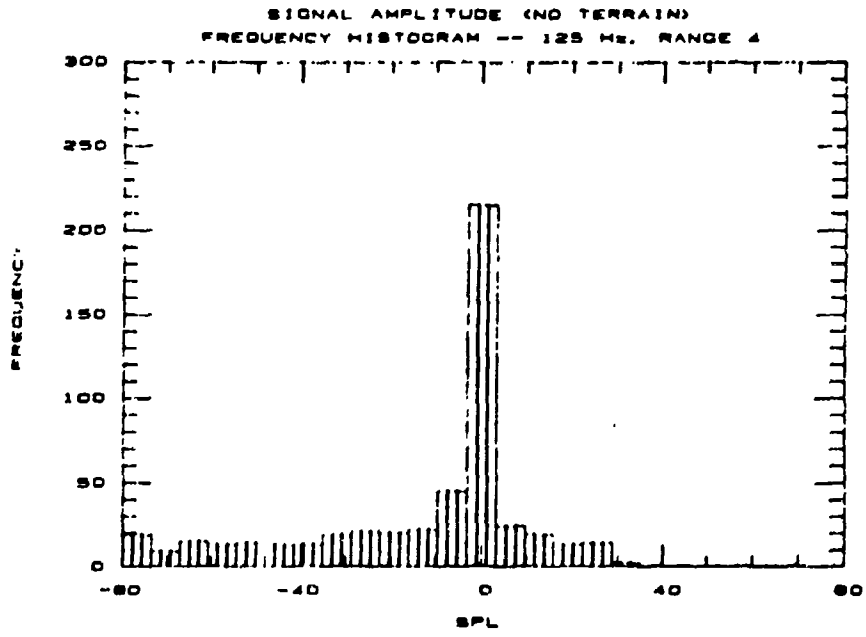

Figure 6.68. Frequency Histogram of the Signal Amplitude, Range 4, 1 July, 125 Hz, Flat Terrain

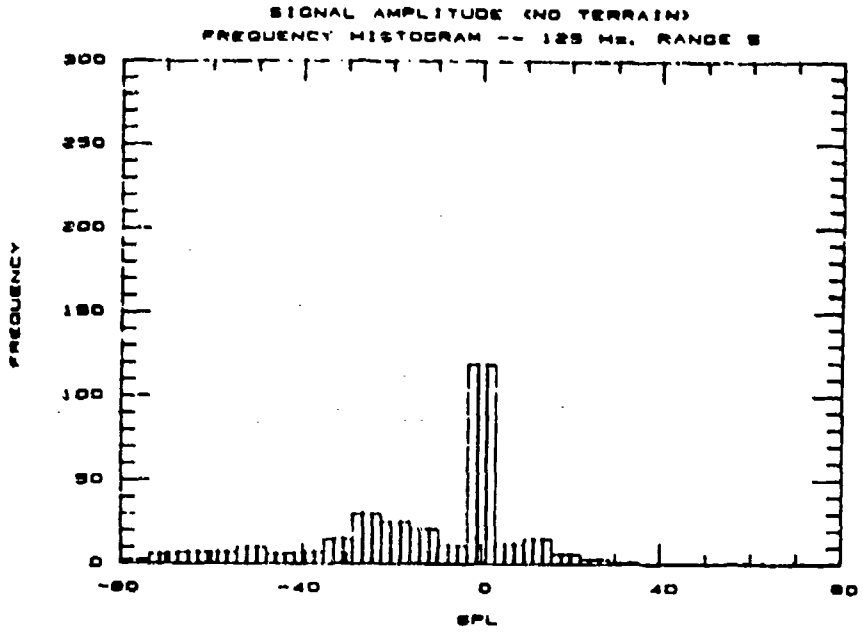

Figure 6.69. Frequency Histogram of the Signal Amplitude, Range 5, 1 July, 125 Hz, Flat Terrain

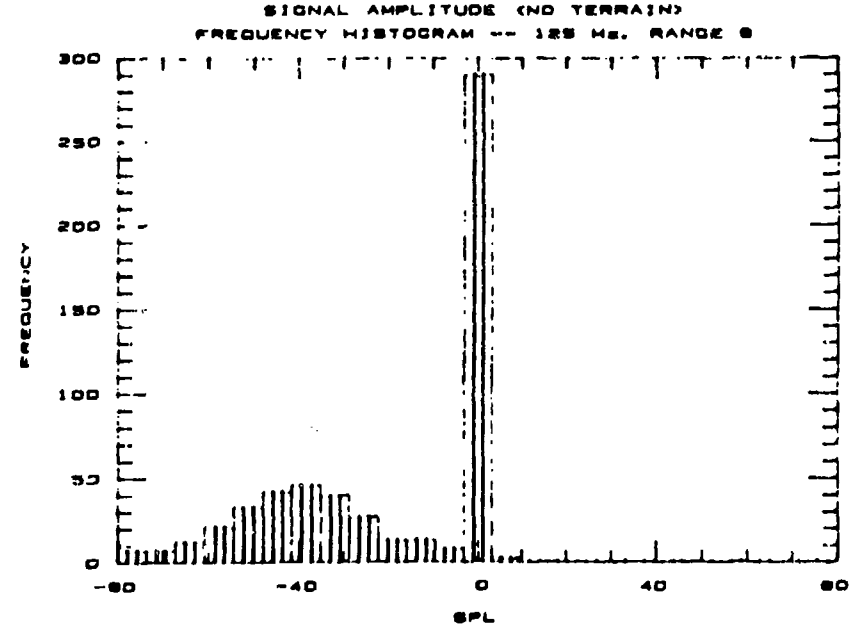

Figure 6.70. Frequency Histogram of the Signal Amplitude, Range 6, 1 July, 125 Hz, Flat Terrain

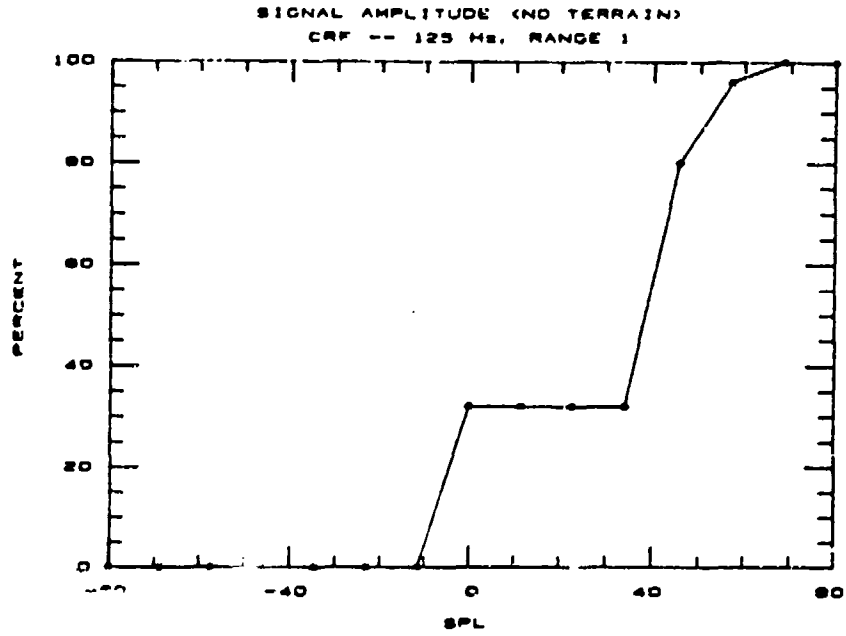

Figure 6.71. Cumulative Relative Frequencies of the Signal Amplitude, Range 1, 1 July, 125 Hz, Flat Terrain

well as differences show up in the frequency histograms.

In Range 3, the topography data set is characteristic of intermittent propagation. For the NT case, the signal remains continuous. Again note the number of the shadow zone values with respect to the other values. In both cases the shadow zone has the largest number of values. However, a shadow zone is in existence 67% of the time for topography and only 29% of the time for no topography. As is evident in the ray trace with flat topography none of the rays are blocked from propagating out to the maximum distance. Thus all of the targets are hit. Therefore, in a region with a continuous signal the only time zero values will appear is when rays are refracted upwards and never reach a target. Thus for such a region the percent of time a shadow zone is in existence represents the percent of time a negative sound speed gradient is present.

The second point to be discussed regarding the continuous/intermittent comparison concerns the breadth of the distribution. The data from NT spans values from -80 dB to +48 dB. With topography the values range from -48 dB to +42 dB. Not only is the no topography distribution wider but the numbers of values in the negative bins are more numerous. The CRF shows negative values 52% of the time and positive 19% for the NT environment. The CRF for the topography environment shows only 5% of the time as negative values and 28% as positive.

The importance of this distinction in the shape of the distribution lies more in the statistical evaluation itself than in the noise impact evaluation. Both environments have an upper limit of

about +45 dB. This is equivalent to the level of conversation in a quiet room (Kryter, 1985, p.8) The percent of time with positive versus negative values is less important if the upper limit is relatively low. What can be very important in a noise impact study is the percent of time with positive values compared to the percent of time with zero values. However, the relative numbers of positive, negative and zero values will determine where the means will fall. For example, in the no terrain data, a range with a high percent of negative numbers has a negative mean. But a high number of zero values with a few negative numbers would fictitiously raise and keep the mean close to zero.

At the furthest regions a comparison can be made between intermittent and sporadic signals. The 125 Hz histogram for Range 5 is shown in Figure 6.69. For NT this is an intermittent region. Recall, however, that at Range 5 with topography the signal is sporadic. In the former case a nice spread of values exists. The lower limit is -80 dB and the upper is +35 dB. The case with topography has the majority of its values at zero and only a few between zero and -10 dB. The relative sizes of the shadow zones also significantly differs. Without topography it is 23% and with topography it is 97%. In fact all of the sporadic ranges have a shadow zone sizes in excess of 96%. Of importance in discussing the percent of time ascribed to a shadow zone for the flat terrain environment is the observation that this percentage is smaller for the intermittent regions than for the continuous regions. In general however, this percentage does not vary much from any one range to any

other range. The minimum is 23% and the maximum is 38%.

The histograms, being a collection of the SPLs over a whole day, characterize the sound in the different ranges. It is obvious from the broader distributions and the smaller shadow zone size that flat topography can facilitate the propagation of sound to large distances.

The distinction between the two sets of means is that the mean from the topography environment is higher than the mean from the flat environment (Figures 6.72 - 6.77). A probable explanation in the farther ranges was already given in the discussion of the percent of time with negative, positive, and zero values. The large shadow zone keeps the mean close to zero, a value that mathematically appears greater than other negative values found as the no topography means. A terse summary of the flat topography's ray traces could possibly explain the differences in the means for the near ranges. Each ray experiences more boundary reflections and possibly travels a longer ray path. These events in general decrease the SPL. Another event is that more rays enter into a single target. This may increase the SPL when considering only incoherent addition.

The change from an actual to a flat environment also alters the resulting standard deviation as well as the percentile deviation. As it turns out for the flat topography all of the percentile standard deviations are small except for the ones at Range 2 with the 125 and 500 Hz signal. Their magnitudes are so small that they do not show up on the graphs. Each percentile standard deviation falls between the values 0.5 and 1.6. In other words the magnitude of the deviation is comparable to the magnitude of the mean. The percentile standard

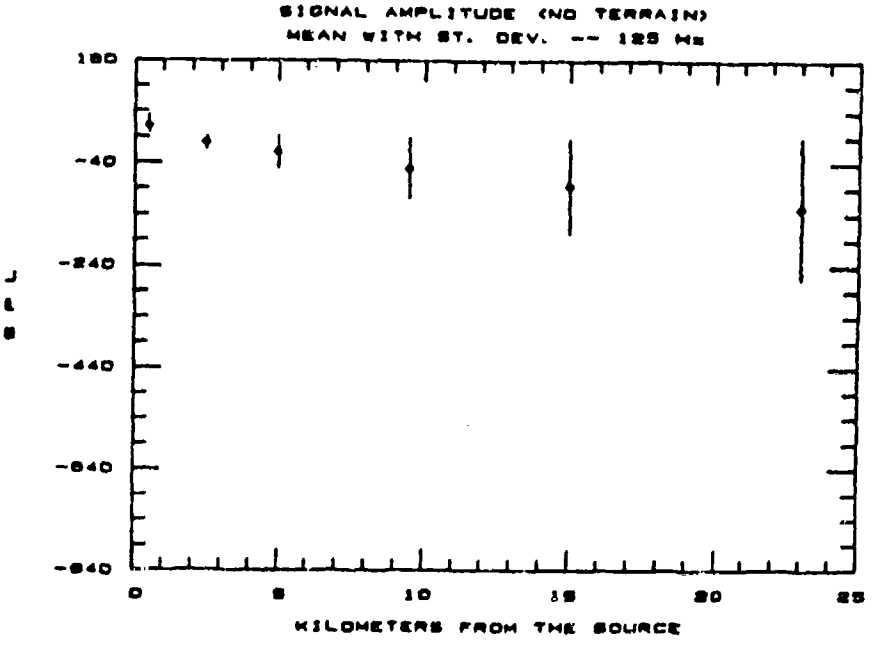

Figure 6.72. Mean and Standard Deviation of the Signal Amplitude by Range, 1 July, 125 Hz, Flat Terrain

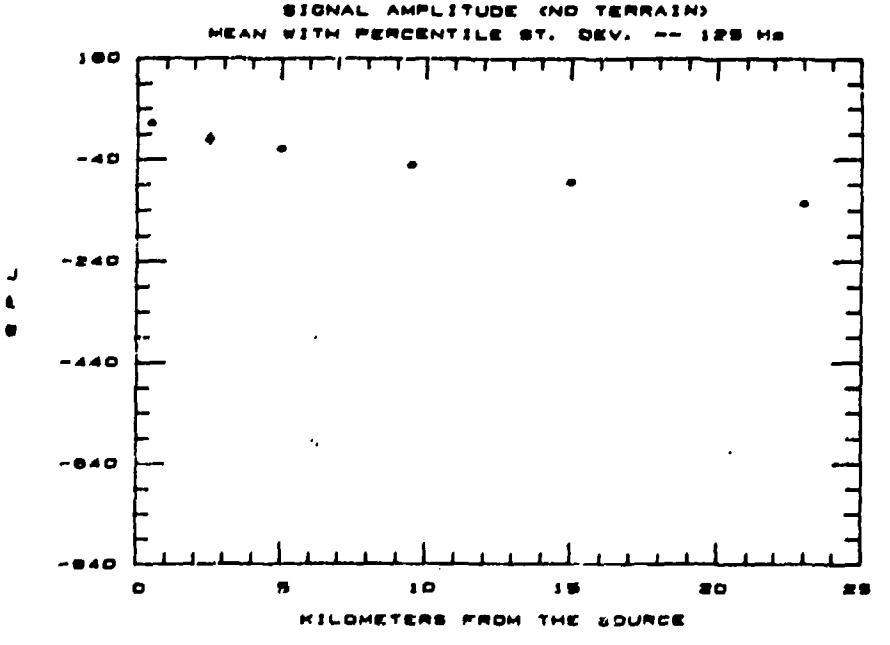

Figure 6.73. Mean and Percentile Standard Deviation of the Signal Amplitude by Range, 1 July, 125 Hz, Flat Terrain

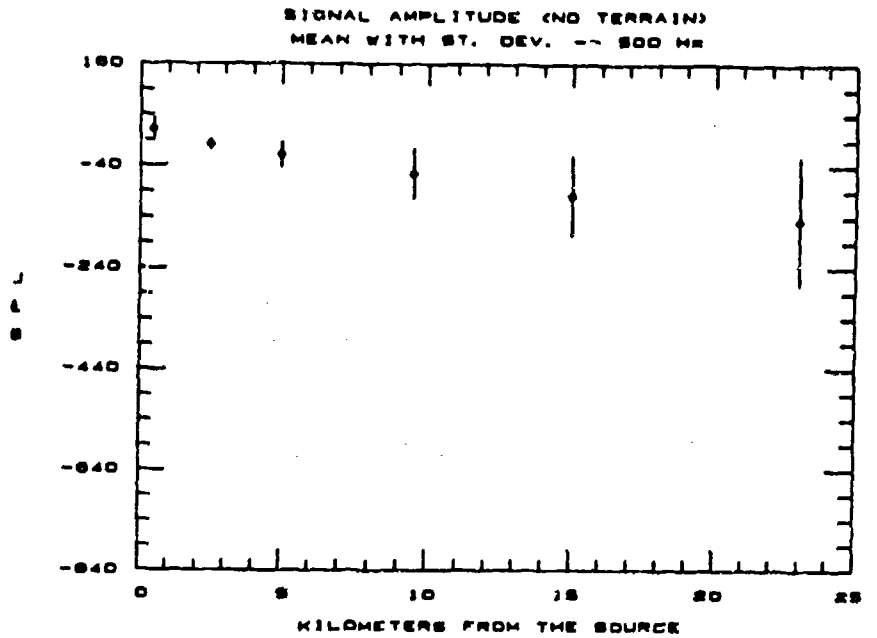

Figure 6.74. Mean and Standard Deviation of the Signal Amplitude by Range, 1 July, 500 Hz, Flat Terrain

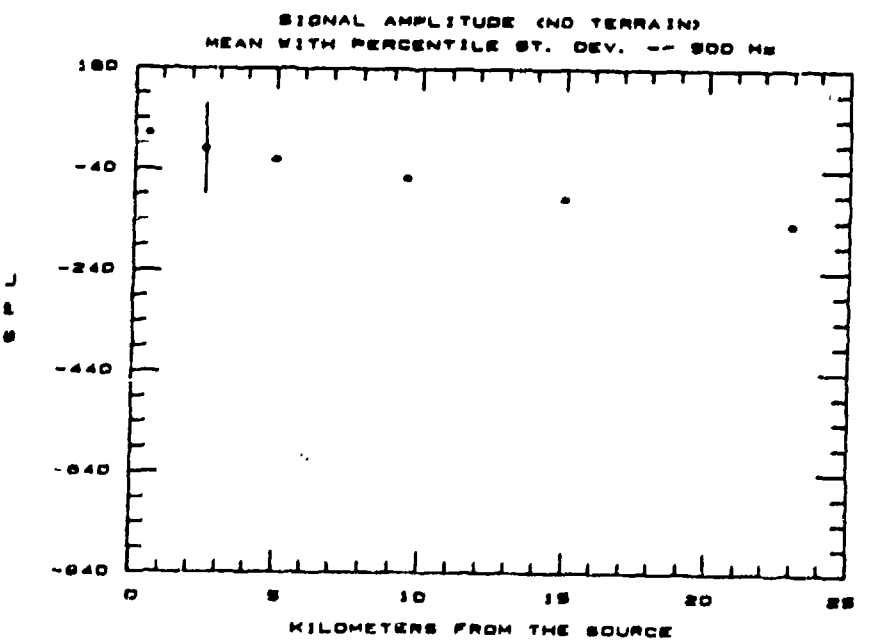

Figure 6.75. Mean and Percentile Standard Deviation of the Signal Amplitude by Range, 1 July, 500 Hz, Flat Terrain

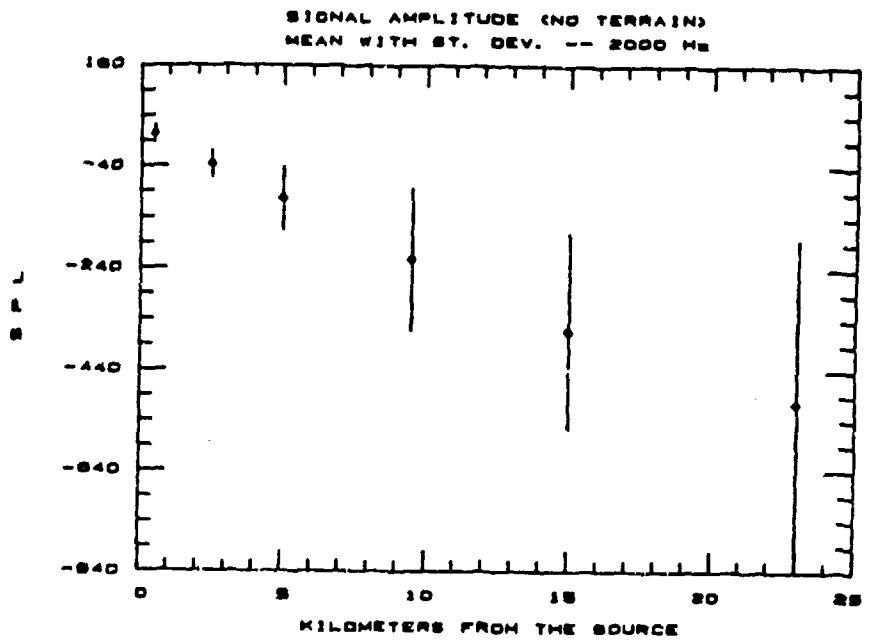

Figure 6.76. Mean and Standard Deviation of the Signal Amplitude by Range, 1 July, 2000 Hz, Flat Terrain

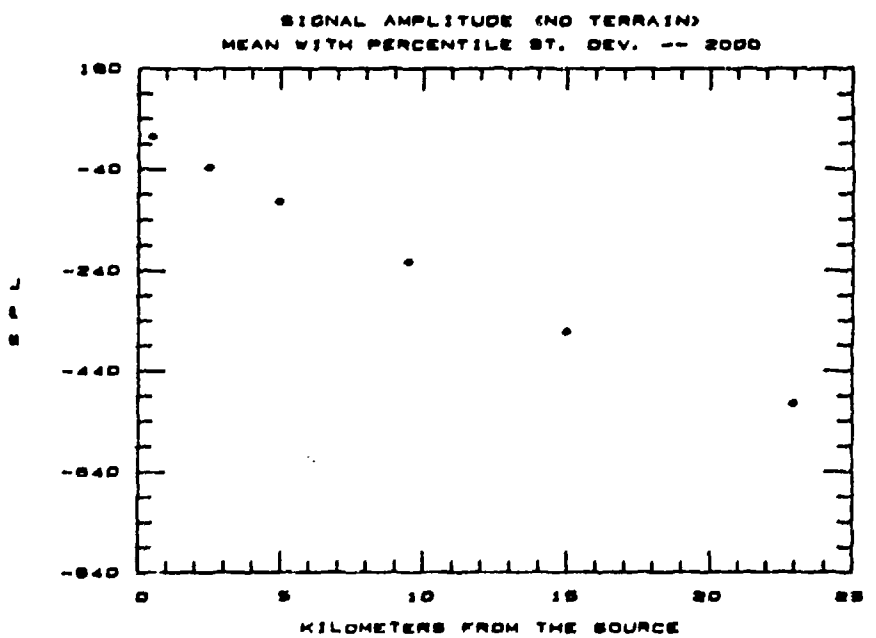

Figure 6.77. Mean and Percentile Standard Deviation of the Signal Amplitude by Range, 1 July, 2000 Hz, Flat Terrain

deviation for the actual topography, on the other hand, increases as the distance increases and eventually reaches values around 23.0.

Characteristics of sound such as the percent of time an absence of sound occurs and the range of the SPL values can be gathered from the CRFs and the frequency histograms. Clearly, they as well as the mean and standard deviation are dependent upon the topography. Also notable in this comparison, drawn from the CRF or frequency histogram, is that in a continuous range the size of the shadow zone represents the percent of time when sound propagates upwards or when a positive lapse rate for the sound velocity profile exists. This comparison shows that using the exact topography is essential for noise prediction studies.

6.3.2.3. PHASE

As discussed earlier the signal phase is that resulting from the vector sum of the rays. In the model runs made for this thesis there were up to four rays whose phases were changing with time that entered a target. These phases made up the sum which, therefore, also changed with time. Instead of the accumulated phase, this sum modulo 2π was recorded. Thus, a possible wide range of cumulative values was redistributed within the smaller range. The distribution of the signal phases, as expected, was uniform random. The statistical results, especially in the frequency histograms demonstrate this type of distribution.

Changing atmospheric conditions alter the ray path length by either effectively stretching or shrinking it. Consequently path length changes correspondingly extend or shorten the travel time from the source to a particular target. This means that the phase of each ray will be increased or decreased from one time to the next. These changes in phase can be compared in either an absolute or relative sense. The propagation model was programed to calculate the difference between the actual phase of a ray and a reference value. The reference phase is the phase a ray would have if it had traveled from source to receiver in a straight horizontal line through a windless, isothermal atmosphere.

It is possible to think of the atmosphere as a complicated system that controls the phase. It has multiple inputs each of which is operated on by the same transfer function. Each output from the transfer function also has time dependent noise added to it. For a final result these outputs are then summed together. Figure 6.78 explains this concept using a block diagram. Each input is one ray with a unique launch angle. All rays have a zero initial phase angle and the inputs are fixed with respect to time. The transfer function, also time independent, is just the reference ray's travel time multiplied by the angular frequency of the signal. In other words it is the minimum phase for whatever target is being considered. Noise is represented by a random number generated by the atmosphere. The final result is the sum of the phases of all the rays as they would be measured at a particular target. It might be interesting to see how this sum would differ at each time interval from a sum calculated for

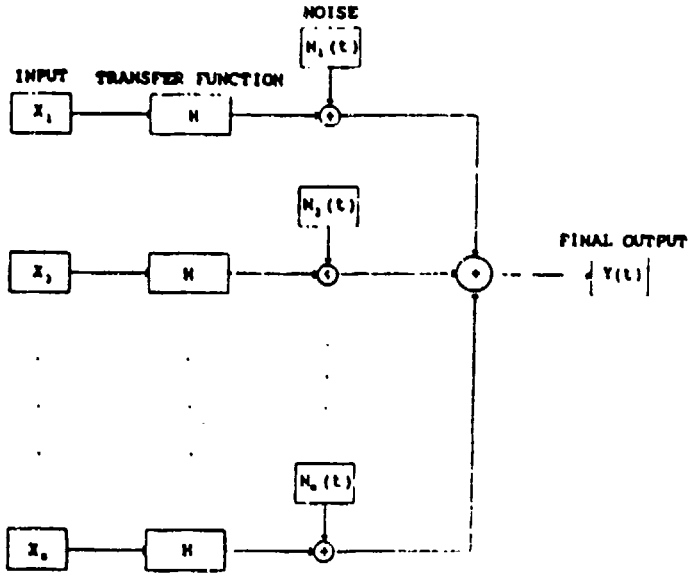

Figure 6.78. Block Diagram of the Atmosphere as a Multiple Input/Single Output System

a hypothetical no wind, isothermal, time-invariant atmosphere. However, experimental verification of such signal behavior would have been well beyond the scope of this thesis and thus no attempt was made to monitor the differences in total phase. Instead the model was used only to examine the differences using a single ray. It outputs how the phase of one ray (with noise) differed each time from a minimum phase. Figure 6.79 shows the frequency histogram of the phase differences for the 26th ray at target 500 meters from the source for the conditions on 1 July. There are values on both sides of the zero, i.e. both lesser and greater phases than the minimum. These differences which in this explanation of the atmospheric effects on phase can be considered to be noise are displayed in chronological order in Table 6.5. With increasing time the differences generally

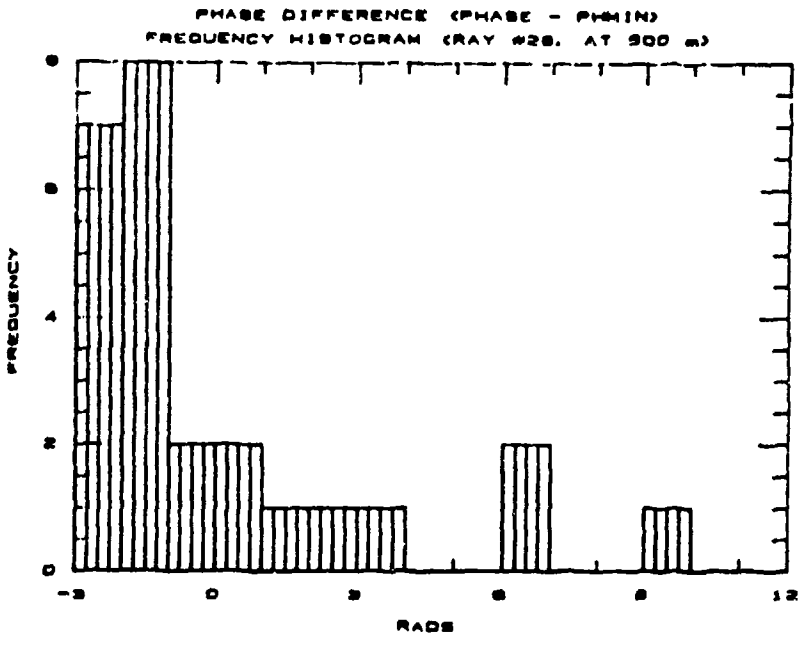

Figure 6.79. Frequency Histogram of Phase Differences for the 26th Ray, 1 July, 500 Meters from the Source

Table 6.5. Phase Differences versus Time for the 26th Ray, 1 July, 500 Meters from the Source

Time	Phase Difference (rads)
1700	9.27
2000	6.73
2300	6.58
0200	3.60
0230	2.51
0300	1.73
0330	0.94
0400	0.12
0430	-0.64
0500	-1.39
0530	-1.53
0600	-1.69
0630	-1.74
0700	-1.73
0730	-1.66
0800	-1.85
0830	-1.83
0900	-2.13
0930	-2.41
1000	-2.61
1030	-2.77
1100	-2.88
1130	-2.46
1200	-2.02
1400	-0.49

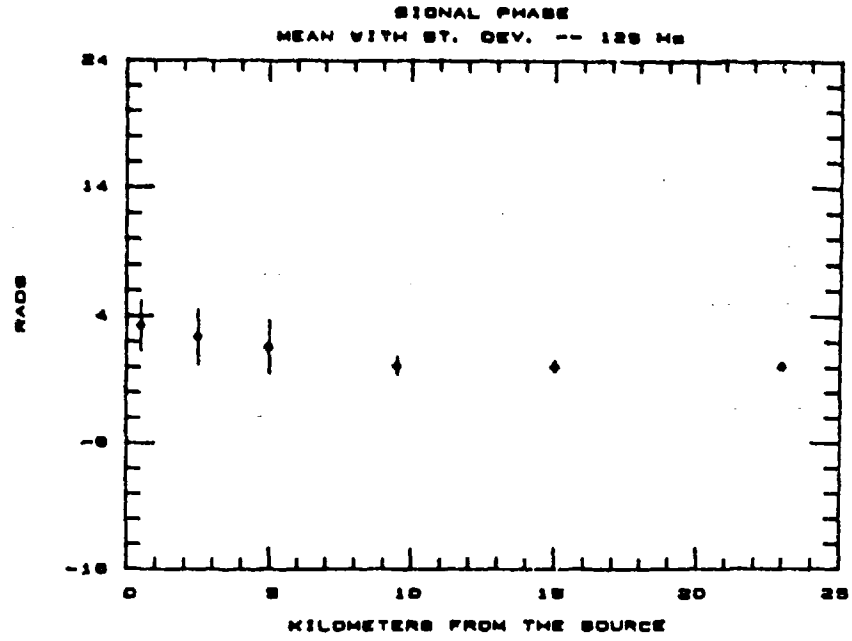

Figure 6.80. Mean and Standard Deviation of the Signal Phase by Range, 1 July, 125 Hz

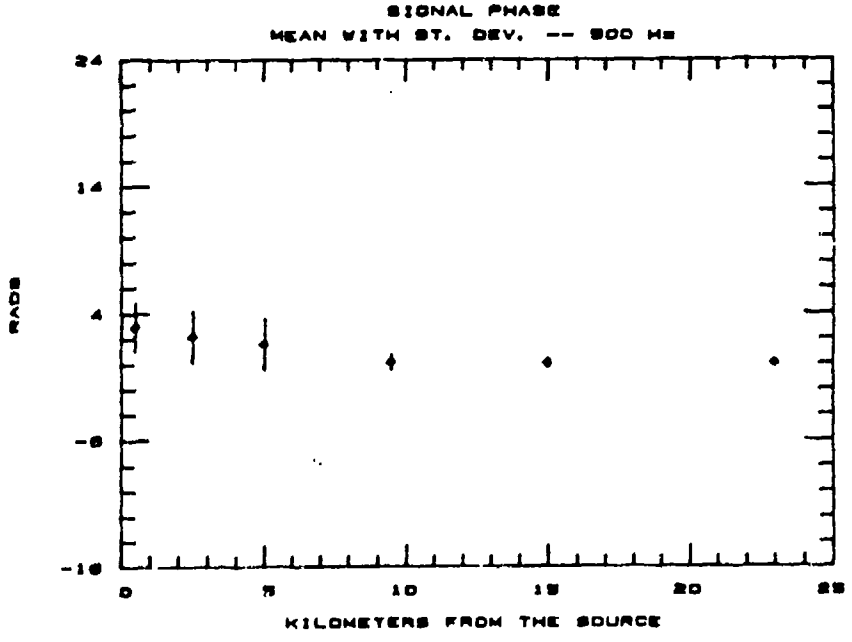

Figure 6.81. Mean and Standard Deviation of the Signal Phase by Range, 1 July, 500 Hz

decrease in value, shifting from a positive value to a negative value between the times 0400 and 0430. At 1130 they begin to increase again. This indicates that over some time intervals that noise will not necessarily be random. In the interests of minimizing repetitiveness, discussion of the statistical properties of the phase variations will focus on the first three ranges. As with the signal amplitudes, signal phases in the last three ranges when sound was absent was assigned a zero value. Because of the large shadow zones in the farther ranges the means of the signal phases are thus forced to be close to zero and the percentile standard deviations end up being correspondingly large.

Figures 6.80 and 6.81 display the mean and standard deviation for the 125 and 500 Hz signals, respectively. In the first three ranges, note that the means appear to fall off at the same rate regardless of the frequency. Although the means for a single frequency are slightly different at the various ranges the standard deviation is similar. This implies that the distribution within each range has a similar shape.

The frequency histograms indicate that at a single range there is an equal probability that the phase will have any value between 0 and 2π. For example note the nearly uniform height of each bar, excluding the shadow zone's in both Range 2 and Range 3 in Figures 6.82 and 6.83.

The CRFs also show uniform distributions within each range. The CRFs for Range 2 and Range 3, Figures 6.84 and 6.85, are close to being straight lines each with a different y-intercept and therefore

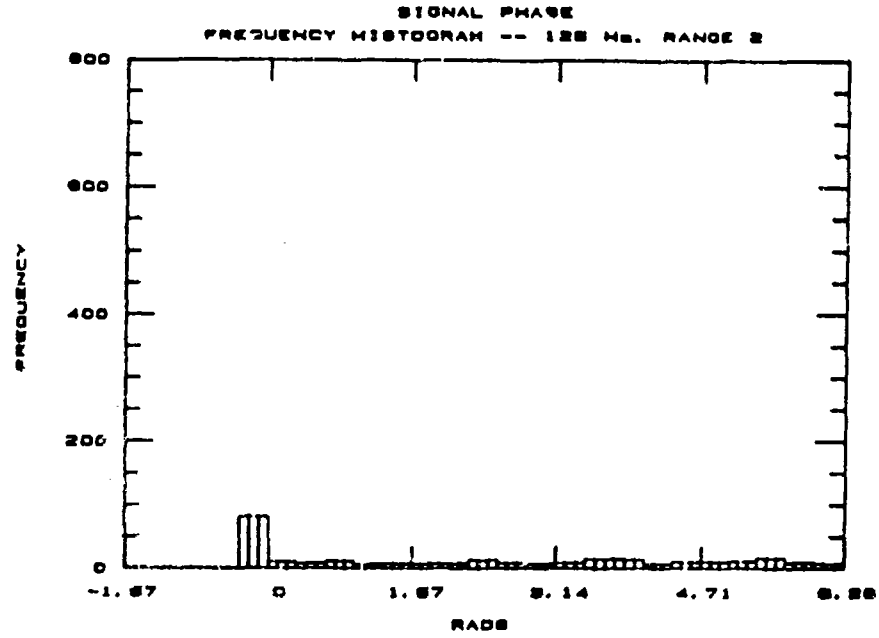

Figure 6.82. Frequency Histogram of the Signal Phase, Range 2, 1 July, 125 Hz

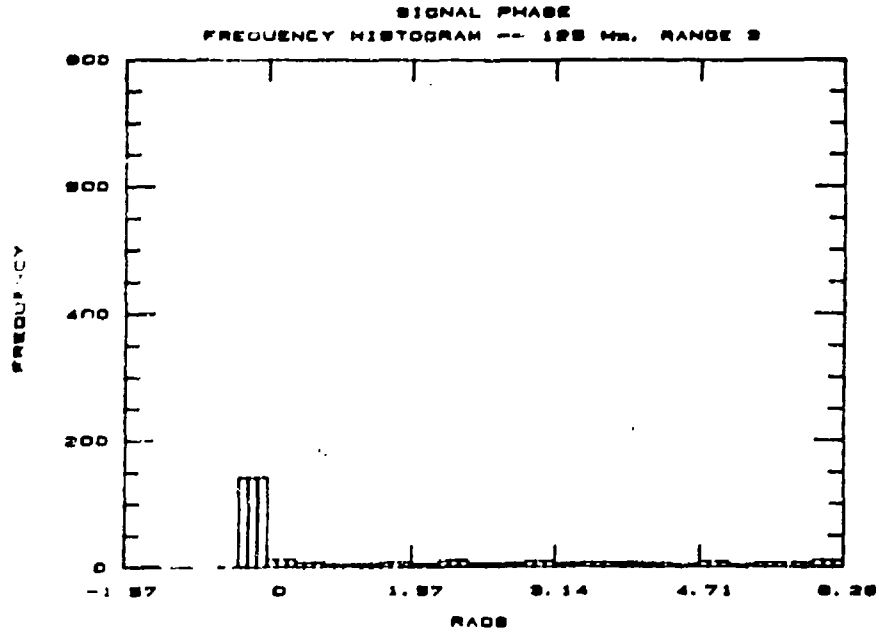

Figure 6.83. Frequency Histogram of the Signal Phase, Range 3, 1 July, 125 Hz

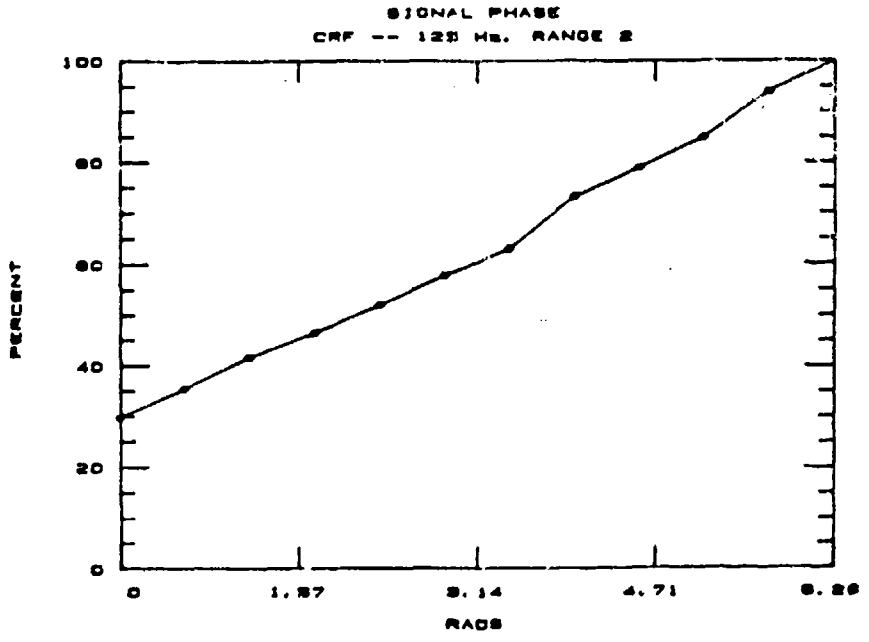

Figure 6.84. Cumulative Relative Frequencies of the Signal Phase, Range 2, 1 July, 125 Hz

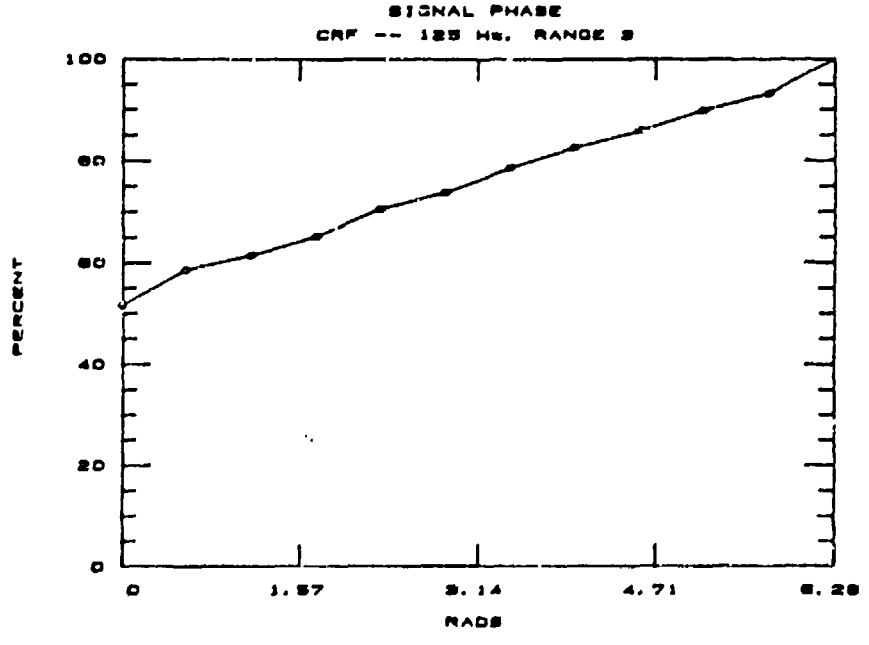

Figure 6.85. Cumulative Relative Frequencies of the Signal Phase, Range 3, 1 July, 125 Hz

also slope. The y-intercept represents the percent of time with zero values. For each range, the graph shows a similar percentage jump from one class to the next. Any differences are under 3 percentage points. The CRF for Range 1, Figure 6.86, however, shows more curvature, suggesting that some values might occur more frequently than others. To the author's knowledge field experiments of the type required to assess such signal behavior have not yet been performed.

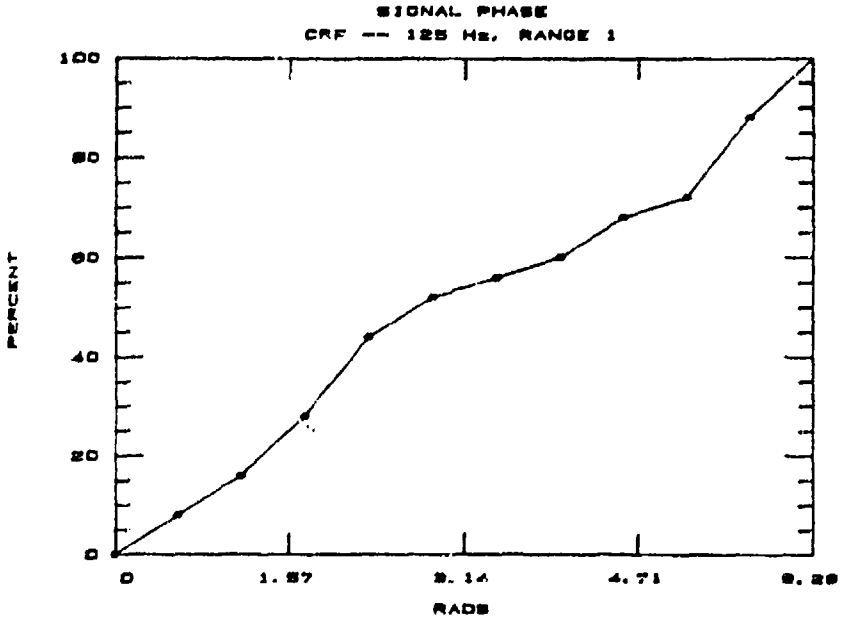

Figure 6.86. Cumulative Relative Frequencies of the Signal Phase, Range 1, 1 July, 125 Hz

Chapter 7

CASE STUDY - II

A second case study was performed using composite atmospheric data from a forest environment. The purpose of this study was twofold. One, it was to demonstrate the utility of the prediction model for calculations on smaller distance scales. Two, it was to investigate some aspects of the possible temporal variability of sound propagation in a forest environment. For these calculations both the vertical and horizontal scales were reduced by a magnitude of one hundred. Thus, instead of the calculations including heights of up to 3000 m the refractive layer considered was only ten meters deep. Fictitious targets were then placed at five meter intervals out to only 600 m. In the first case study, the intervals were 500 m out to 25 km. The theory of sound transmission including attenuation for forests was discussed both by Martens (1981) and Price, et al. (1988). Roth (1983) had also analyzed some time series of acoustic data obtained under a forest canopy.

7.1. PREPARATION

One classical study of the forest microclimate is presented in Geiger (1965). Meteorological data he used had been archived by A. Baumgartner (1956, 1967). Baumgartner's forest stand consisted of young firs, five to six meters in height, located 30 km southeast of

Munich, Germany. Wind, temperature, and water vapor pressure data for whole days were averaged over a period of about a week, from 29 June to 7 July, 1952. For this thesis the data from Baumgartner's original paper was extracted and organized into a working format by Kathleen K. Hodgdon.

The original data was given at time intervals of one hour over a diurnal cycle. The temperature and vapor pressure profiles consisted of measurements at 0.2, 1.5, 2.5, 3.0, 5.0, and 10.0 m. Vapor pressures were converted into humidity mixing ratios. The original wind profiles were measured at 0.0, 4.2, 5.1, 6.4, 8.0, 9.8, 12.2, and 16.0 m. Wind was given as a speed only, no direction. For this study we assumed the values corresponded to a downwind (source-receiver bearing) u component. The v component was set to zero at every height and every time. The listed u components were then splined in order to have values at the same levels as those for the temperature and vapor pressure. Next all three sets of profiles were splined to create thirty values at equal intervals of 0.33 m from zero to ten meters. An extra value at 0.11 m was found by interpolation using the data at zero and 0.33 meters. This meteorological data was placed into the input file JLWK52.DAT, standing for data averaged over the week in July, 1952. Some changes to the model were necessary to enable it to use these new profiles. For example, the user could now input the vertical profile's interval at the beginning of the run. Previously this interval had been forced to be at 100 m with the extra data point at 10 m.

Other important preparations for the execution of this case study were as follows. First, an absorption coefficient file, JLWKAC.DAT was made by simply running the meteorological data file through the program COEF.FOR. The static atmospheric pressure for Munich at an elevation of 1640 feet, $\bar{p}$ = 954.6 mbars, was changed inside COEF.FOR. Since the terrain was considered flat, the topographic values were immediately set to zero. To force the wind component along the transmitter-receiver line to be a maximum, 90° bearing was specified. Other modifications had to be made to the model in order to accommodate the target spacing of only five meters. Again, the user now was allowed through the questions at the beginning of the run to input the necessary horizontal spacing. A hypothetical source was placed two meters above the ground at the 0.0 meter point in the x direction. The best launch angles to use for this forest situation were found to be between ±5.5°, differing by 0.5°.

7.2. SPEED OF SOUND PROFILES

A surface plot of the speed of sound profiles calculated from the splined temperature and wind profiles is shown in Figure 7.1. The ten meter profiles reach above the forest canopy. There is an inversion evident all of the time at most of the heights. However, some positive lapse regions appeared at some earlier times within limited height intervals of the profile. For example at 0100 there is a positive lapse region between two and three meters.

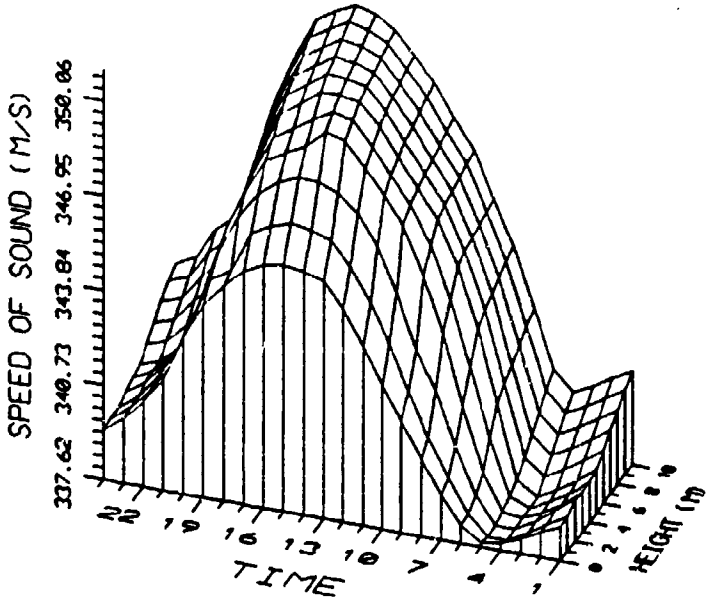

Figure 7.1. Speed of Sound Profiles from the Forest Data

7.3. RESULTS

7.3.1. RAY TRACES

The prediction model successfully produced raytraces even though distances were scaled down by a magnitude of one hundred. We had been concerned that computational roundoff errors might give rise to problems. Figures 7.2 - 7.4 are representative of the modeled traces. These figures are the results only for the local times: 0100, 0700, and 1700. Every ray trace shows all of the rays continually refracted downwards. This is due to the persistent inversion in the sound speed profiles. Most of the ray traces are similar to the one shown for 0700. All of the rays reached a vertex before exiting the top of the forest canopy. Because of the flat terrain each ray reached the maximum possible horizontal distance -- but with a multitude of ground reflections. Figure 7.4 is the ray trace at 1700 local time. Compared to the trace at 0700, some of the rays at this time traveled to a greater height before reaching their vertices. It is small differences in the sound speed gradients which cause the differences in the rays' maximum height. Figure 7.2, the ray trace at 0100, shows an example of rays traveling through a lapse region. On some of the rays an upward curved path is noticeable between two and three meters. Also noticeable is the vertex being as high as 10 m, a much higher height than that at 1700 or 0700. Referring back to the speed of sound profiles this difference is confirmed by a smaller slope in general at 0100.

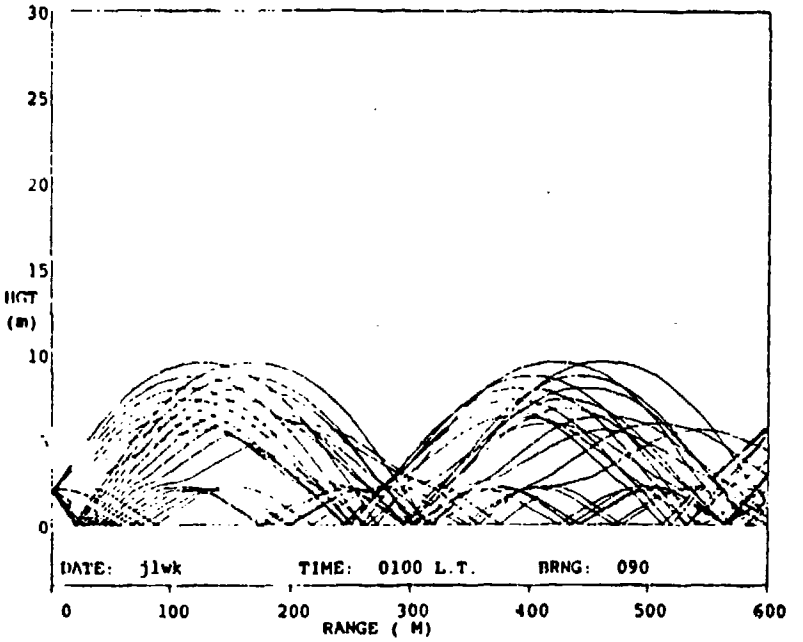

Figure 7.2. Ray Trace from the Forest Data, 0100 L.T.

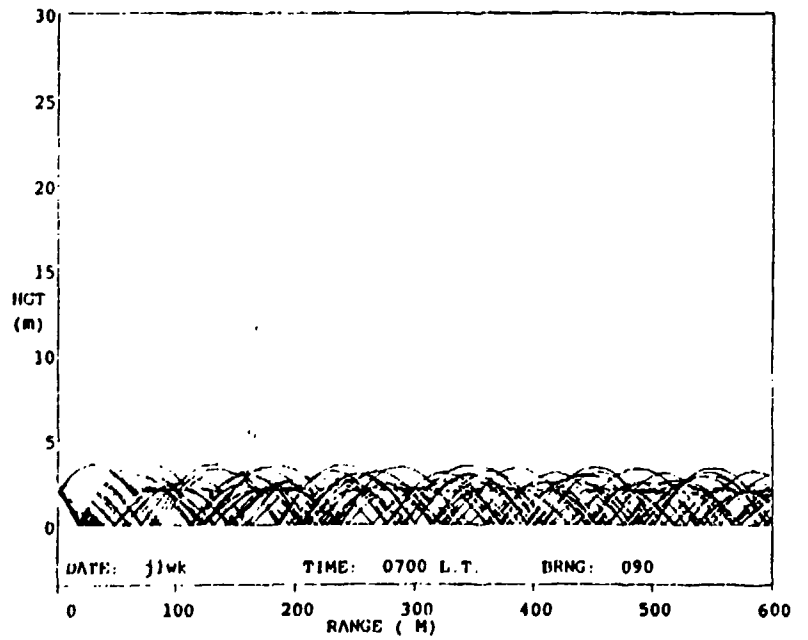

Figure 7.3. Ray Trace from the Forest Data, 0700 L.T.

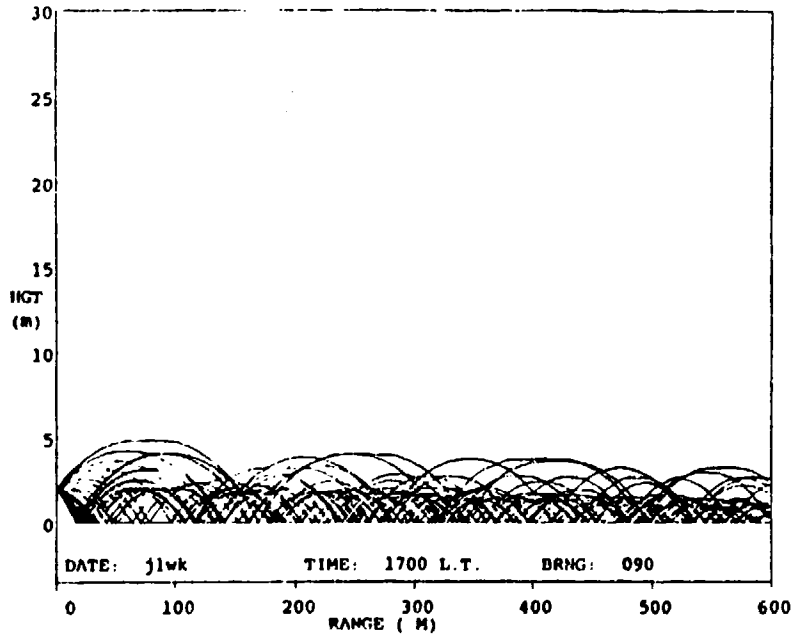

Figure 7.4. Ray Trace from the Forest Data, 1700 L.T.

7.3.2. AMPLITUDE

The SPL diagrams for propagation in the forest environment, Figures 7.5 - 7.7, show sound occurring continuously with small fluctuations out to the maximum distance. Once in a while peaks appeared but they were not as often nor as large as some of the peaks that were evident in the no terrain results from the previous study. The continuously high sound levels are a result of most, if not all, of the rays remaining under five meters. The model uses zero to five meters as the target size. The distance dependence is weak. What there is is caused primarily by the attenuation due to atmospheric absorption and ground reflections.

A better way to examine the SPLs is to examine how they vary with time instead of distance. Figures 7.8 - 7.11 are the SPLs versus time of a 63 Hz signal at four different distances: 20, 100, 300, and 595 meters. The mean SPL for each target was removed from each time before plotted. It is evident on each graph that the values do change significantly from one time to the next. Furthermore the range of the signal fluctuations grows as the distance from the source increases. For example at 20 meters the range is only over seven decibels; at 595 meters the range is over 70 dB. From the closer targets, 20 and 100 meters, the variation appears to be random. But at the furthest distances the pattern suggests the possibility of a diurnal trend. Higher values are present before sunrise (0600) and after sunset (1900) than at other times during the day.

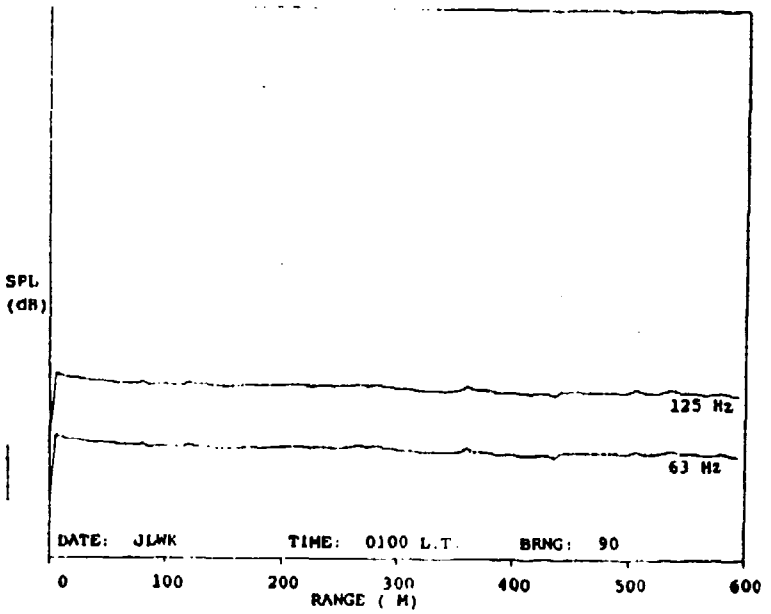

Figure 7.5. Sound Pressure Level versus Distance from the Forest Data, 0100 L.T.

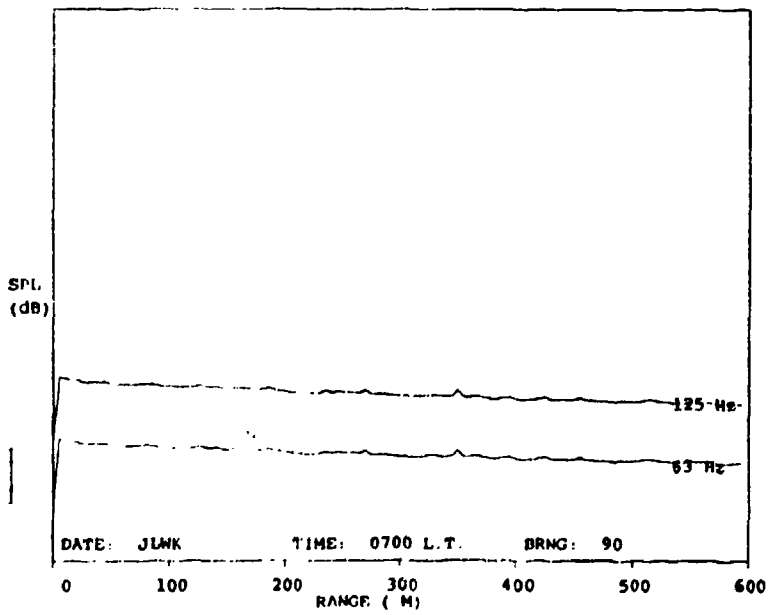

Figure 7.6. Sound Pressure Level versus Distance from the Forest Data, 0700 L.T.

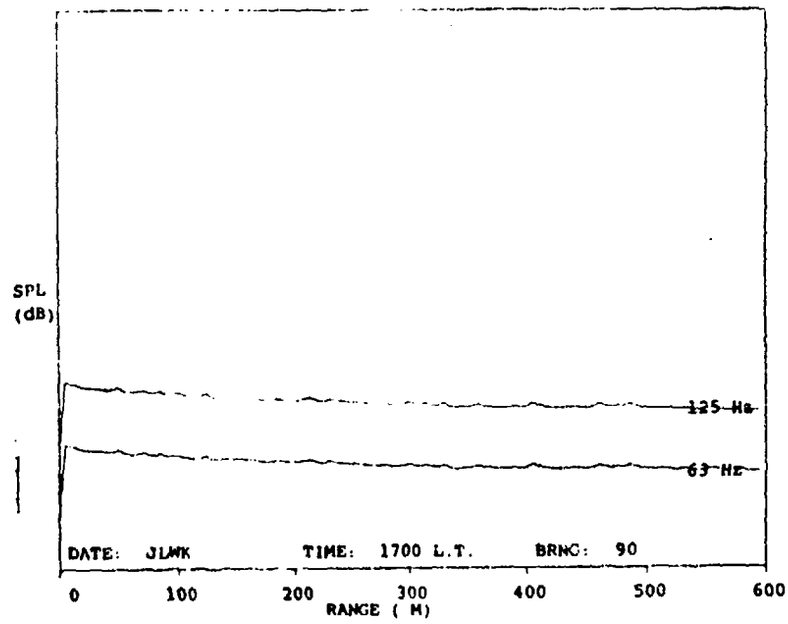

Figure 7.7. Sound Pressure Level versus Distance from the Forest Data, 1700 L.T.

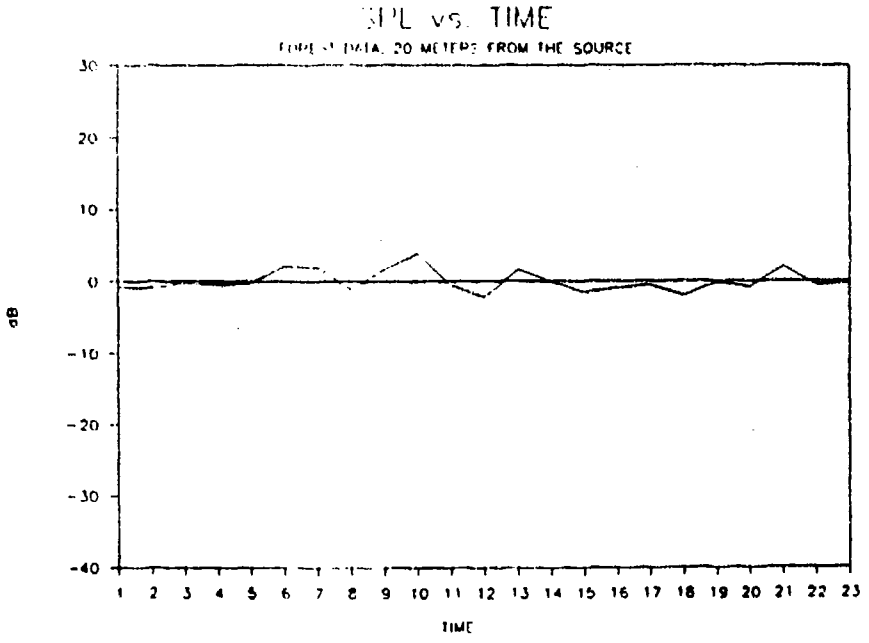

Figure 7.8. Sound Pressure Level versus Time from the Forest Data, 20 Meters from the Source

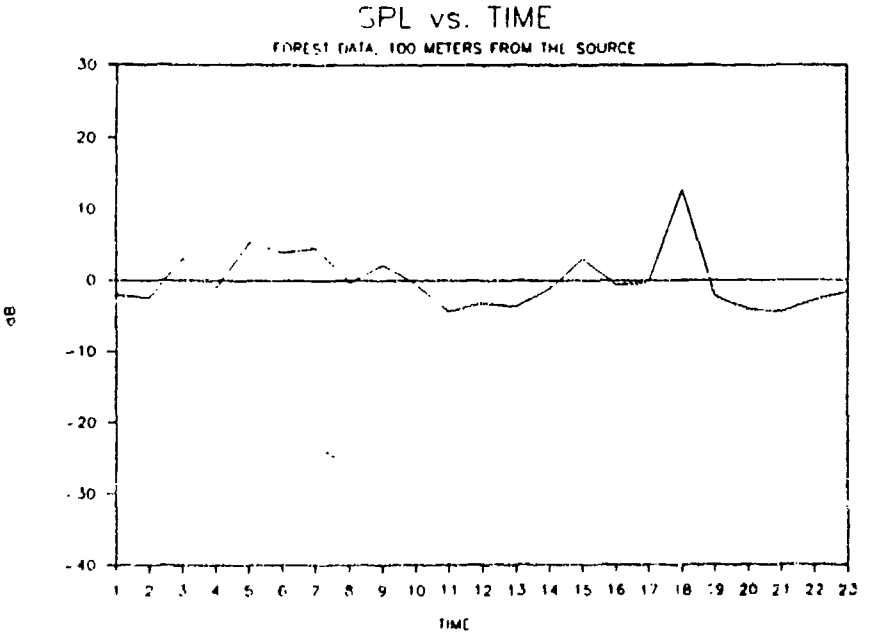

Figure 7.9. Sound Pressure Level versus Time from the Forest Data, 100 Meters from the Source

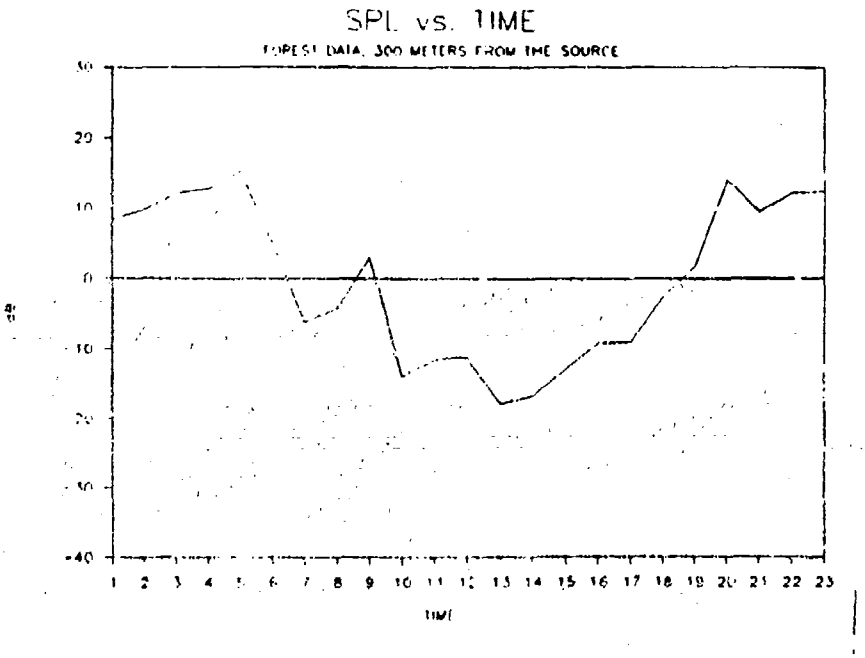

Figure 7.10. Sound Pressure Level versus Time from the Forest Data, 300 Meters from the Source

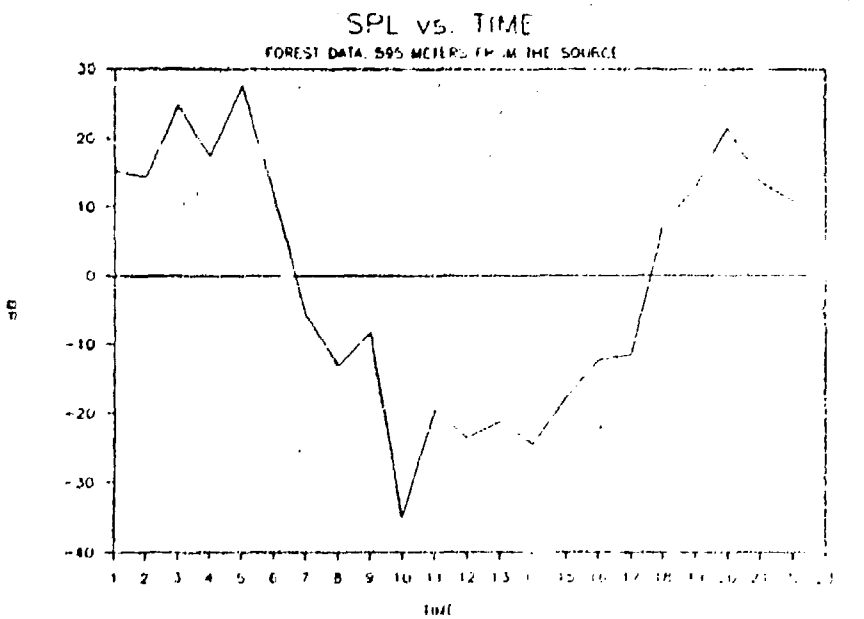

Figure 7.11. Sound Pressure Level versus Time from the Forest Data, 595 Meters from the Source

Chapter 8

CONCLUSIONS

In addition to documenting the comprehensive computer code for the RAYPS model, accomplishments in this thesis research included the addition of signal phase calculations into the prediction model, and the evaluation of several statistical methods for summarizing both the temporal and spatial variations of signal phase and amplitude. With the possibility of predicting signal phase at hand, future work could include examining the potential for using tomographic methods for studies of the structure of the atmospheric planetary boundary layer (Thomson, 1987). The thesis also provides examples of how environmental noise impact prediction studies could be improved. Current standards and prediction models need to be reexamined to see how temporal and spatial fluctuations might be incorporated into them.

8.1. FUTURE WORK -- TOMOGRAPHIC ANALYSIS OF ATMOSPHERIC STRUCTURE

Beginning with Munk and Wunsch's (1979) examination a number of studies of underwater acoustical tomographic analyses have been performed. Spiesberger (1985) discusses and analyzes the forward problem in which paths of the individual rays arriving at a single receiver are identified. Cornuelle (1985) experiments with inversion methods. Inversion methods are used to extract the information from individual rays and to infer the subsurface speed of sound profile.

The RAYPS program, specifically the calculation of phases and phase differences of the individual rays, can be used in a forward sense for similar atmospheric studies. The phases and phase differences which are related to travel time and travel time differences could then be used as input for a tomographical model. Basically, the travel time differences define the time between individual and reference rays. The reference travel time is the time it would take a ray to reach the receiver for a specified sound speed profile. For this thesis study the reference speed of sound profile was that for an isothermal, windless atmosphere.

8.2. OTHER STATE-OF-THE-ART MODELS AND STANDARDS

RAYPS is designed for making predictions based on specific environmental inputs, such as real meteorological and topographical data. It can be used to predict the temporal and spatial variations of sound pressure levels. Prediction models and standards currently in use in the acoustical noise community are not so sophisticated. For example, the Integrated Noise Model (INM) is a computer program required by the Federal Aviation Administration (FAA) for use in airport noise impact studies. The System for Predicting Acoustical Detectability (SPreAD) is one used for the prediction of sound in recreational areas. SPreAD is intended for use in forest environments, over small distance scale similar to the environment examined in the second case study in this thesis. Two standards on the measurement of outdoor noise, one from the American National

Standards Institute (ANSI) and one from the American Society for Testing and Materials (ASTM) are currently being updated.

The Integrated Noise Model was written by the FAA for predicting noise around airports. Its use of meteorological data is primitive. Basically, noise charts that give noise versus distance for different aircraft source power settings are used. The charts have been compiled from real measurements of aircraft noise and adjusted to a "standard day." The defined standard day has the following meteorological conditions: 15° C, 70% relative humidity, and no wind at a sea level elevation. The procedure of measurement and adjustment is from the FAA-36 Test Certification Standard (Connor, 1989).

In reality the effects of refraction, turbulence, atmospheric absorption, and ground impedance are all essential propagation controlling factors. By adjusting the data to a single day's conditions and thereby assuming that these will be the conditions at every airport at any and all times is, from a meteorological point-of-view, contrary to all reason. Another limitation of the model is the absence of topographical input. Although the area around many airports is flat, there are also many airports in regions of complex terrain.

Besides restricting the predictions to predetermined conditions, the INM model output also fails to provide any information regarding temporal variations. Although adjustments are made to the levels provided by the charts to account for day, evening, and night differences, only a single set of contours is provided to cover a whole day's scenario. As can be seen by the studies performed in this

thesis, environmental noise impact studies should somehow include some descriptors of the temporal fluctuations of the sound pressure levels.

The System for the Prediction of Acoustic Detectability, SPreAD, was developed by the U.S. Forest Service, Department of Agriculture, to predict noise impact in outdoor recreation areas. Although SPreAD is ultimately concerned with detectability as well as noise impact, it outlines step-by-step hand calculations to determine the SPL at the listener's location.

Unfortunately SPreAD's usefulness is also limited. Although the Project Record, SPreAD's written documentation (Harrison, 1980), thoroughly explains the basic theory of refraction, no use of the theory is made in SPreAD. The documentation shows the reader variation with height of both the temperature and wind. It explains the nature of positive temperature lapse rates during the day and inversions during the night. It also mentions how the wind generally increases with altitude. Figures are even included to show the refractive consequences of these profiles. But then the user is asked only for a single temperature, and wind direction and speed to describe the conditions for which the acoustic impact is to be predicted. The example provided by the report failed even to mention from what height the data was or should be obtained. In the actual calculation of the refraction related loss only the direction of the wind with respect to the source-listener bearing is considered.

Following the deficient guidance regarding the effects of refraction, one then finds erroneous interpretation of the ground absorption phenomenon. The user is given no insight regarding the

predicted number nor angle of bounces that rays will encounter between a source and receiver. Instead SPreAD uses a table of ground cover loss versus distance from source to receiver.

SPreAD's accounting of temporal variations may also lead to erroneous predictions. Although this model recognizes that a set of input data is specific to the conditions for which the prediction is to take place, it assumes that the atmospheric parameters change only seasonally. A differentiation between day and night is also made (Harrison, 1980, p. 19). As was shown in the first case study in this thesis, large differences occur on the different days. Seasonal resolution is not sufficient.

SPreAD also suggests that the daily averages for the atmospheric parameters are "... good enough and [do] not produce any serious inaccuracy (Harrison, 1980, p. 19)." In SPreAD the daily averages are used to determine the absorption coefficient. Thomson (1987) has shown for diurnal, monthly, and seasonal variations that the use of mean meteorological variables (temperature, and relative humidity) to calculate the "mean" absorption coefficients can result in large errors. Furthermore, when only a single number is used, potentially important information about signal variations is lost. Although detailed statistical representation of the variations as shown in this thesis may not be needed, predictions at enough times during the day to illustrate the diurnal variability could be very helpful. The question of concern is: for many practical applications what is a sufficient presentation of the results from a prediction model so that a spatially and temporally variable noise environment will be

adequately described?

Similar questions might be asked regarding field measurements. How should a noise environment be properly described? Standards are supposed to be designed to supply the answer to such questions. Currently many of the standards on the measurement of outdoor sound are either being newly written or revised. Both the ASTM E-33 committee and the ANSI S12-27 working groups now recognize the need to incorporate the effects of meteorology and to represent the temporal as well as the spatial variations.

Transcripts of an October meeting (Putnam, 1987) provide some insight into current thoughts of the acoustic community. One purpose of this October meeting, in summary, was to identify areas of environmental noise in which needed standards can be developed for effective monitoring, characterization, and control of the acoustic environment. The standardization tasks identified at the meeting included: temporal characterization of sound at a point, design of spatial and temporal sampling programs, processing and presentation of noise data, and assessment of meteorological effects. The work presented in this thesis, especially the use of real meteorological data as input to the prediction model and the use of statistics to display and discuss the temporal and spatial variations of signal amplitude has, hopefully, helped define the nature of some of the standardization problems.

8.3. SUGGESTED ENHANCEMENTS TO RAYPS

Enhancements to the RAYPS program fall into two categories -- some theoretical, others operational. First to be considered is the calculation of atmospheric absorption coefficients. The coefficients used in RAYPS were taken from the tables supplied by the ANSI S1.26 standard (1978). There are nine tables for nine different temperatures. Each table provides a coefficient for different frequencies and relative humidities. In order to find the coefficient for a particular time, the supplementary program, COEF, uses the table whose associated temperature is closest to the surface temperature during this particular time. In other words, the program groups several temperatures onto one table. Once the table is selected, for each frequency, interpolation is used to determine the absorption coefficient for the current relative humidity. Current relative humidity is determined from the surface mixing ratio.

The same standard provides the equations necessary to calculate the absorption coefficient. According to the standard, these equations not only calculate the absorption loss outside the ranges of the tables but with potentially a greater accuracy. Both the necessary acoustic and meteorological variables appear in the formulae -- the temperature, the molar concentration of water vapor which is similar to the mixing ratio, and the atmospheric pressure. The absorption coefficient is not linearly dependent upon either temperature or mixing ratio. However, a linear dependency was implied

as a consequence of the particular method of grouping and interpolation that was used.

Use of the equations would not only produce more precise results but save unnecessary calculations. The mixing ratio would no longer need to be transformed into relative humidity. One additional variable, the atmospheric pressure in Pascals, however, would be required. When the coefficients were calculated for the tables the atmospheric pressure was set equal to the reference atmospheric pressure of one atmosphere. This substitution could also be done in the program or, better yet the actual pressure used.

Another part in which a computational algorithm could be improved is the method used to deal with the wind profiles when the topography is assumed to be flat. Currently, the model allows the topography profile to include negative values. Normally the minimum elevation cannot exceed -400.0 meters. This lowest possible elevation is made to be the point at which the wind speed goes to zero. After setting the wind speed at this bottom point, the wind speeds between it and the first given data point, usually at ten meters, are estimated. Consequently, the wind speed at the zero meter elevation may have a small non-zero value. This procedure is applied without regard to the actual topography. So when flat terrain is specified the wind is not forced to zero at the ground. Better routines to set the wind values for the negative elevations are needed. In the current version the one for irregular terrain is satisfactory. However, for flat topography, all the points between and including -400.0 and zero meters should be initialized to a wind speed of zero

m/s. Then, in both cases the same number of points would be maintained in the wind profile. This is important to all of the subroutines that use this profile.

There are at least three simple changes which could improve the usability of this model. The first would be to read in from file the complex frequency dependent ground impedances and propagation constants. Currently they are hard coded. This data could then be quickly replaced without having to recompile the model. Sound propagation over different types of ground could then be much more easily studied.

A second change is concerned with the number of points written out to the ray trace file. Even though all the points are calculated, in most cases it is not necessary to record every point, especially for the larger distance scales. A sufficient visual plot could still be achieved with fewer points. The user should be able to adjust the frequency at which the points are recorded.

The last suggestion regards a general improvement to the user-interface. Answers to all the organizational questions at the beginning of the program should be stored in a file that could be read in at start up. This would allow the user to change only those parameters that needed to be changed from the previous run.

REFERENCES

American National Standard: Method for the Calculation of the Absorption of Sound by the Atmosphere. ANSI S1.26 (American Institute of Physics, New York, 1978).

Baumgartner, A., "Untersuchungen Über den Wärme- und Wasserhaushalt eines Jungen Waldes," Berichte des Deutschen Wetterdienstes Nr. 28, Band 5, 3-53 (1956).

Baumgartner, A., "Beobachtungswerte und Weitere Studien zum Wärme- und Wasserhaushalt eines Jungen Waldes," Wissenschaftliche Mitteilungen Nr. 4, 1-37 (1957).

Chessel, C. I., "Propagation of Noise along a Finite Impedance Boundary," The Journal of the Acoustical Society of America 62, 825-834 (1977).

Clay, C. S., and H. Medwin, *Acoustical Oceanography: Principles and Applications* (John Wiley & Sons, New York, 1977).

Clifford, S. F., and E. H. Brown, "Propagation of Sound in a Turbulent Atmosphere," The Journal of the Acoustical Society of America 48, 1123-1127 (1970).

Connor, T.L., Personal Communication. (1989).

Cornuelle, B., et al., "Tomographic Maps of the Ocean Mesoscale. Part I: Pure Acoustics," Journal of Physical Oceanography 15, 133-152 (1985).

Fleagle, R. G., and J. A. Businger, *An Introduction to Atmospheric Physics* (Academic Press, New York, 1963).

Fried, D. L., "Remote Probing of the Optical Strength of Atmospheric Turbulence and of Wind Velocity," Proceedings of the IEEE 57, 415-420 (1969).

Geiger, R., trans. by Scripta Technica, Inc., *The Climate Near the Ground* (Harvard University Press, Cambridge, 1965).

Harrison, R. T., R. N. Clark, and G. H. Stankey, Predicting Impact of Noise on Recreationists. Project Report (Forest Service -- U. S. Department of Agriculture, San Dimas, 1980).

Herzog, P., A. C. Berry, and J. Nicolas, "Long-Range Atmospheric Sound Propagation Near the Ground," in *Proceedings of Noise-Con 88* (Noise Control Foundation, New York, 1988).

Janes, H. B., A. W. Kirkpatrick, D. M. Waters, and D. Smith, "Phase and Amplitude Diversity in Over-Water Transmissions at Two Microwave Frequencies," in *National Bureau of Standards Technical Note 307* (U.S. Government Printing Office, Washington, D. C., 1965).

Janes, H. B., M. C. Thompson, Jr., D. Smith, and A. W. Kirkpatrick, "Comparison of Simultaneous Line-of-Sight Signals at 9.6 and 34.5 GHz," IEEE Transactions on Antennas and Propagation AP-18, 447-451 (1970).

Kinsler, L. E., A. R. Frey, A. B. Coppens, and J. V. Sanders, *Fundamental of Acoustics* 3rd ed. (John Wiley & Sons, New York, 1982).

Kryter, K. D., *The Effects of Noise on Man* 2nd ed. (Academic Press, Inc., Orlando, 1985).

Lahti, T., and H. T. Tuominen, "Calculation of Noise Propagation with Multiple Ground Reflections in an Inhomogeneous Atmosphere," in *Proceedings of Inter-Noise 81* (Nederlands Akoestisch Genootschap, Delft, 1981).

Little, C. G., "Acoustic Methods for the Remote Probing of the Lower Atmosphere," Proceedings of the IEEE 57, 571-578 (1969).

Mandics, P. A., "Line-of-Sight Acoustical Probing of Atmospheric Turbulence," Doctoral Thesis, Stanford University, Stanford, CA (1971).

Martens, M. J. M., "Noise Abatement in Plant Monocultures and Plant Communities," Applied Acoustics 14, 167-189 (1981).

Munk, W. and C. Wunsch, "Ocean Acoustic Tomography: A Scheme for Large-Scale Monitoring," Deep Sea Research 26 A, 123-161 (1979).

Nesterova, T. N., A. I. Oterzov, A. S. Smirnov, and I. P. Chunchuzov, "Effect of Temperature and Wind Stratification in the Bottom Layer of the Atmosphere on the Phase of Low-Frequency Sound Waves," Izvestiya, Atmospheric and Oceanic Physics 23, 157-158 (1987).

Oke, T. R., *Boundary Layer Climates* (Methuen, London, 1978).

Panofsky, H. A., and J. A. Dutton, *Atmospheric Turbulence: Models and Methods for Engineering Applications* (John Wiley & Sons, New York, 1984).

Price, M. A., K. Attenborough, and N. W. Heap, "Sound Attenuation through Trees: Measurements and Models," The Journal of the Acoustical Society of America 84, 1836-1844 (1988).

Putnam, R. A., ed., Needs in community Noise: Description, Measurement and Analysis. ASTM E-33.96 Workshop Report (American Society for Testing and Materials, Bal Harbour, 1987).

Roth, S. D., "Acoustic Propagation in the Surface Layer Under Convectively Unstable Conditions," Doctoral Thesis, The Pennsylvania State University, State College, PA (1983).

Spiesberger, J. L., "Ocean Acoustic Tomography: Travel Time Biases," The Journal of the Acoustical Society of America 77, 83-100 (1985).

Tatarski, V. I., trans. by R. A. Silverman, *Wave Propagation in a Turbulent Medium* (McGraw-Hill Book Company, Inc., New York, 1961).

Thomson, D. W., Potential Noise Impact from Proposed Operations at the Davis canyon, Utah Site: Evaluation of Atmospheric Acoustic Refractive Index Profiles. Final Report (Department of Meteorology, The Pennsylvania State University, State College, 1986).

Thomson, D. W., "Regarding the Temporal Variability of Frequency-Dependent Atmospheric Acoustic Absorption Coefficients," in *Proceedings of Noise-Con 87* (Noise Control Foundation, New York, 1987).

Thomson, D. W., Personal Communication. (1988).

Wessels, H. R. A., and C. A. Velds, "Sound Propagation in the Surface Layer of the Atmosphere," The Journal of the Acoustical Society of America 74, 275-280 (1983).

Appendix

FLOW CHARTS

RAYPS

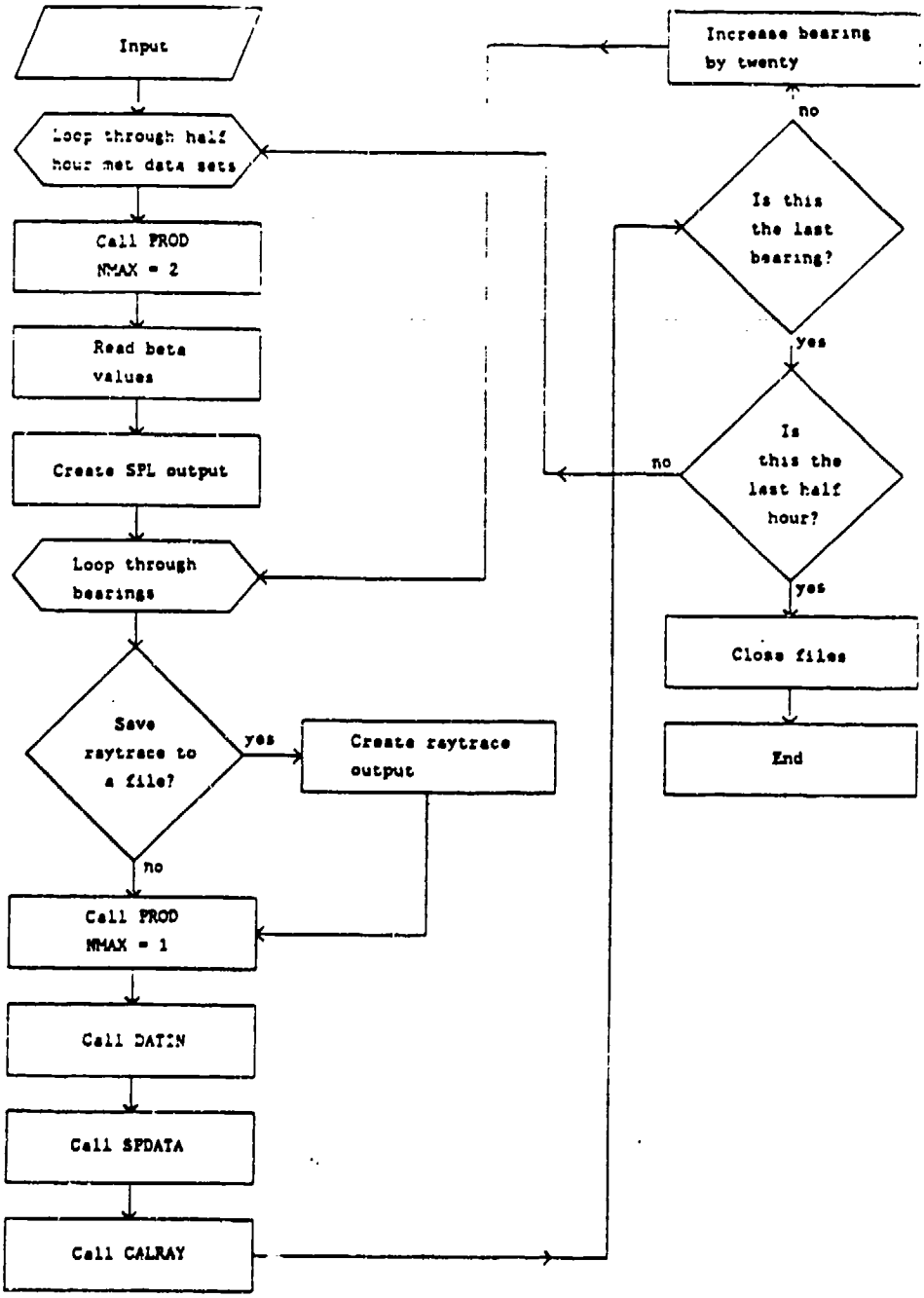

Figure A.1. Flow Chart for Program Rayps

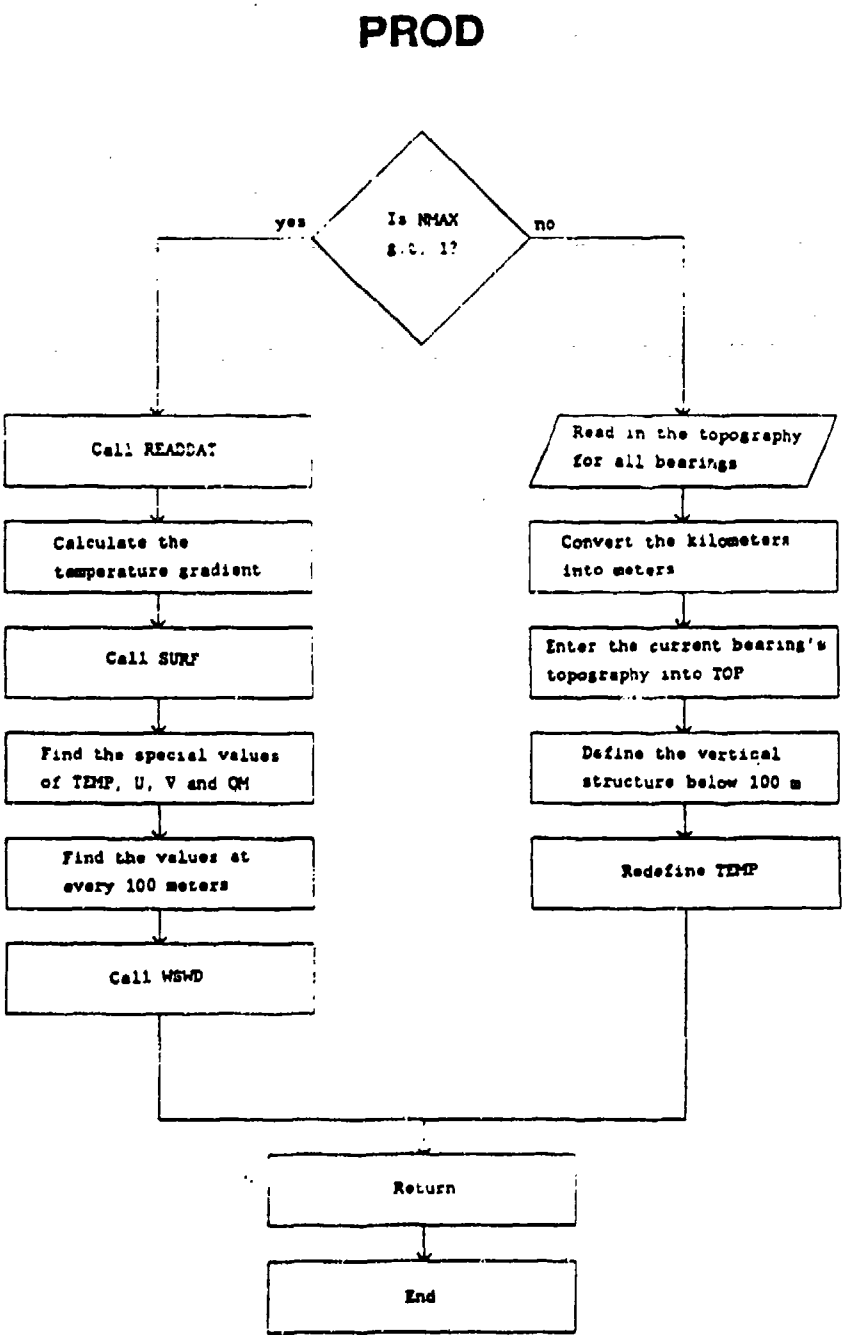

Figure A.2. Flow Chart for Subroutine Prod

READDAT

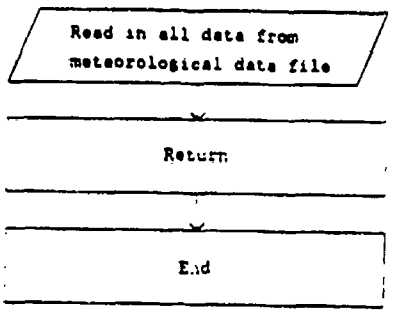

Figure A.3. Flow Chart for Subroutine Readdat

SURF

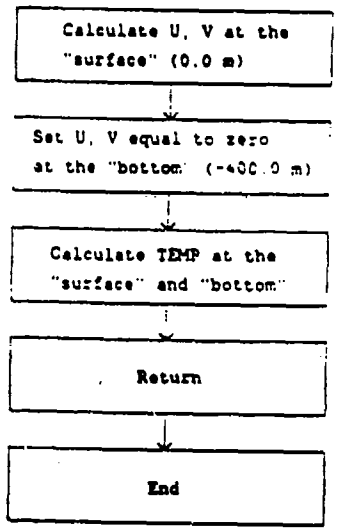

Figure A.4. Flow Chart for Subroutine Surf

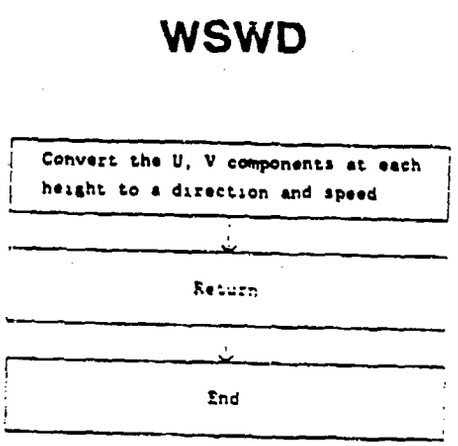

Figure A.5. Flow Chart for Subroutine Wswd

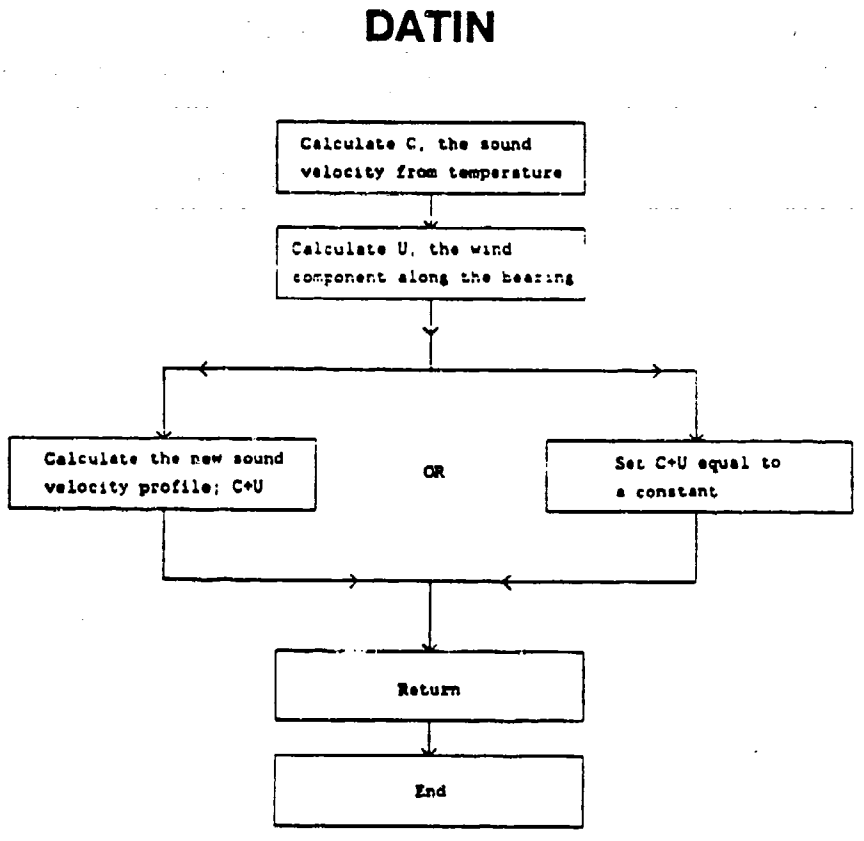

Figure A.6. Flow Chart for Subroutine Datin

SPDATA

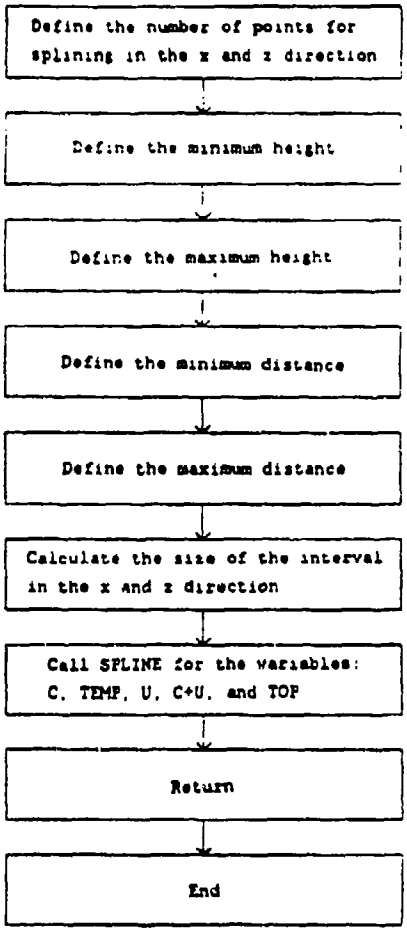

Figure A.7. Flow Chart for Subroutine Spdata

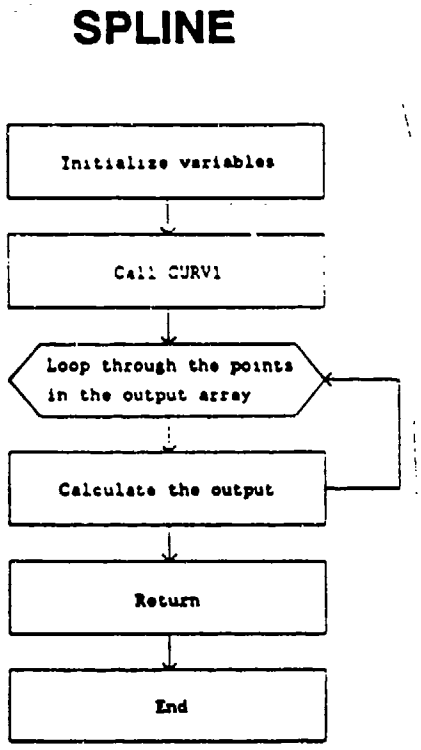

Figure A.8. Flow Chart for Subroutine Spline

CALRAY

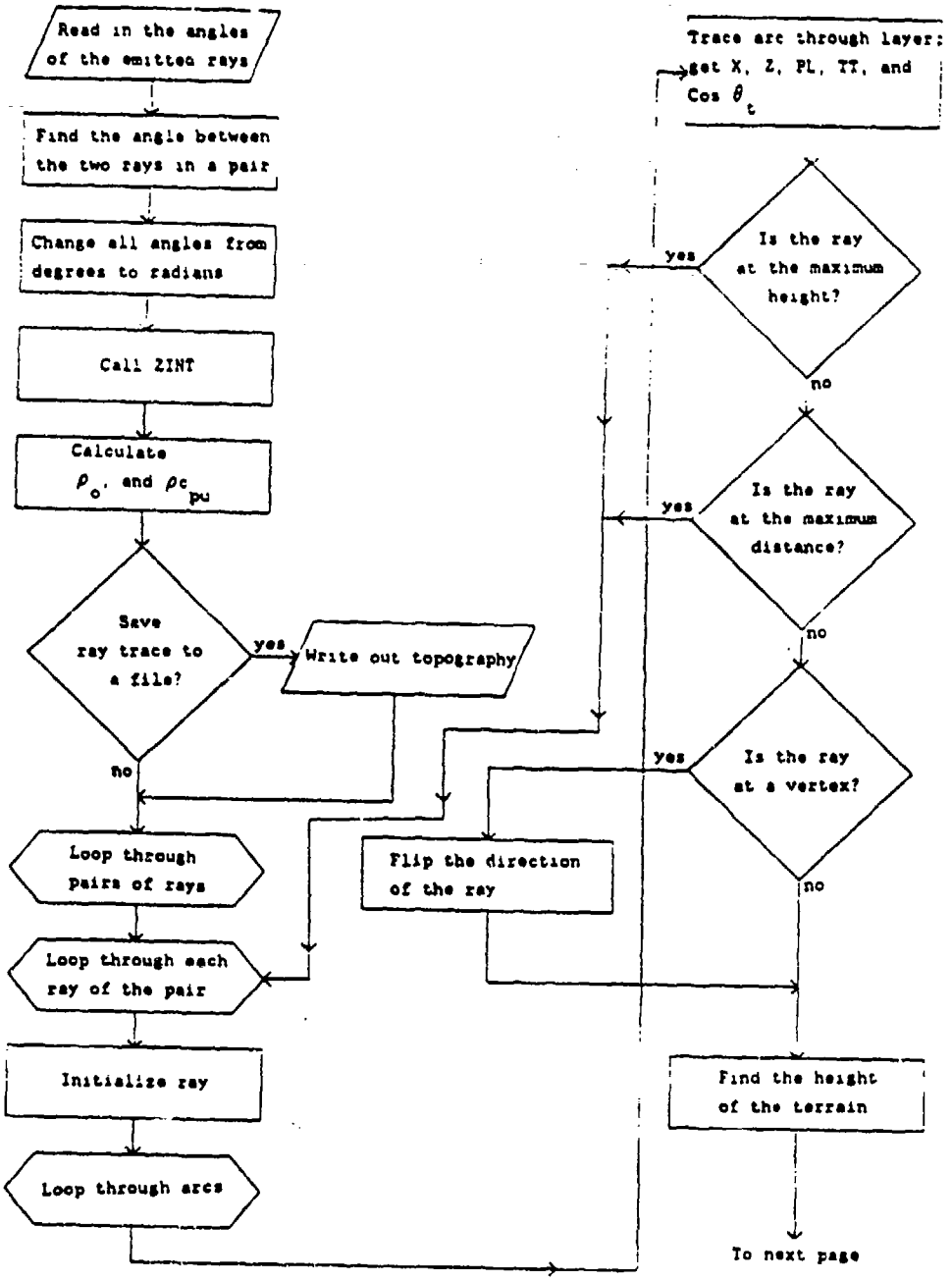

Figure A.9. Flow Chart for Subroutine Calray (Page 1 of 3)

CALRAY (Continued)

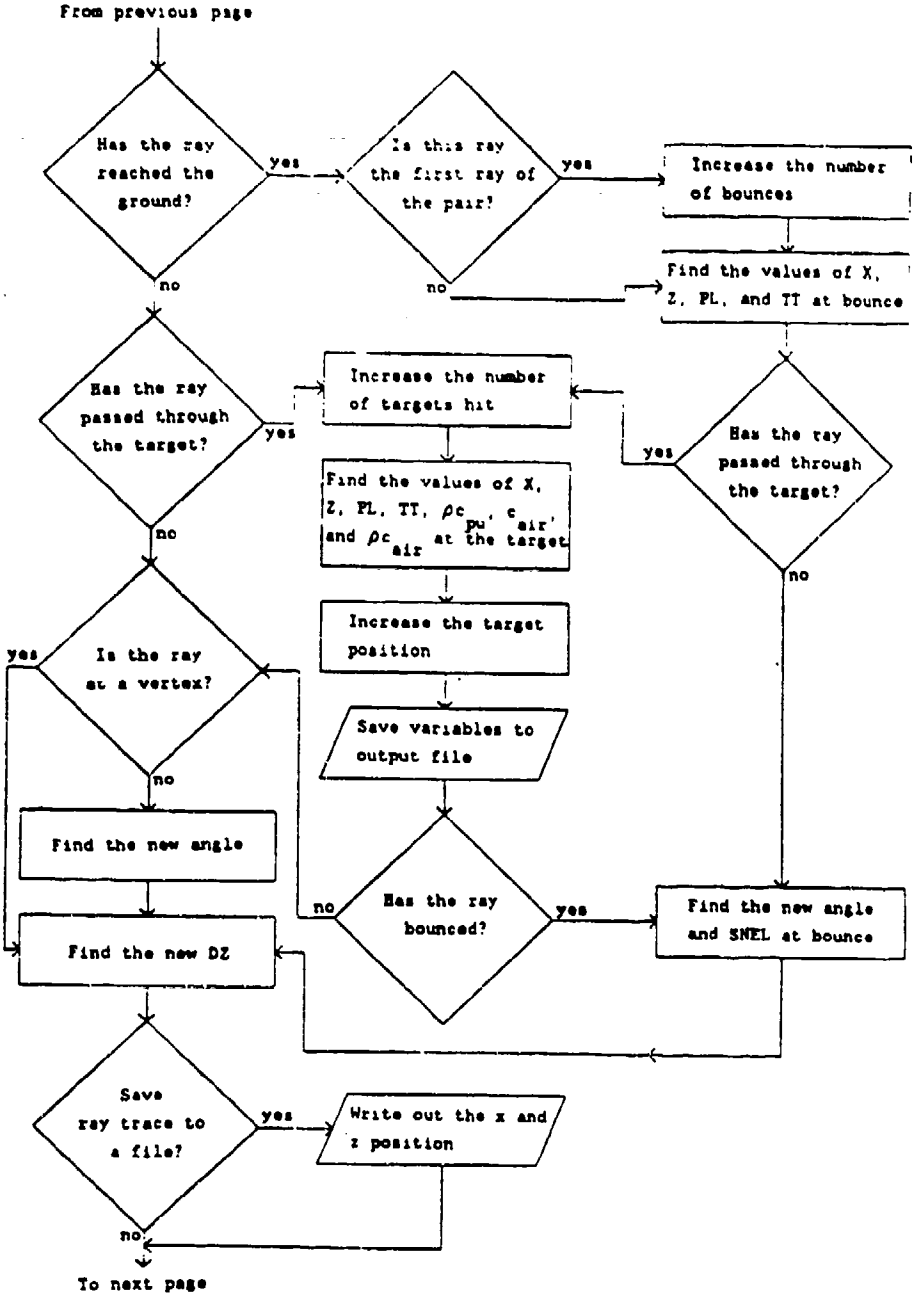

Figure A.10. Flow Chart for Subroutine Calray (Page 2 of 3)

CALRAY (Continued)

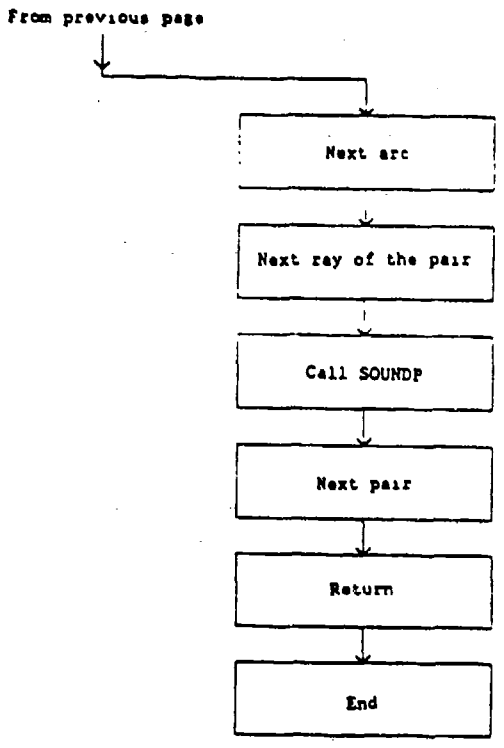

Figure A.11. Flow Chart for Subroutine Calray (Page 3 of 3)

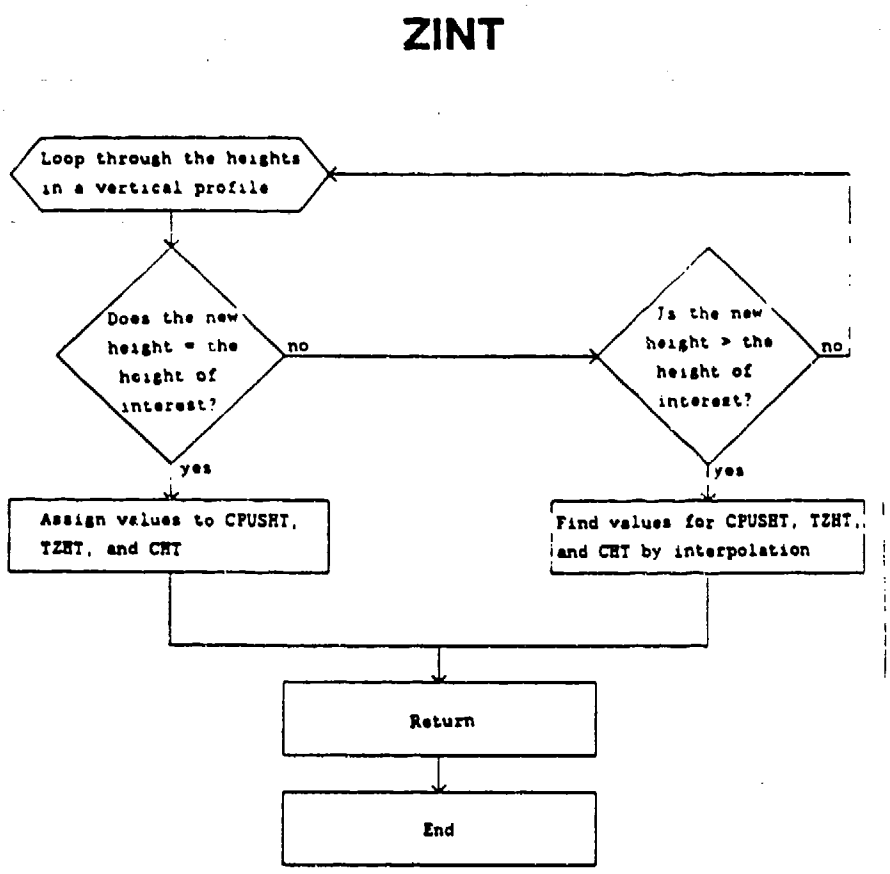

Figure A.12. Flow Chart for Subroutine Zint

SOUNDP

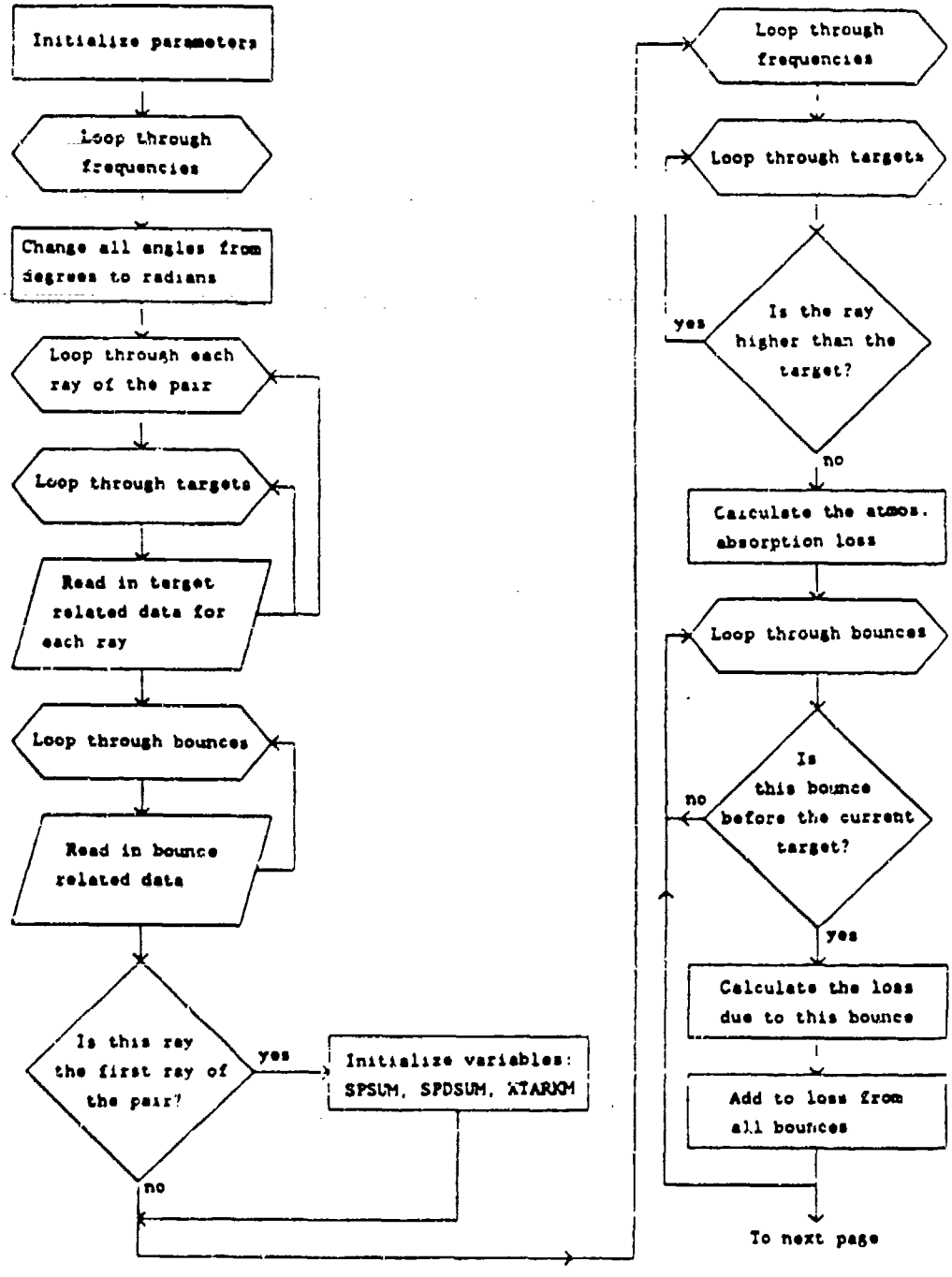

Figure A.13. Flow Chart for Subroutine Soundp (Page 1 of 2)

SOUNDP (Continued)

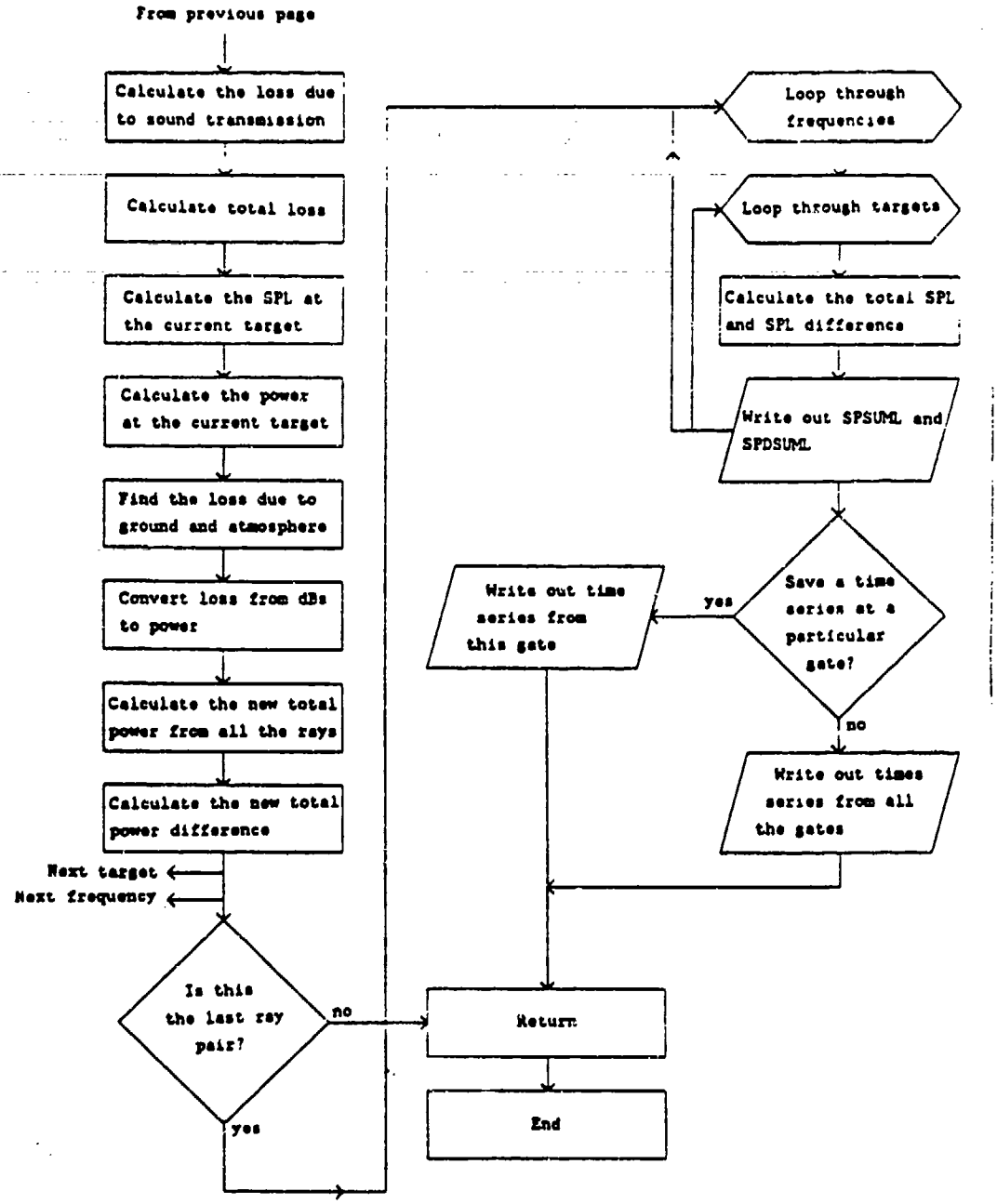

Figure A.14. Flow Chart for Subroutine Soundp (Page 2 of 2)

PHASE

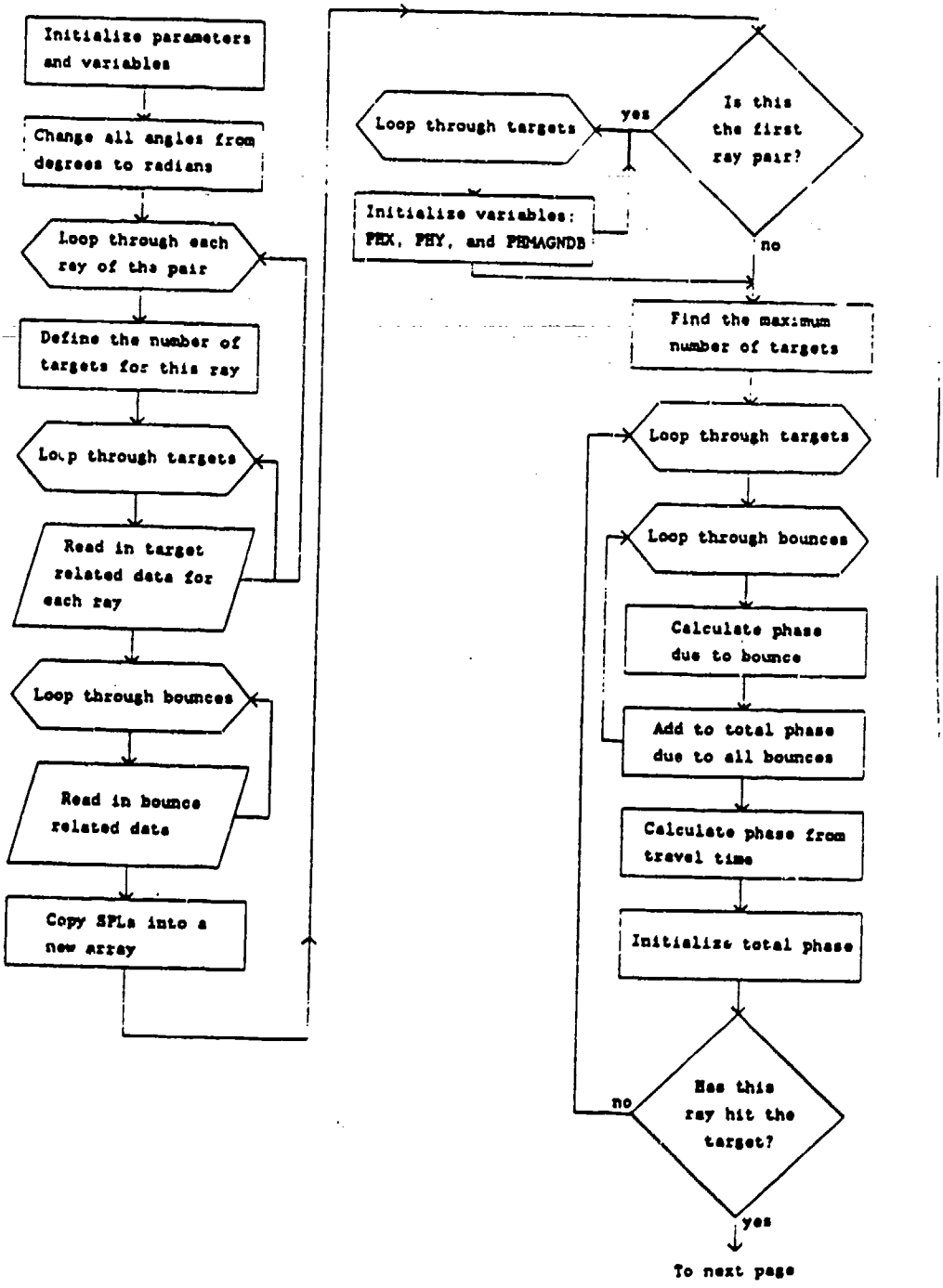

Figure A.15. Flow Chart for Subroutine Phase (Page 1 of 3)

PHASE (Continued)

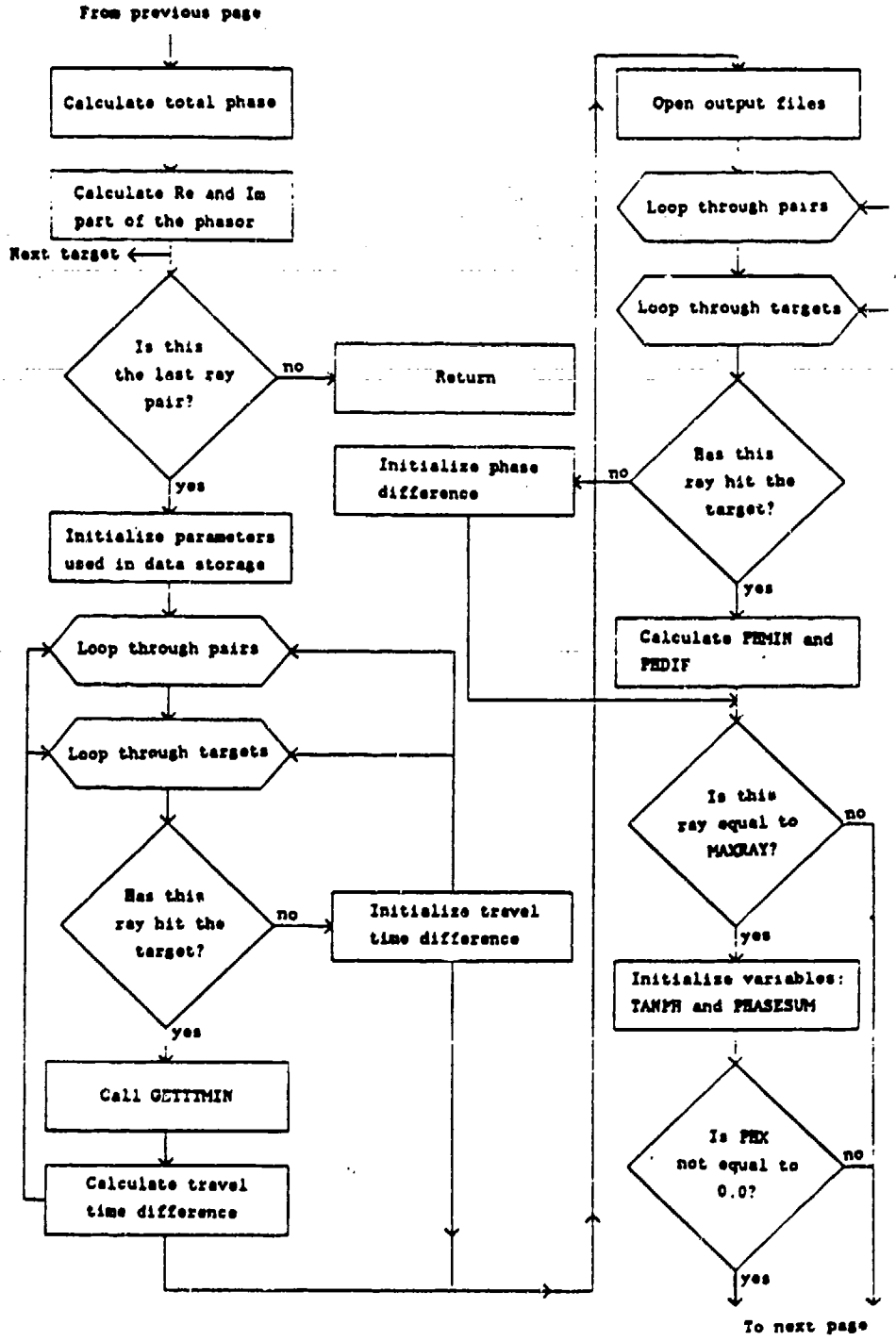

Figure A.16. Flow Chart for Subroutine Phase (Page 2 of 3)

PHASE (Continued)

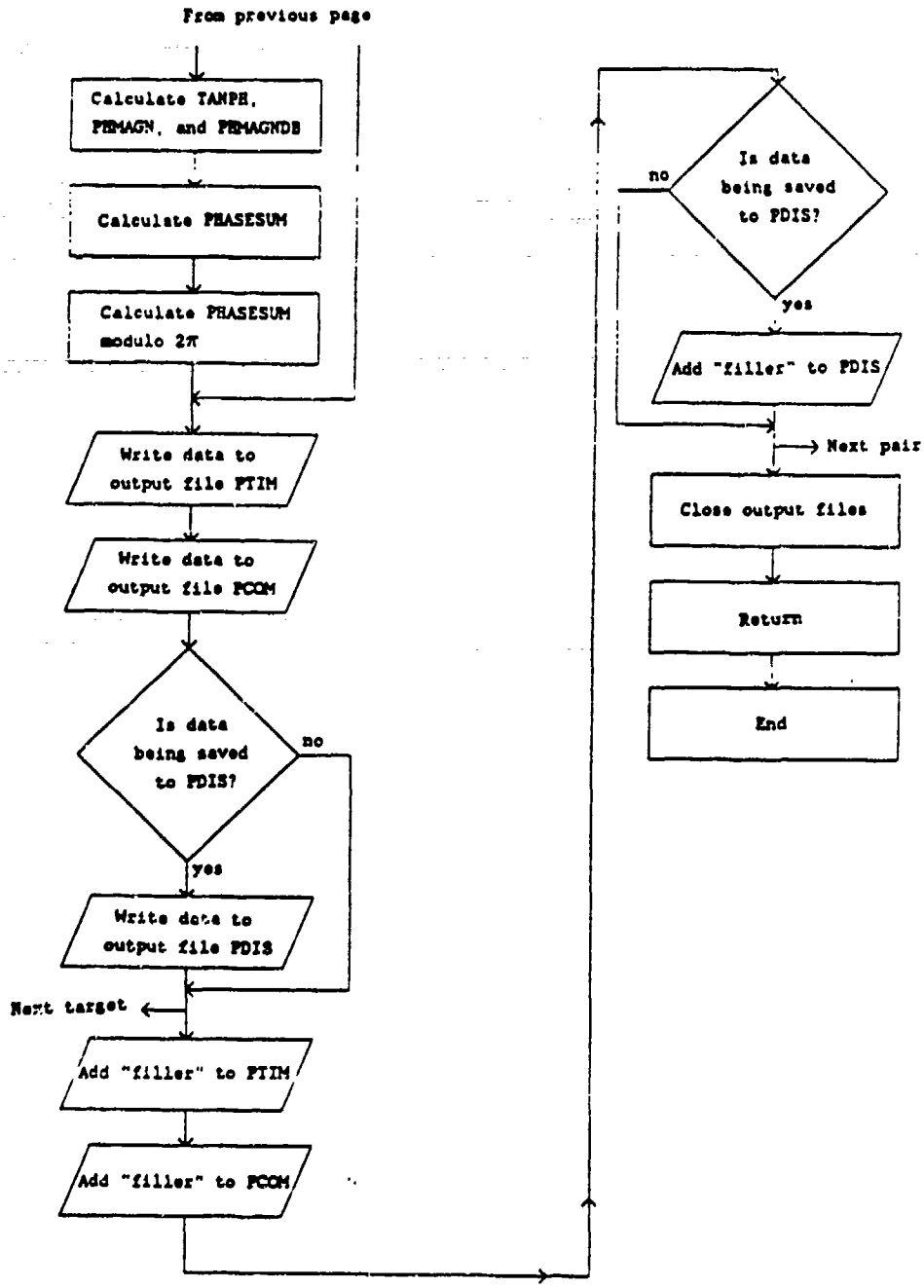

Figure A.17. Flow Chart for Subroutine Phase (Page 3 of 3)